SUPPORTING INFORMATION

A Wagner-Meerwein-like rearrangement shapes the structures of the fischerazoles, cyanobacterial polychlorinated lipopeptides.

Sandra A. C. Figueiredo,[§,1] Kathleen Abt,[§,1,2] Konrad Viehrig,[§,1] Peter J. Jervis,[1] Teresa P. Martins,[1] Iñaki Lacomba,[1] Chuhan Li,[3] Daniele Castagnolo,[3] Pedro N. Leão*[,1]

[1]Interdisciplinary Centre of Marine and Environmental Research (CIIMAR/CIMAR), University of Porto, Avenida General Norton de Matos, s/n, 4450-208 Matosinhos, Portugal;
[2]ICBAS—School of Medicine and Biomedical Sciences, University of Porto, Rua de Jorge Viterbo Ferreira, 228, 4050-313, Porto, Portugal:
[3] Department of Chemistry, University College London, Marshgate Building, Manufacturing Futures Lab, 7 Sidings Street, E20 2AE, London, United Kingdom.
[§] these authors contributed equally to this work

Table of Contents

Experimental Procedures

General experimental procedures

Stable-isotope labeled fatty acids (d_{11}-hexanoic, d_{15}-octanoic, d_{19}-decanoic d_{23}-dodecanoic, d_{27}-tetradecanoic, d_{31}-hexadecanoic acids and and potassium d_{35}-octadecanoate) were obtained from CDN Isotopes Inc. [U-^{13}C]-hexadecanoic acid was obtained from Cambridge Isotope Laboratories. *L*-methionine-(methyl-^{13}C, d_3) sodium salt was obtained from Sigma-Aldrich. All solvents, purchased from VWR Chemicals, Thermo Fisher Scientific, Carlo Erba and Chem Lab NV were ACS grade, except for HPLC solvents (HPLC gradient grade) and LC-MS solvents (MS-grade). Deuterated solvents for NMR were purchased from Cambridge Isotope Laboratories and Alfa-Aesar. LC-HRESIMS and LC-HRESIMS/MS analyses were obtained on a Thermo Scientific UltiMate 3000 HPLC system, which consists of the following components: LPG-3400RS pump, WPS-3000RS autosampler, TCC-3x00RS column compartment, and MWD-3000RS UV/VIS detector coupled to a Q Exactive Focus Hybrid Quadrupole Orbitrap Mass Spectrometer (Thermo Fisher Scientific), controlled by Q Exactive Focus (Exactive Series) 2.9 and Thermo Scientific Xcalibur 4.1.31.9 software. Optical rotations were obtained on a P-2000 polarimeter (Jasco) in a 1 mL sample cell. The electronic circular dichroism (ECD) spectrum of **2** was acquired on a J-815 CD Spectrometer (Jasco). UV spectra were acquired on a UV-1600PC spectrophotometer (VWR). Infrared spectra were determined on a Thermo Scientific Nicolet™ iS™ 5 Fourier transform IR spectrometer controlled by OMNIC 9.8.372 software. NMR spectra were acquired using a DMSO-matched Shigemi tube on a Bruker Avance III HD, 600 MHz, equipped with a 5 mm cryoprobe and controlled by TopSpin 3.6.1., in the Materials Center of the University of Porto (CEMUP) and the NMR data were analyzed in MestReNova 12.0.3 (MestrelabResearch). The chemical shifts values (δ) are presented in parts per million (ppm) and the coupling constants (*J*) in hertz (Hz). The purification of **1**-**3** was performed on a Thermo Scientific UltiMate 3000 HPLC system and fitted with an ACE 10 C18 column (250 mm × 10 mm, 10 µm, 100 Å, ACE).

Strains and culture conditions

The cyanobacterium *Fischerella* sp. PCC 9431 was acquired from Pasteur Culture Collection of Cyanobacteria (PCC), Institute Pasteur (France). Cyanobacterial cultures were carried out in glass Erlenmeyer flasks (small-scale culturing) or in 20-L polycarbonate carboys (large-scale culturing), in Z8 medium with aeration, 25 ºC, 30 µmol photons m^{-2} s^{-1} (16 h light/ 8 h dark cycle). For large-scale cultures, the biomass was harvested in late-exponential to early-stationary phase by centrifugation (5000 *g*), freeze-dried and stored at -20 ºC until further use.

LC-HRESIMS and MS/MS analysis of fischerazole metabolites

HRESIMS data were obtained in Full Scan positive mode with a capillary voltage of HESI set to 3.5 kV and the capillary temperature to 263 °C. Sheath gas flow rate was set to 50 units. For LC-HRESIMS analyses, separation was performed in an ACE UltraCore 2.5 SuperC18 column (75 x 2.1 mm, ACE).

For flow injection analysis (during HPLC isolation of **1-3**), the ESI parameters were 3.8 kV a capillary temperature of 300 °C and a sheath gas flow rate of 5 units.

Samples from stable isotope supplementation experiments (full MS) and pure compounds were separated at a flow rate of 0.3 mL min^{-1} with a mobile phase of 0.1% formic acid in H_2O (eluent A), MeOH (eluent B) and iPrOH (eluent C). The gradient for the crude extracts started with 5% B increasing to 100% B over 20 min, held for 15 min, then B was decreased to 30% while C was increased to 70% over 5 min which was held for 7 min before returning to initial conditions over 2 min.

Samples during the isolation of **1-3** (after VLC, flash chromatography and HPLC) were separated with a shorter gradient at a flow rate of 0.4 mL min^{-1} and employed a mobile phase of 0.1% formic acid in MeOH/H_2O 1:1 (v/v) (eluent A) and in iPrOH (eluent B). The gradient started with 10% B for 1 min, a gradient from 10% to 65% B over 5 min, held at 65% B for 12 min, then a gradient to 85% B over 2 min, and held again at 85% B for 9 min, before returning to the initial conditions.

Samples from stable isotope supplementation experiments for MS/MS analysis were separated over a similar shorter gradient of MeOH/H2O 1:1 (v/v) (eluent A) and in iPrOH (eluent B), both containing 0.1% formic acid. Starting with 10% B for 1 min, the gradient increased to 23% B over 2 min, which was held for 10 min until another increase to 90% B over 2min. This was held for 7 min, then returned to initial conditions in 2 min.

Identification of new mass features in LC- HRESIMS data from the initial d_{11}-hexanoic acid substrate incorporation experiments was performed with MZmine 2.53 as previously described,[SI-1] with the additional use of Natural Product Atlas[SI-2] as a database for dereplication.

LC-HRESIMS and MS/MS analysis of ACP-bound fatty acids

After trypsination, quenched enzymatic assays were separated in an Aeris peptide XB-C18 column (3.6 µm particle size, 150 × 4.6 mm), injecting 10 µL. The column oven was set to 40 °C. At a flow of 0.5 mL/min with a mobile phase of H_2O with 0.1% formic acid (eluent A) and ACN with 0.1% formic acid (eluent B). The gradient started isocratic at 100 % A for 2 min, gradient from 100 % A to 100 % B over 16 min, held at 100 % B for 4 min, before returning to the initial conditions within 1 min and equilibrating for 2 min.

For LC-HRESIMS analysis, the parameters used were a resolution of 70,000 with an AGC target of 1×10^6 and a scan range of 150-2,000 *m/z*. Extracts from stable isotope labelling experiments were analyzed with the same parameters but a scan range from 100 to 1,500 *m/z*.

LC-HRESIMS/MS analysis was performed using a resolution of 35 000, with a 0.4 *m/z* isolation window, a loop count of 1, AGC target of 2×10^5 and collision energy of 25 (arbitrary units). For low abundance compounds, the full MS scan range was between *m/z* 400 and 650. For enzymatic assays the resolution was 17 500, AGC target 5×10^4 and stepped normalized collision energy 20, 30 and 40.

LC-HRESIMS analysis of free fatty acids

Cleared enzymatic assays were separated in an ACE UltraCore 2.5 SuperC18 column (75 x 2.1 mm, ACE), injecting 3 µL. The column oven was set to 40 °C. At a flow of 0.35 mL/min with a mobile phase 10 mM NH_4OAc in MeOH/H_2O 1:1 (v/v) (eluent A) and in iPrOH (eluent B). Separation started with 10% B for 3 min, then a gradient from 10% to 65% B over 5 min, held at 65% B for 2 min, then a gradient to 90% B over 10 min, then returning to 10% B over 1 min and 1min hold at 10% B. Between each sample, a blank run was inserted to avoid carry-over.

GC-MS analysis of FAMEs

Aliquots of the samples containing free fatty acids were esterified to obtain fatty acid methyl ester (FAME) derivatives for GC-MS analysis (details given at a later section). Extracts and standards were analyzed using a triple quadrupole gas chromatography–tandem mass spectrometry system consisting of a TSQ 9610 mass spectrometer coupled to a Thermo Scientific TRACE 1600 gas chromatograph. Sample introduction was carried out using a Thermo Scientific AI 1610 autosampler. Chromatographic separation was achieved on an Agilent J&W capillary column with a length of 30 m, an internal diameter of 0.250 mm, and a film thickness of 0.25 µm. A volume of 1 µL of each sample was injected into the GC inlet, which was maintained at 220 °C and operated in splitless mode using a split/splitless quartz wool liner (4mm ID, 78.5mm). Splitless time was 0.5 minutes and speptum purge flow was 1 mL/min. Helium was used as the carrier gas at a constant flow rate of 1.0 mL/min. The oven temperature program started at 40 °C, which was held for 5 minutes, followed by a temperature ramp to 150 °C at a rate of 20 °C/min, ramp two to 210 °C at a rate of 2 °C/min, finishing with ramp three to 225 °C at a rate of 40 °C/min, with a final hold time of 10 minutes. The mass spectrometer transfer line was maintained at 230 °C. Electron ionization was performed at an electron energy of 70 eV, with the ion source temperature set to 230 °C. Data were acquired using full scan (50-550 m/z). Instrument control, data acquisition, and data processing were performed using the Thermo Scientific Chromeleon 7 Chromatography Data System software.

Extraction and MS-guided isolation of compounds 1-3

The freeze-dried biomass resulting from large-scale (80 L) culturing of *Fischerella* sp. PCC 9431 (24.5 g, d.w.) was repeatedly extracted by immersion on a 2:1 mixture of CH_2Cl_2/MeOH. After filtration of the resulting slurry and solvent evaporation, 3.2 g of crude extract were obtained. The extract was subjected to normal-phase (Si Gel 60, 0.040-0.063 mm, Merck) Vacuum Liquid Chromatography (VLC). A gradient of increasing solvent polarity, from *n*-hexane to EtOAc to MeOH, resulting in twelve fractions (A – L). All fractions were subjected to LC-HRESIMS analysis to determine those which contained the mass features corresponding to the polyhalogenated compounds of interest. Fractions F, G and H, eluting between 3:2 and 1:4 *n*-hexane/EtOAc (v/v), were enriched in target ($[M+H]^+$) *m/z* 515.085 and 481.124, and were pooled (combined: 592.2 mg) for further separation. Likewise, fractions D and E, eluting with 4:1 and 7:3 *n*-hexane/EtOAc (v/v), respectively, were enriched in *m/z* 499.091 and 465.130 ($[M+H]^+$)and were combined (520.3 mg) before being further fractionated. Pooled fractions F/G/H were loaded onto a 12 g normal phase silica cartridge (Silicycle), which was fitted to a flash chromatography system (Pure C-815 Flash, Büchi). A gradient from *n*-hexane to EtOAc to MeOH was used for the automated separation. A total of 247 collected fractions were pooled into 18 fractions on the basis of their ELSD and UV profiles. These were analyzed by LC-HRESIMS, which revealed that fractions 8 (16.1 mg) and 9 (15.5 mg) were highly enriched in the two target compounds (*m/z* 515.085 and 481.124, $[M+H]^+$). In addition, fractions 3-5 (combined: 16.4 mg) were enriched in the other two target mass features (*m/z* 499.091 and 465.130). Semi-preparative HPLC separation of fraction 8 (gradient of 50% MeOH aq. (solvent A) and iPrOH (solvent B) starting with isocratic conditions of 33% B for 25 min, increasing to 90% B over 5 min, holding for 10 min and returning to initial conditions over 5 min), afforded pure **1** (t_R = 22.5 min) and **2** (t_R = 26.5 min). Similar HPLC conditions were used to further separate fraction 9 (the initial isocratic step was held for 30 min as the only change), which also afforded pure **1** and **2**. The two aliquots for each compound were pooled to give 3.6 mg of **1** (0.015% of biomass d.w.) and 2.0. mg of **2** (0.008% of biomass d.w.). Pooled fractions D/E and flash chromatography fractions 3-5 were combined and further separated by automated flash chromatography using the same conditions as described above. This procedure afforded 13 fractions, which were analyzed by LC-HRESIMS. The target mass features were present in two fractions with a combined mass of 320.0 mg. These were pooled together and further fractionated by a new round of automated flash chromatography, this time using a 4g normal-phase silica column (Silicycle). Once again, the

resulting fractions were pooled on the basis of ELSD and UV profiles (to give 14 fractions) and analyzed by LC-HRESIMS. This revealed that the mass features of interest were highly enriched in fraction 7 (36.0 mg). This fraction was further separated by semi-preparative HPLC (gradient of 50% MeOH aq. – solvent A – and iPrOH – solvent B – starting with isocratic conditions of 55% B for 23 min, increasing to 95% B over 3 min, holding for 7 min and returning to initial conditions over 3 min) to afford pure **3** (1.0 mg, 0.004% biomass d.w., t_R = 15.0 min) and a small amount (0.2 mg) of a partially purified analogue with an $[M+H]^+$ ion of *m/z* 465.130 (t_R = 18.0 min).

Fischerazole A (1) (pale yellow amorphous solid): $[\alpha]_D^{24}$ +14.7 (*c* 0.1, MeOH); IR (thin film) υ_{max} 3412, 2919, 2851, 1651, 1553, 1496, 1462, 1413, 1028 cm^{-1}; UV (MeOH) λ_{max} (log ε) 234 (3.4), 281 (2.7); ^1H and ^{13}C NMR data, see Table S1; HRESIMS *m/z* 515.0852 $[M+H]^+$ (calcd. for $C_{21}H_{31}O_2N_2{}^{35}Cl_4S$ 515.0855).

Fischerazole B (2) (pale yellow amorphous solid): $[\alpha]_D^{24}$ +17.6 (*c* 0.1, MeOH); IR (thin film) υ_{max} 3417, 2936, 2858, 1658, 1651, 1556, 1495, 1463, 1412, 1311, 1252, 1108, 996, 918, 878, 506 cm^{-1}; UV (MeOH) λ_{max} (log ε) 239 (3.0), 276 (2.0); ^1H NMR (600 MHz, DMSO-d_6) δ8.28 (q, *J* = 4.9 Hz, 1H), 8.14 (s, 1H), 6.12 (t, *J* = 7.4 Hz, 1H), 5.74 (dd, *J* = 17.2, 10.8 Hz, 1H), 5.11 (dd, *J* = 17.3, 2.3 Hz, 1H), 4.98 (dd, *J* = 10.8, 2.3 Hz, 1H), 4.44 (tt, *J* = 8.7, 4.3 Hz, 1H), 4.20 (s, 1H), 3.53 (dd, *J* = 15.4, 4.4 Hz, 1H), 3.38 (dd, *J* = 15.4, 8.8 Hz, 1H), 2.77 (d, *J* = 4.8 Hz, 3H), 2.11 (q, *J* = 7.4 Hz, 2H), 1.88 – 1.80 (m, 1H), 1.71 (dtd, *J* = 14.1, 9.4, 4.6 Hz, 1H), 1.46 (m, 2H), 1.42 – 1.31 (m, 8H), 1.31 – 1.13 (m, 6H); ^{13}C NMR (150 MHz, DMSO-d_6) δ166.5, 160.9, 149.6, 144.8, 131.2, 123.6, 117.9, 111.8, 73.7, 62.5, 41.2, 40.4, 40.3, 37.3, 29.2, 29.1, 27.5, 26.3, 25.8, 22.8, 22.6; HRESIMS *m/z* 481.1242 $[M+H]^+$ (calcd. for $C_{21}H_{32}O_2N_2{}^{35}Cl_3S$ 481.1245).

Fischerazole C (3) (pale yellow amorphous solid): $[\alpha]_D^{24}$ +41.4 (*c* 0.1, MeOH); IR (thin film) υ_{max} 3418, 2922, 2859, 1659, 1551, 1055, 1033 cm^{-1}; UV (MeOH) λ_{max} (log ε) 238 (3.4), 281 (3.1); ^1H and ^{13}C NMR data, see Table S2; HRESIMS *m/z* 499.0908 $[M+H]^+$ (calcd. for $C_{21}H_{31}ON_2{}^{35}Cl_4S$ 499.0906).

Identification of the *fsh* BGC

The genome data of PCC 9431 (NCBI accession number: ALVX00000000) was used to populate a local BLAST database with the Geneious software package 11.1.4 (Biomatters). tBLASTn searches against this database, using the halogenases CylC (NCBI: ARU81117.1) and ArzI (NCBI: DAB41911.1) revealed the candidate *fsh* gene locus (accession numbers in Table S3). The genome was submitted to AntiSMASH (6.0.1 bacterial version) for BGC annotation. Manual annotation of the Fsh proteins was performed using BLASTp searches against the NCBI nr database. Domains were annotated based on NCBI BLAST and InterProScan from within Geneious. Docking domains for sequence alignments were downloaded from the DDAP database,[SI-3] containing 382 entries at the time of accession (November 2020). Sequences of C-terminal heads were aligned using the 100 C-terminal residues of FshA, FshE, FshM, FshG, FshH and FshI; sequences of N-terminal tails were aligned using the 50 N-terminal residues of FshE, FshM, FshH, FshI and FshJ, by using MAFFT with a BLOSUM62 matrix in Geneious.

Stable isotope-labeled substrate incorporation experiments

The initial supplementation of *Fischerella* sp. PCC 9431 with d_{11}-hexanoic (d_{11}-C_6) was performed in three pulses with a final concentration of 0.5 mM in triplicates as previously described.[SI-1] Small-scale (25 mL) cultures in Z8 medium in Erlenmeyer flasks (starting chlorophyll a content of ~0.8–2.9 µg mL^{-1}), were inoculated with d_{15}-octanoic acid (d_{15}-C_8), d_{19}-decanoic (d_{19}-C_{10}), d_{23}-dodecanoic (d_{23}-C_{12}), d_{27}-tetradecanoic acid (d_{27}-C14) and d_{31}-hexadecanoic (d_{31}-C_{16}) acids , to a final concentration of 0.5 mM from a 1000× concentrated solution of each acid in DMSO. L-methionine-(methyl-^{13}C, d_3) was provided directly to the culture at 0.5 mM. Potassium d_{35}-octadecanoate (d_{35}-C_{18}) was provided at a final concentration of 0.25 mM from a 1000× concentrated solution in H_2O. For hexanoic acid, octanoic acid and methionine, DMSO was used as a control, for all others, the control was the respective non-labeled substrate. After a seven-day growth period with continuous orbital shaking (200 rpm, mini shaker, VWR), cells were harvested by centrifugation at 5000 ×g for 15 min, rinsed with deionized water, centrifuged again and the water drained as much as possible. The fresh biomass was extracted with ca. 7 mL of CH_2Cl_2/MeOH (2:1, v/v) and vigorous vortexing. All samples were incubated for 30 min on a nutating mixer in solvent-resistant tubes. The extracts were filtered through Whatman No. 1 filter paper, concentrated using a rotary evaporator (R-210, Buchi) and transferred to glass vials. The solvent was fully evaporated. Crude extracts were analyzed by LC- HRESIMS at a concentration of 2 mg mL^{-1}. For improved incorporation from [U^{13}C]-hexadecanoic acid ([U^{13}C]-C_{16}), small-scale (25 mL) cultures of PCC 9431 in Z8 medium in Erlenmeyer flasks (starting chlorophyll a content of ~4.0 µg mL^{-1}), were inoculated with 0.25 mM [U^{13}C]-hexadecanoic acid and harvested after an incubation of 48 h with continuous orbital shaking (200 rpm, mini shaker, VWR). Centrifugation, extraction and LC- HRESIMS analysis were performed as for the other supplementation samples as described above. To achieve fragmentation of [U^{13}C]-C_{16}-**3**, the extract

was concentrated by solid phase extraction (Strata C_{18}-E, 100 mg, 1 mL, 55 µm, 70 Å, Phenomenex) over a stepwise gradient of MeOH in H_2O, starting with 30% MeOH. [$U^{13}C$]-C_{16}-**3** was more concentrated in the fraction eluting with 100% MeOH.

Cloning, expression and purification of C-His$_6$-FshA, N-His$_6$-FshE, N-His$_6$-FshM, N-His$_6$-FshF, C-His$_6$-'tesA, C-His$_6$-'tesA-mCherry and C-His$_6$-Sfp

Primers used in this work.

gene	primer	sequence
fshA	Fw	ATGAGAGCTCGATGAGTCTAATGGAAAACC
	Rv	GTCAGTCGACAGTAGGGACATTCG
fshE	Fw	GCGCCATATGGAAACTCAAAATGCTC
	Rv	GCGCCTCGAGTTATAAAGAATTGGTATG
fshM	Fw	GCGCCATATGGATACTGAAATTTCTC
	Rv	GTACCTCGAGTTAGTTTCCTTCAG
fshF	Fw	GATCCATATGGCTACGAACACTG
	Rv	GATCCTCGAGTTACTTACGGGG
'tesA	Fw	CGGTCATATGGCGGACACGTTATTG
	Rv	GGCACTCGAGTGAGTCATGATTTACTAAAGGCTG

Gene expression conditions.

Protein	predicted MW [kDa]	Expression conditions					
		plasmid	*E. coli* strain	media	Temp [°C]	IPTG [mM]	time
FshA	69.6	pET29b(+)	C43(DE3)	TB	25	0.5	2d
FshE	14.3	pET28a(+)	BL21(DE3)	TB	25	1	overnight
FshM	13.5	pET28a(+)	BL21(DE3)	TB	25	1	overnight
FshF	36.3	pET28a(+)	BL21(DE3)	TB	25	0.5	overnight

Ca. 100 mg (wet weight) frozen biomass of PCC 9431 was homogenized with liquid N_2 and mortar and pestle. The resulting powder was extracted with a plant/fungi gDNA isolation kit (Nzytech) according to the manufacturer's instructions (using buffer PNL1). gDNA was eluted in 40 µL warm H_2O. The *fsh*A gene was amplified with primers containing restriction sites for SacI and SalI, while the primers for the genes *fshE, fshM* and *fshF* contained restriction sites for NdeI and XhoI – Table S4. The reaction for *fshA* contained 1x Q5 master mix (New England Biolabs), 0.5 µM of each primer and 1 µL of gDNA in 50 µL total reaction volume. The PCR was performed using the following conditions: initial denaturation at 98 °C for 30 seconds, 35 cycles of denaturation at 98 °C for 10 seconds, annealing at 66 °C for 30 seconds, extension at 72 °C for 1 min, followed by final extension at 72 °C for 10 min. The reaction for *fshE, fshE* and *fshF* contained 1x Phusion HF Buffer, 400 µM dNTPs, 0.5 µM of each primer, 0.4 U Phusion polymerase (Thermo Scientific) and 0.5 µL of gDNA. The PCR conditions were as follows: initial denaturation at 98 °C for 30 seconds, followed by 40 cycles of denaturation at 98 °C for 10 s, annealing at 65 °C (*fsh*E), 61 °C (*fshM*) or 58 °C (*fsh*F) for 30 s, extension at 72 °C for 1 min (*fshE, fshM*) or 2 min (*fshF*), followed by final extension at 72 °C for 7 min. PCR products were gel purified, restricted with the corresponding enzymes SacI/ SalI (ThermoScientific) or XhoI/ NdeI (New England Biolabs) for 1 h at 37 °C followed by 65 °C inactivation for 20 min and gel purification. Digests were ligated into linearized and Quick CIP-treated (New England Biolabs) His$_6$-Tag-containing pET-29b (+) or pET-28a (+), using T4 DNA ligase (New England Biolabs), according to the manufacturer's instructions. An insert to vector ratio of 3:1 (*fshA*, *fshE, fshM*) or 9:1 (*fshF*) was used and the reaction mixtures were incubated overnight at 16 °C. Chemically competent *E. coli* TOP10 cells (Invitrogen) were transformed with 5 µL of the ligation reaction using the heat shock method. After recovery, the mixture was plated onto LB plates containing 50 µg mL^{-1} kanamycin. Colonies were screened by colony PCR using 1 µM primers for each gene (Table S4), 0.5 units of GoTaq Flexi DNA Polymerase (Promega), 1× Green GoTaq reaction buffer and 250 µM dNTPs (each). The PCR program was defined as: initial denaturation at 95 °C for 5 min; 35 cycles of denaturation at 95 °C for 45 s, primer annealing at 48 °C for 30 s and extension at 72 °C for 2 min; then final extension at 72 °C for 5 min. Positive colonies were inoculated in LB medium supplemented with 50 µg mL^{-1} kanamycin and used for plasmid DNA extraction with the NZYMiniprep kit (NZYtech). The purified plasmids were sequenced to verify construct identity and amplification fidelity. The four generated constructs were transformed into chemically competent *E. coli* OverExpress C43(DE3) (*fshA*-pET29) or BL21(DE3) (*fshE*-pET28, *fshM*-pET28 and *fshF*-pET28, pET29_'tesA and pET29_'tesAmCherry) using the heat shock method. Protein expression was optimized in small-scale studies with different temperatures and IPTG concentration – Table S5. For large-scale expression, glycerol stocks were used to inoculate 20 mL of LB medium supplemented with 50 µg mL^{-1} kanamycin and grown overnight at 37 °C. The overnight cultures were then used to inoculate 2 L of TB medium supplemented with 50 mg mL^{-1} kanamycin. The cultures were grown to an OD of 0.5 to 0.8, induced with the optimized concentration of IPTG (Table S5) and allowed to grow overnight or for 2 nights (FshA).

Cells were harvested by centrifugation (10 min, 4,000 *g*), transferred to 50 mL falcon tubes and flash frozen in liquid nitrogen. The thawed pellets were resuspended in approximately 20 mL of chilled lysis buffer (50 mM HEPES, 300 mM NaCl, 30 mM imidazole, 10 % glycerol, pH 8.0; for FshA purification additionally containing 1% triton X-100*) supplemented with Pierce Protease Inhibitor Tablets EDTA-free (ThermoScientific). The cell suspension was lysed in a cell disruptor (CF Range, Constant Sytems Ltd) by passing it twice through the high pressure chamber (20,000 psi). Lysates were centrifuged for 30 min at 19,500 *g*. A prepacked Protino Ni-IDA 1000 column was washed with 5 mL lysis buffer before the supernatant of the lysate was loaded onto it. The column was washed again with another 5 mL lysis buffer. The protein was eluted with 5 mL of elution buffer (20 mM HEPES, 300 mM NaCl, 200 mM imidazole, 10 % glycerol, pH 8.0; for FshA purification additionally containing 1% triton X-100*). For purification of 'tesA and 'tesAmCherry protein, frozen cell pellets were disrupted by sonication following standard protocols. Lysates were centrifuged for 60 min at 18,000 *g* and the cleared filtered lysate loaded onto a His-trap HP 1 mL column. Protein was isolated on an ÄKTA prime HPLC using a linear gradient from 25 mM to 500 mM imidazole over 20 column volumes. Eluate fractions were analyzed by SDS-PAGE and fractions containing target protein were concentrated in Pierce Protein Concentrator tubes, 10 K MWCO or 3 K MWCO (FshE, FshM) (5 mL, Thermo Scientific). For FshA and FshF, buffer exchange was performed by concentrating the eluate to ca. 250 µL (7,000 *g*), filling the filter up twice with dialysis buffer (20 mM HEPES, 50 mM NaCl, 10 % glycerol, pH 8.0; for FshA purification additionally containing 0.1% triton X-100) and concentrating again to 150-200 µL; in the case of FshE and FshM, the imidazole-containing buffer was exchanged by running the sample (concentrated to 2.5 ml) through a PD-10 desalting column (GE Healthcare) as per the manufacturer's instruction (gravity protocol, using the same dialysis buffer as above) before further concentration – Fig. S27, SDS-PAGE of all proteins. The protein concentration was measured with a spectrophotometer (DS-11 FX, DeNovix). The concentrated protein solution was frozen in liquid nitrogen in 10-100 µL aliquots and stored at –80 °C.

'tesA was amplified with primers containing restriction sites for *Nde*I and *Xho*I from plasmid pKS1 and cloned into pET29b. pKS1 was a gift from Jay Keasling (Addgene plasmid # 24636 ; http://n2t.net/addgene:24636 ; RRID:Addgene_24636). Due to degradation issues of purified recombinant 'tesA protein (see Fig. S31), the *'tesA* gene was excised from pET-29b_'tesA with *Xba*I and *Xho*I and cloned into a linearized previously generated pET-29b_mCherry plasmid via standard ligation to express a 'tesA-mCherry fusion protein, which was later used to hydrolyze fatty acids bound to FshE. Expression of 'tesA and 'tesAmCherry was done in LB auto-induction medium (NZY) at 24 °C in 0.5 L scale.

* Avoiding the use of detergent in FshA purification yielded mostly inactive protein which was not able to convert enough substrate to reach detection levels at least in the assays described here.

C-His_6-Sfp was used from a purification described previously.[SI-4]

FshA competition assay with FshE/ FshM ACP

Briefly, in a 25 µL reaction, 100 µM of apo-FshE (stock conc. 10 µg μL^{-1}) or apo-FshM (stock conc. 19 µg μL^{-1}) and 7 µL of the FshA purification (stock conc. 42 µg μL^{-1} total protein) were incubated with 10 µM Sfp, 1 mM coenzyme A, 5 mM $MgCl_2$, 2 mM ATP and 1 mM dodecanoic, tetradecanoic, hexadecanoic, *cis*-9-hexadecenoic, octadecanoic and *cis*-9,10-methylenehexadecanoic acid (only hexadecanoic acid for FshM) in 50 mM HEPES pH 8.0. Reactions were incubated overnight at 30 °C and digested with an equal volume of MS-grade trypsin (Pierce, 0.1 µg mL^{-1} in 0.1 M ammonium bicarbonate buffer, pH 7.4). After 4 h at 37°C, samples were quenched with 25 µL of 25 % formic acid. The reactions were centrifuged at 17,000 *g* for 10 min and analyzed by LC-HRESIMS/MS.

FshF activity assay

Briefly, in a 25 µL reaction, 100 µM of apo-FshE and 3.5 µL of the FshA purification (42 µg μL^{-1} total protein) were incubated with 10 µM C-His_6-Sfp, 1 mM coenzyme A, 5 mM $MgCl_2$, 2 mM ATP, 10 µM FshF, 1 mM unlabeled or d_3-labeled S-adenosyl methionine (SAM) and 1 mM *cis*-9-hexadecenoic acid in 50 mM HEPES pH 8.0. Reactions were incubated overnight at room temperature and digested with an equal volume of MS-grade trypsin (Pierce, 0.1 µg mL^{-1} in 0.1 M ammonium bicarbonate buffer, pH 7.4). After 4 h at 37°C, samples were quenched with 25 µL of 25% formic acid. The reactions were centrifuged at 17,000 *g* for 10 min and analyzed by LC-HRESIMS/MS.

FshF activity assay for free fatty acid analysis

Approximately 100 µM apo-FshE, 25 µM FshA, 25 µM FshF, 10 µM Sfp, 1 mM coenzyme A, 5 mM $MgCl_2$, 2 mM ATP, 1 mM SAM and 1 mM palmitoleic acid (16:1n-7) or iso-palmitoleic acid (16:1n-8) were combined in 50 mM HEPES pH 8.0. Reactions were incubated for 12-20h at 25°C followed by addition of 25 µM 'tesA-mCherry. The reactions were incubated at 25°C for another 12-24h, then an equal volume of MS-grade MeOH was added to each reaction. After freeze-thawing, each reaction was

centrifuged at 17,000 *g* for 45 min and analyzed by LC-HRESIMS for detection of substrate and product free fatty acid target masses.

Methyl ester synthesis of FshF-modified fatty acids for FAMEs analysis

The free fatty acids released from the FshF activity assay via 'tesA-mCherry (see above) were converted to their corresponding fatty acid methyl ester (FAME) derivatives using a standard acid-catalyzed esterification procedure.[SI-5] The dried enzymatic reaction products from FshF-catalyzed methylenation of (*Z*)-8-hexadecenoic acid (**FA-5**, ~100 µg) were dissolved in MeOH (1.0 mL). *p*-Toluenesulfonic acid (2.0 mg) and anhydrous Na_2SO_4 (50 mg) were then added, and the mixture was heated at 60 °C overnight. TLC analysis confirmed consumption of the fatty acid and formation of the corresponding methyl ester. After cooling, the reaction mixture was filtered and diluted with EtOAc (3 mL) and 2.0 M aqueous $NaHCO_3$ (3 mL). The organic layer was separated, dried (Na_2SO_4), filtered, and concentrated under reduced pressure to afford the corresponding FAME, which was analyzed by GC–MS.

The methyl ester synthetic standards **FAME-6** and **FAME-7** had already been accessed as synthetic intermediates during the synthesis of fatty acid synthetic standards **FA-5**, **FA-6** and **FA-7**. For details, see 'Synthetic procedures and compound characterization' section.

Supplemental Texts, Figures and Tables

Text S1. Structure elucidation of **1**.

The structural elucidation of **1** as major compound isolated was deduced through a combined analysis of its MS (Fig. S1) and NMR in DMSO-d_6 (Table S1, Fig. S2-S8) data. The characteristic isotopic pattern displayed by the $[M+H]^+$ ion at *m/z* 515/517/519/521 in a ratio of 8/10/5/1 in the (+)-HRESIMS of **1**, indicating the presence of four chlorine atoms, along with the monoisotopic $[M+H]^+$ ion at *m/z* 515.0852 (calcd. for $C_{21}H_{30}O_2N_2Cl_4S$ *m/z* 515.0855), allowed us to determine its molecular formula.

The ^{1}H NMR spectrum of **1** showed several conspicuous resonances, namely two protons above 8.0 ppm (one quartet at δ_H 8.28 and one singlet at δ_H 8.14), four olefinic protons (δ_H 6.2-5.0), two methine triplets of triplets (δ_H 4.45 and 4.16), a sharp singlet resonating at δ_H 4.27, and a doublet corresponding to a methyl group (δ_H 2.77). Other overlapped resonances of several aliphatic methylene were also observed.

^{13}C NMR (APT) data revealed two sp^2 non-protonated carbon signals above 160 ppm (δ_C 166.5 and 160.9), six aromatic/olefinic carbons (δ_C 150-110, four of which protonated), one non-protonated oxygenated carbon (δ_C 73.7), two methine carbons (δ_C 62.5 and 61.9), several methylenes (δ_C 41-20), and one methyl carbon (δ_C 25.8).

Analysis of the combined 1D and 2D NMR data for **1**, mainly obtained from COSY, HSQC and HSQC-TOCSY experiments, displayed five spin systems, namely a terminal vinyl moiety, an isolated aromatic proton, a NHMe group, and two chlorinated aliphatic chains (Fig. 1C) that were connected through a HMBC experiment.

The three terminal vinylic protons (H-16, δ_H 5.75; H-17a, δ_H 5.13 and H-17b, δ_H 5.00) showed HMBC-cross signals to the non-protonated carbon at δ_C 73.7 (C-8), which in turn displayed a HMBC correlation to an exchangeable hydroxy proton that resonated as a singlet at δ_H 4.27. Hence, this moiety was consistent with an allylic alcohol group.

The non protonated carbon resonances at δ_C 149.6 (C-19) and δ_C 166.5 (C-1) along with the methine carbon at δ_C 123.6 (C-18), connected through a HSQC experiment to the isolated aromatic singlet signal at δ_H 8.14 (H-18), were characteristic of a disubstituted thiazole,[SI-6] which was consistent with the presence of the N and S heteroatoms in the molecular formula of **1**.

The strong HMBC correlations between the NH proton at δ_H 8.28 to the carbon C-19 at δ_C 149.6 and between the *N*-methyl protons at δ_H 2.77 (Me-21) and the carbonyl carbon at δ_C 160.9 (C-20), allowed us to connect the NHMe spin system to the C-19 of the thiazole ring through the C-20 carbonyl group.

One of the four chlorine atoms was located at C-3 in the first aliphatic chain from the key HMBC correlations between H-3 at δ_H 4.45 and methylene carbons C-4 (δ_C 37.3) and C-2 (δ_C 41.2) and the thiazolinic carbon C-1 (δ_C 166.5). The multiplicity of the methine proton H-3 as a triplet of triplet, indicating that is surrounding by two methylene groups, confirmed this assignment. Key HMBC correlations between H-6 and H-7 protons to the non-protonated carbon C-8 at δ_C 73.7, connected this chlorinated aliphatic chain to the allylic alcohol moiety in the other end.

The remaining three chlorine atoms were placed in the second aliphatic chain spin system. Firstly, the presence of a *gem*-dichlorovinylidene moiety was deduced by the characteristic non protonated carbon at δ_C 120.1 (C-15) and the methine carbon at δ_C 127.4 (C-14) which is in turn connected to the olefinic proton at δ_H 6.18 through a HSQC experiment. The HMBC correlation between the H-14 and C-15 confirmed the presence of this group. The fourth Cl atom was located at C-12 from the key HMBC correlations from H-12 at δ_H 4.16 to the methylene carbons C-11 (δ_C 37.8) and C-13 (δ_C 38.1) and to the methine carbon C-14 (δ_C 127.4) of the *gem*-dichlorovinylidene moiety. As for H-3, the triplet of triplet multiplicity of the H-12 proton signal is agreement with this assignment. Finally, the second trichlorinated aliphatic chain was linked to the allylic alcohol group by the HMBC correlations between H-9 and H-10 protons to the non-protonated carbon C-8. (+)-HRESIMS/MS analysis supported the NMR-based structure elucidation, although the spectra interpretation was not straightforward due to HCl losses dominating low-energy fragmentations (Fig. S9). In this way, the planar structure of **1**, named as fischerazole A, was established as shown in Figure 1.

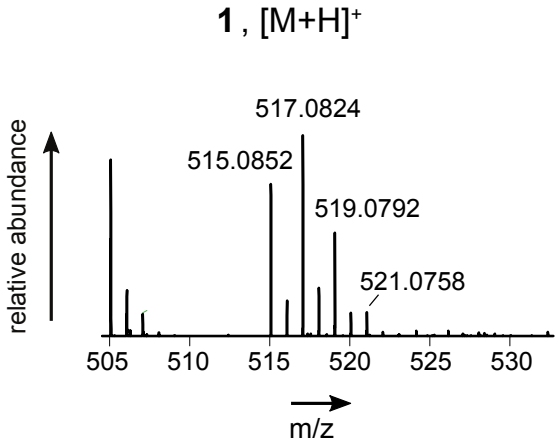

Figure S1. HRESIMS spectrum of compound **1** ([M+H]$^+$ isotope cluster).

Table S1 - NMR Spectroscopic Data (^{1}H 600 MHz, ^{13}C 150 MHz, DMSO-d_6) for fischerazole A (**1**).

Position	δ_C	Type	δ_H[a]	mult., *J* (Hz)	HMBC[b]	COSY
1	166.5	C=N	-	-	-	-
2a	41.2	CH_2	3.53	dd, 15.4, 4.4	1, 3, 4, 18, 19	2b, 3
2b			3.38	dd, 15.4, 8.8	1, 3, 4	2a, 3
3	62.5	CH	4.45	tt, 8.7, 4.3	1, 2, 4, 5	2a, 2b, 4a, 4b
4a	37.3	CH_2	1.84	m	2, 3, 5, 6	3, 4b, 5a, 5b
4b			1.71	m	2, 3, 5, 6	3, 4a, 5a, 5b
5a	26.3	CH_2	1.46	m	3, 4, 6, 7	4a, 4b, 5b, 6b
5b			1.39	m	3, 4, 6, 7	4a, 4b, 5a, 6b
6a	22.6	CH_2	1.33	m	5, 7, 8	6b
6b			1.20	m	5, 7, 8	5a, 5b, 6a, 7
7	40.4	CH_2	1.40	m	4, 5, 6, 8, 9, 16	6b
8	73.7	C	-	-	-	-
		OH	4.27	s	8, 9, 16	-
9	39.8[c]	CH_2	1.40	m	8, 10, 16	-
10a	20.2	CH_2	1.42	m	11, 12	10b, 11a, 11b
10b			1.37	m	11, 12	10a, 11a, 11b
11a	37.8	CH_2	1.71	m	9, 10, 13	10a, 10b, 11b, 14
11b			1.62	m	9, 10, 12, 13	10a, 10b, 11a, 14
12	61.9	CH	4.16	tt, 8.8, 4.5	10, 11, 14	11a, 11b, 13a, 13b
13a	38.1	CH_2	2.64	ddd, 15.3, 6.6, 4.6	11, 12, 14, 15	12, 13b, 14
13b			2.55	ddd, 15.4, 7.8, 7.8	11, 12, 14, 15	12, 13a, 14
14	127.4	CH	6.18	dd, 7.7, 6.6	12, 13, 15	13a, 13b
15	120.1	C	-	-	-	-
16	144.6	CH	5.75	dd, 17.3, 10.7	7, 8, 9	17a, 17b
17a	112.0	CH_2	5.13	dd, 17.3, 2.2	7, 8, 9	16, 17b
17b			5.00	dd, 10.7, 2.2	7, 8, 9	16, 17a
18	123.6	CH	8.14		1, 19, 20	-
19	149.6	C	-	-	-	-
20	160.9	C=O	-	-	-	-
		NH	8.28	q, 4.8	18, 19, 20, 12	21
21	25.8	CH_3	2.77	d, 4.8	19, 20	20-NH

[a]from HSQC; [b]from proton to indicated carbon; [c]extracted from HMBC.

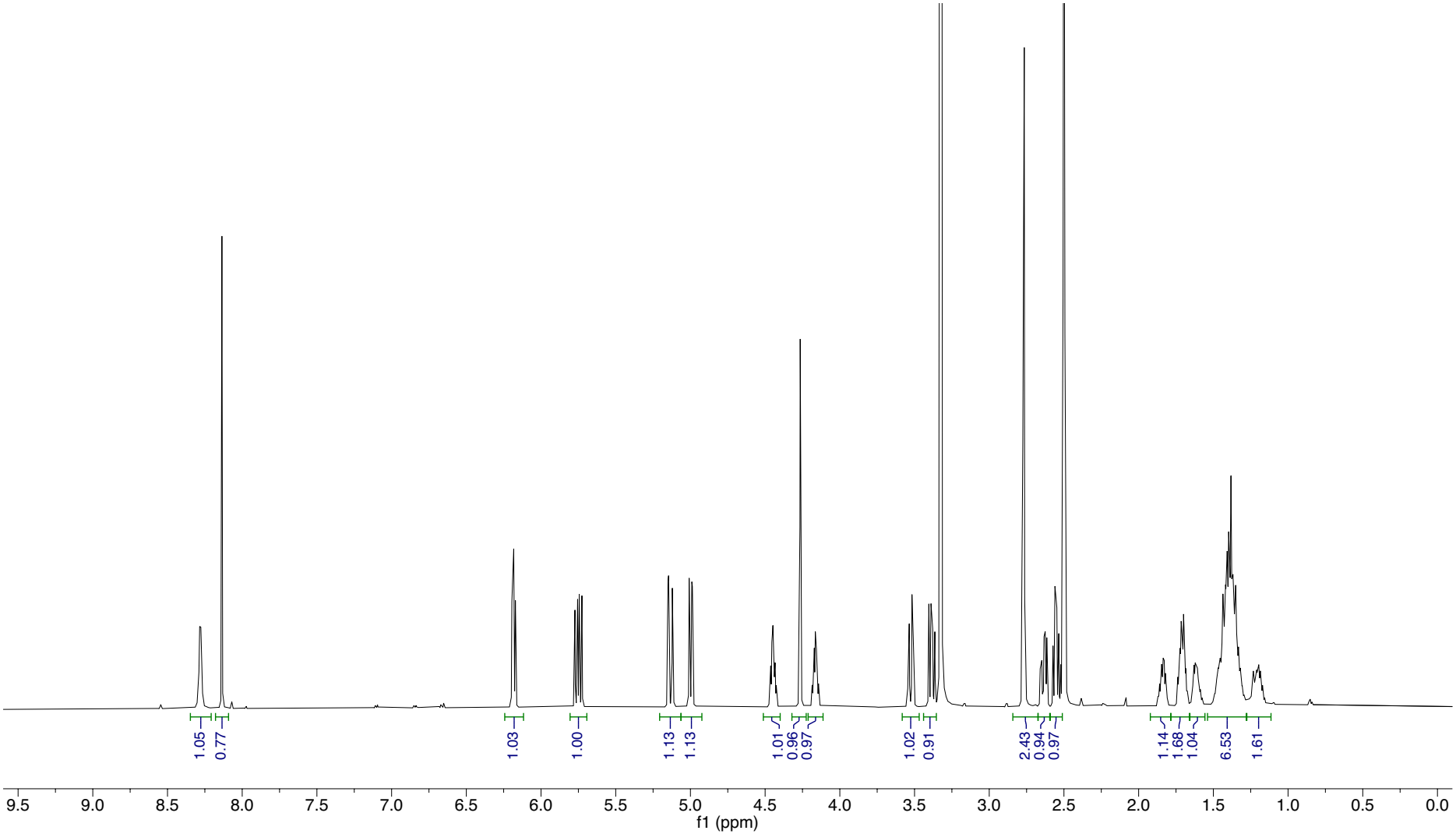

Figure S2. ^{1}H NMR (DMSO-d_6, 600 MHz) spectrum of compound **1**.

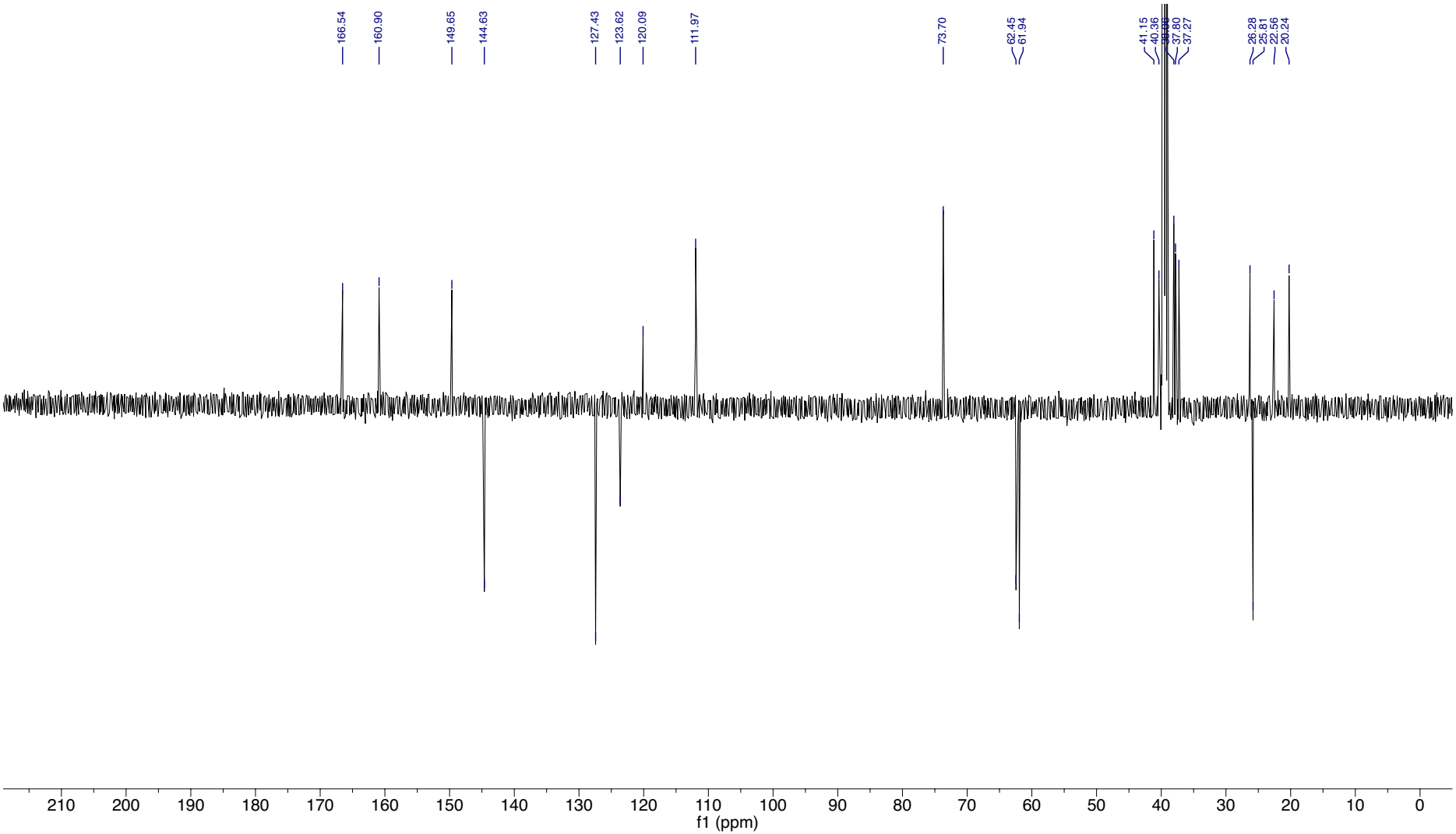

Figure S3. ^{13}C NMR (APT, DMSO-d_6, 150 MHz) spectrum of compound **1**.

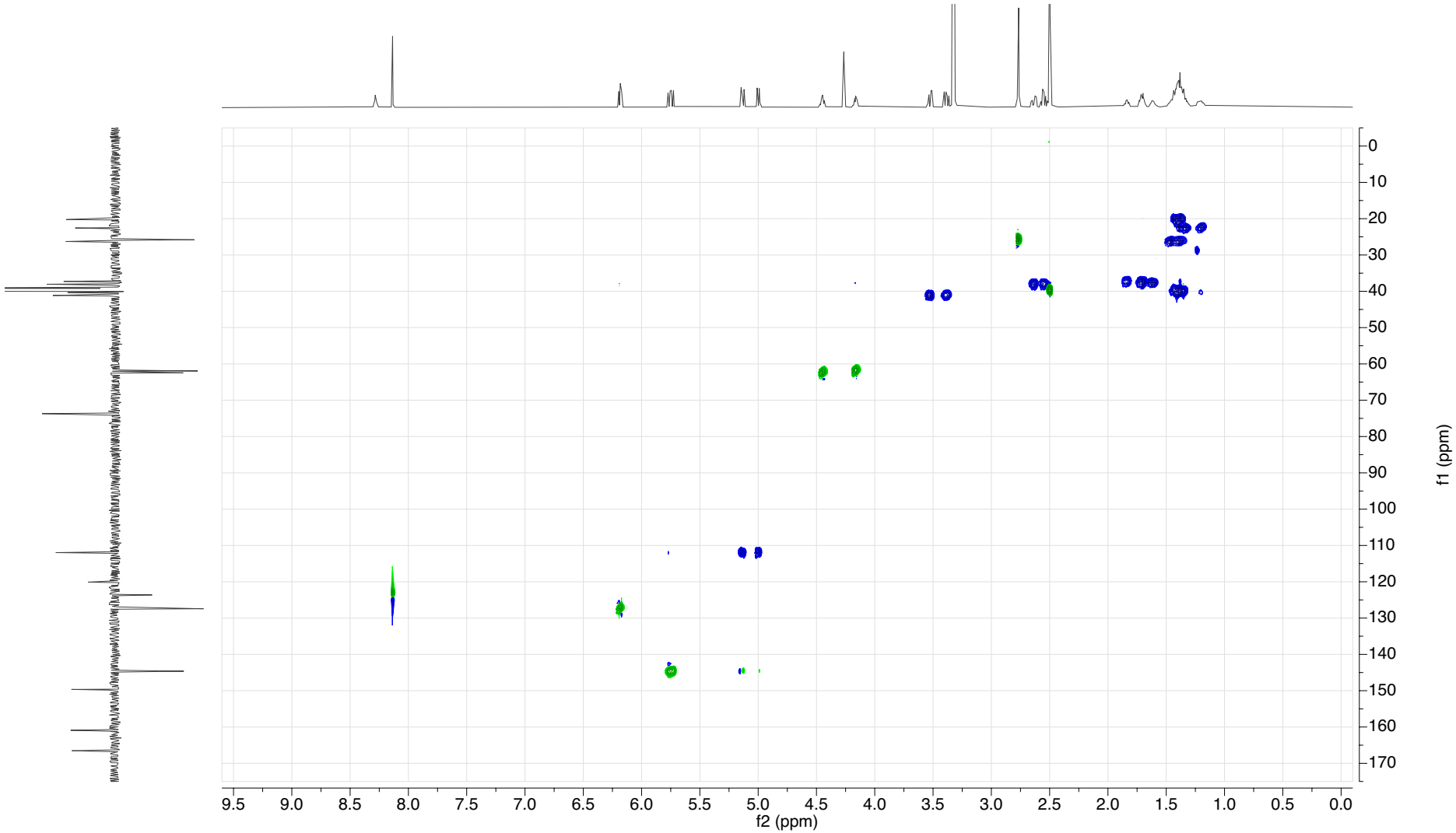

Figure S4. HSQC (DMSO-d_6, 600 MHz) spectrum of compound **1**.

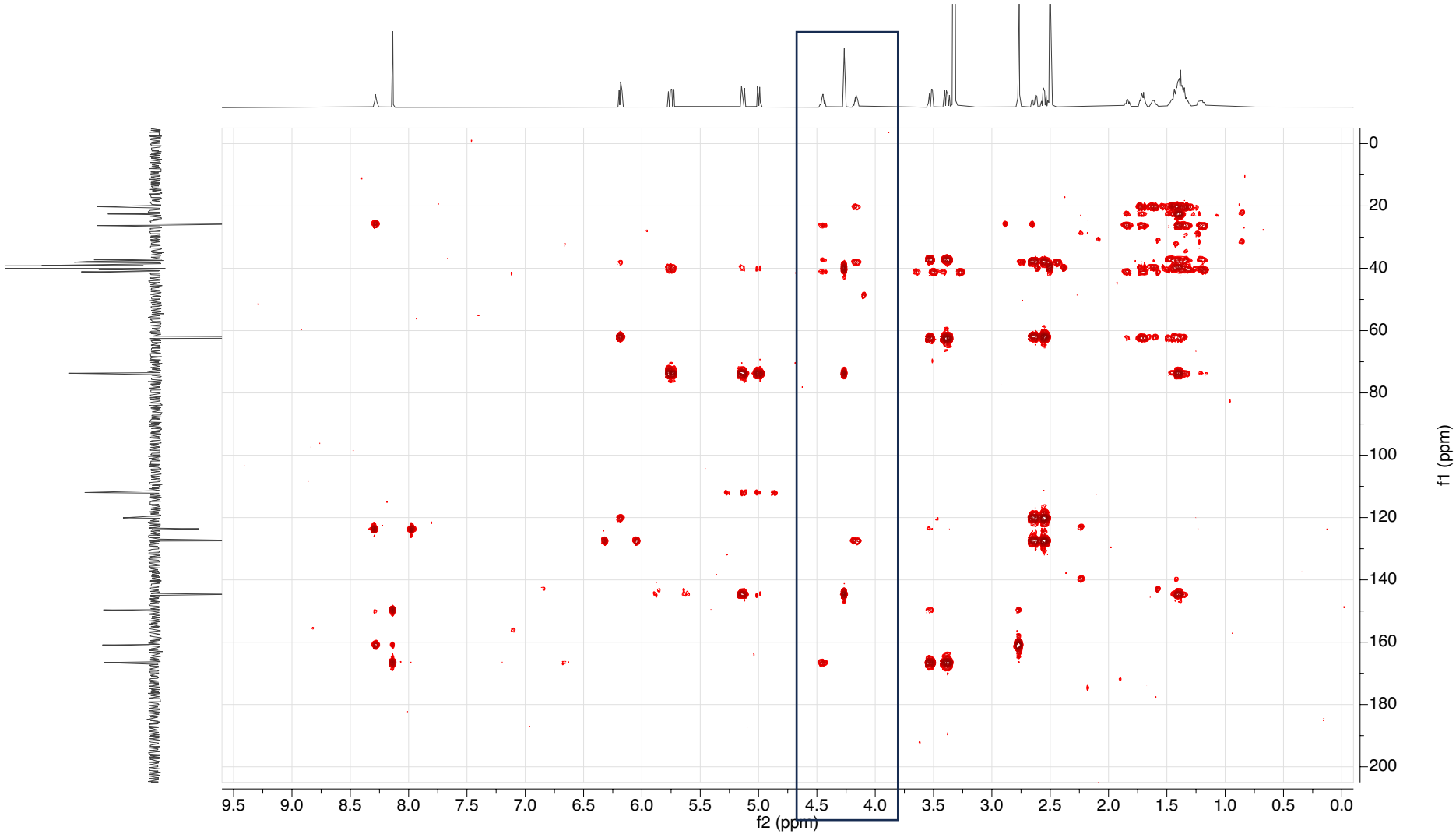

Figure S5. HMBC (DMSO-d_6, 600 MHz) spectrum of compound **1**. The box highlights the region where correlations of H-3 and H-12 can be observed.

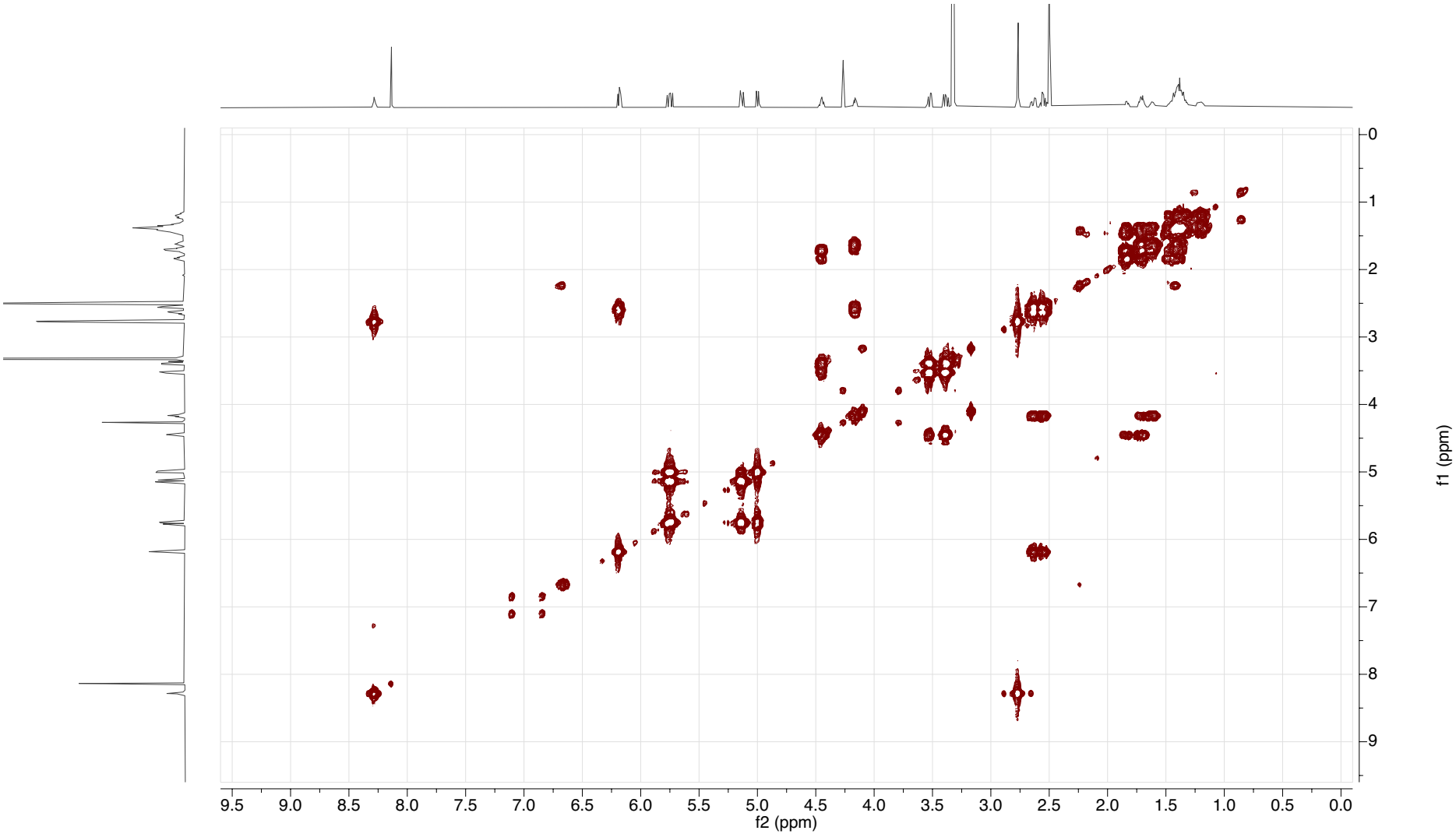

Figure S6. COSY (DMSO-d_6, 600 MHz) spectrum of compound **1**.

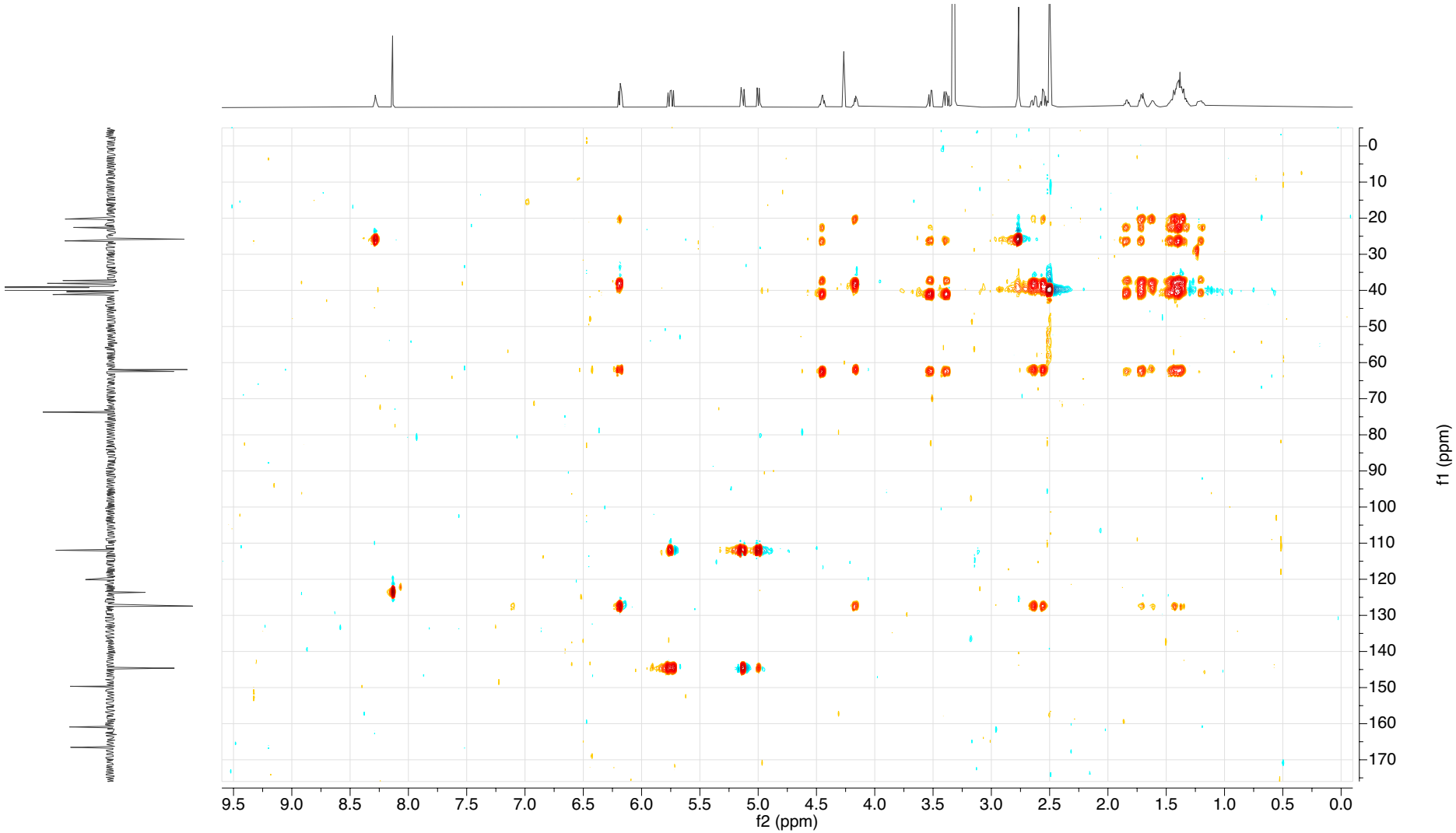

Figure S7. HSQC-TOCSY (DMSO-d_6, 600 MHz) spectrum of compound **1**.

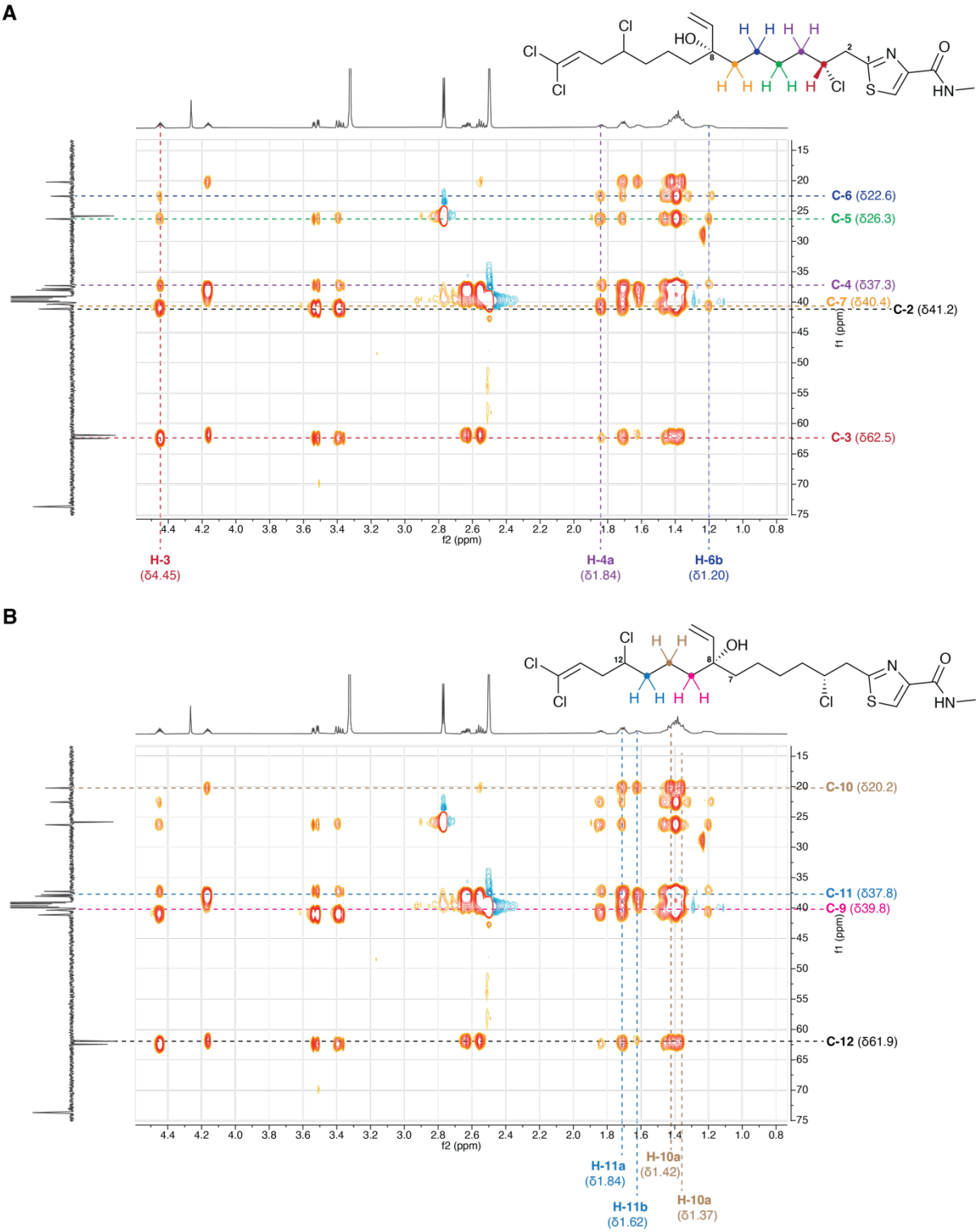

Figure S8. HSQC-TOCSY (DMSO-d_6, 600 MHz) data for **1** enabled to unambiguously assign the resonances for the aliphatic methylene positions and extend the COSY-derived spin systems. A – Correlations establishing the progression from CH-3 to CH_2-7; B – correlations establishing the progression from CH_2-9 to CH-12

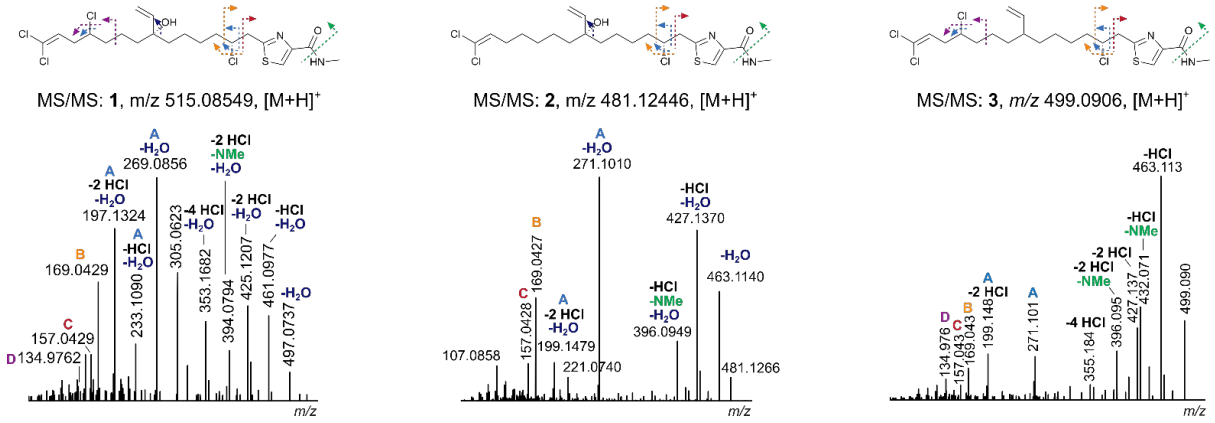

Figure S9. Annotated (+)-HRESISMS/MS spectra (HCD 25.0) of fischerazoles A-C (**1**-**3**, $[M+H]^+$).

Text S2. Structure elucidation of **2** and **3**.

The NMR-based structure elucidation of **2** and **3** used the proposed structure for **1** as reference. Compound **2** showed a monoisotopic $[M+H]^+$ ion of *m/z* 481.1242 (calcd. 481.1245, Fig. S10). This corresponded to a molecular formula of $C_{21}H_{31}O_2N_2Cl_3S$ and therefore **2** differs from **1** by one less Cl atom and one more proton. This was confirmed by the characteristic isotopic cluster for a compound with three chlorine atoms displayed by the $[M+H]^+$ ion at *m/z* 481/483/485 in a 10/9/3 ratio. Comparison of the ^1H and ^{13}C NMR data for **2** (Figs. S11-12) to those of **1** allowed us to unambiguously determine that the difference lied at position 12. The NMR spectra of **2** display the lack of the resonances for the CH-12 at δ_C 61.9/δ_H 4.16 present in those of **1**, showing instead a larger methylene envelope. Additionally, the identical carbon and proton chemical shift values of the spin system containing CH-3 (C-2 to C-7) for both compounds (see NMR data for both compounds and Figs. S13-S14) is in agreement with the assignment. Compound **3** showed a characteristic $[M+H]^+$ ion isotopic cluster in its (+)-HRESIMS spectrum, indicating the presence of four chlorine atoms. The complete formula of **3** as $C_{21}H_{30}ON_2Cl_4S$ was established from the monoisotopic $[M+H]^+$ ion peak at *m/z* 499.0908 (calcd. 499.0906, Fig. S15). Therefore, the composition of **1** and **3** differed by a single O atom. We considered that in **3**, the hydroxyl group (OH-8) was not present. We acquired 1D and 2D NMR data for this compound in DMSO-d_6 (Table S2, Figs. S16-S20). Analysis of the combined NMR data indicated that the difference was in fact in position 8. The non-protonated C-8 and the exchangeable hydroxyl proton in **1** are not found in the NMR data for **3**, which instead features an additional methine (CH-8, δ_C 43.2, δ_H 1.94). ^1H and ^{13}C NMR resonances in the vicinity of this moiety are also shifted in **3**, relative to those in **1** (Tables S1-S2). The NMR-derived structures for **2** and **3** were consistent with the respective (+)-HRESIMS/MS data (Fig. S9).

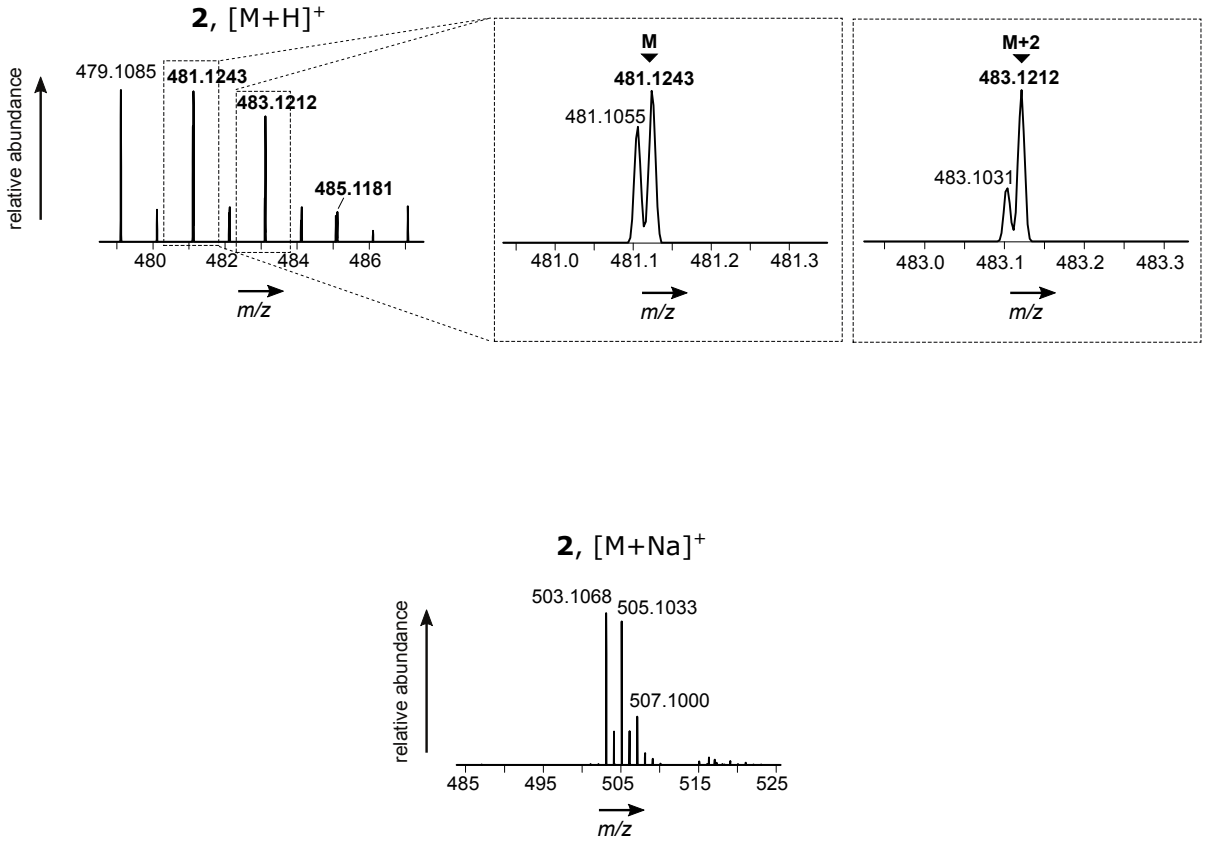

Figure S10. HRESIMS spectrum of purified compound **2** (shown are the $[M+H]^+$ isotope cluster and blow-outs allowing for distinguishing it from another isotope cluster with monoisotopic peak at *m/z* 479.1085 as well as the $[M+Na]^+$ isotope cluster).

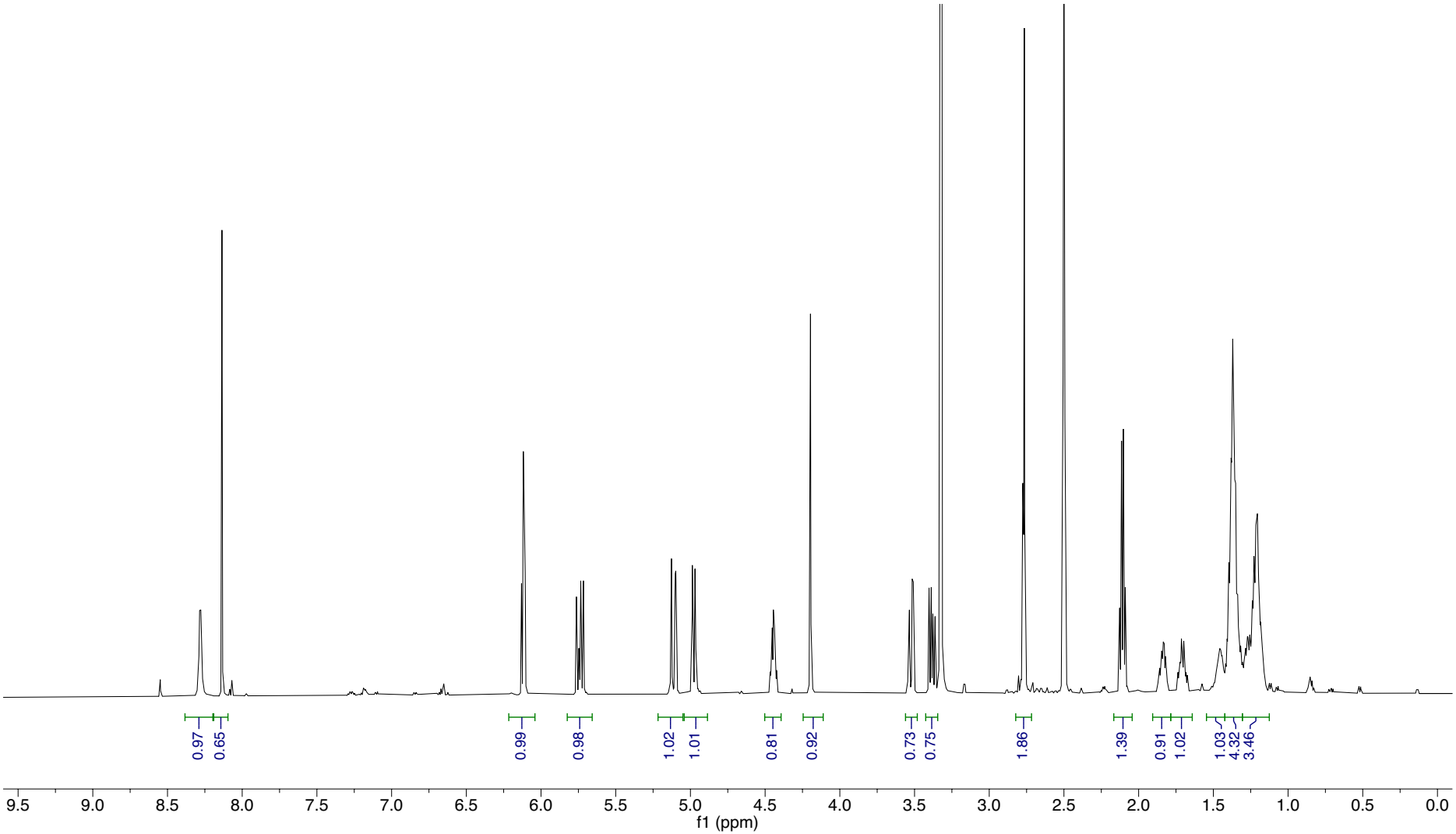

Figure S11. ^{1}H NMR (DMSO-d_6, 600 MHz) spectrum of compound **2**.

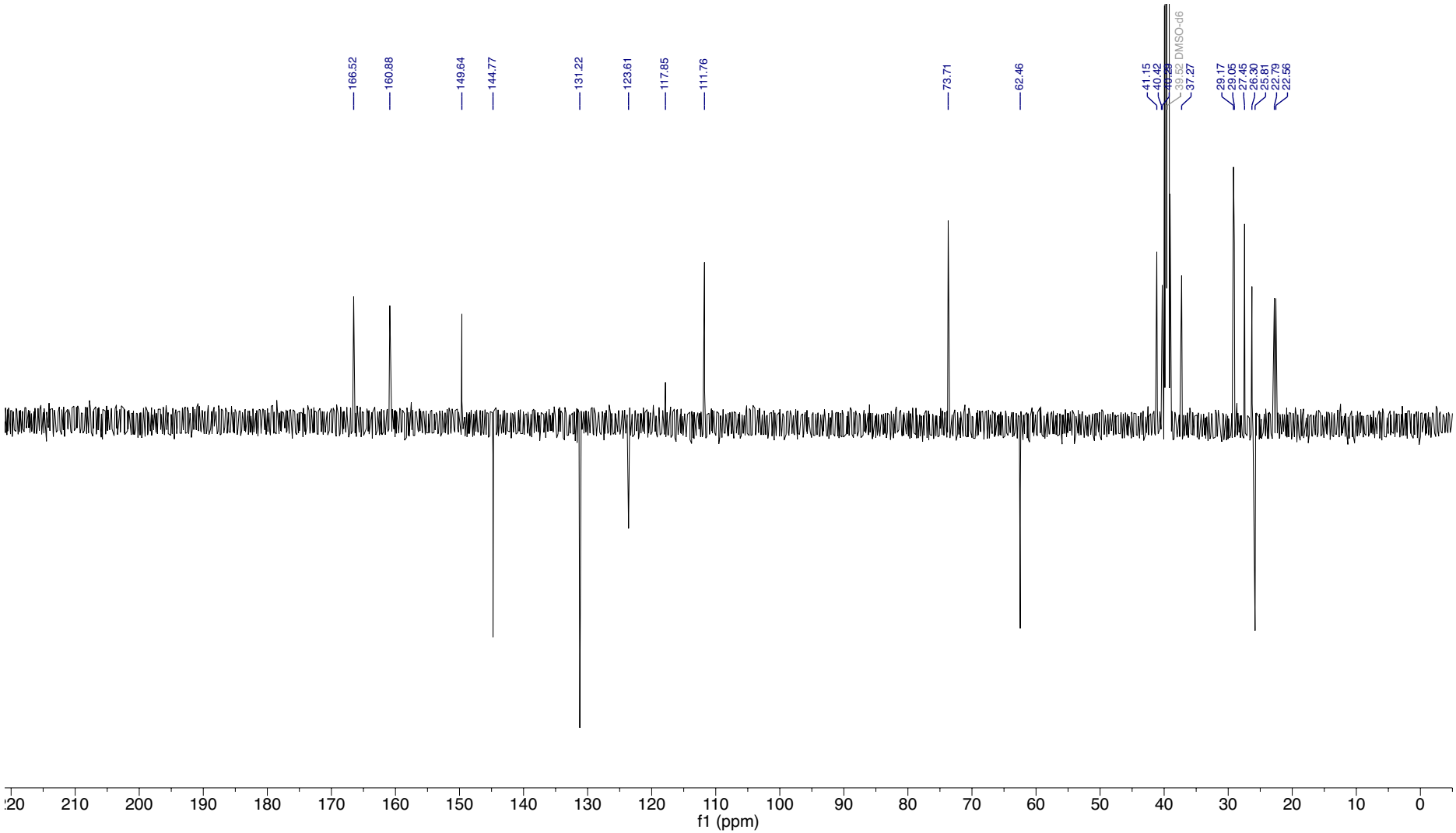

Figure S12. ^{13}C NMR (APT, DMSO-d_6, 150 MHz) spectrum of compound **2**.

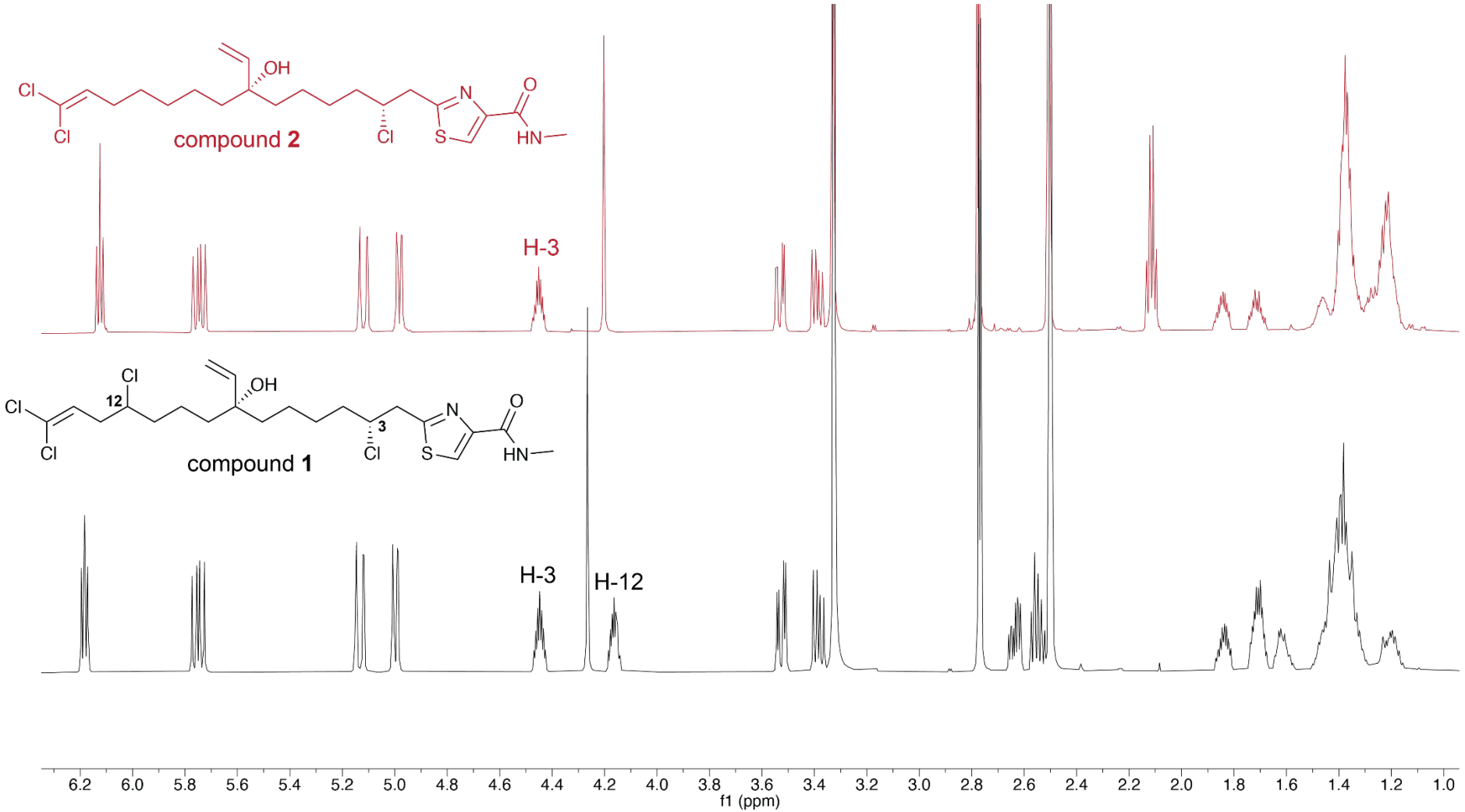

Figure S13. Comparison of the ^{1}H NMR spectra for **1** and **2**, highlighting the absent H-12 chlorinated methine protons in **2**.

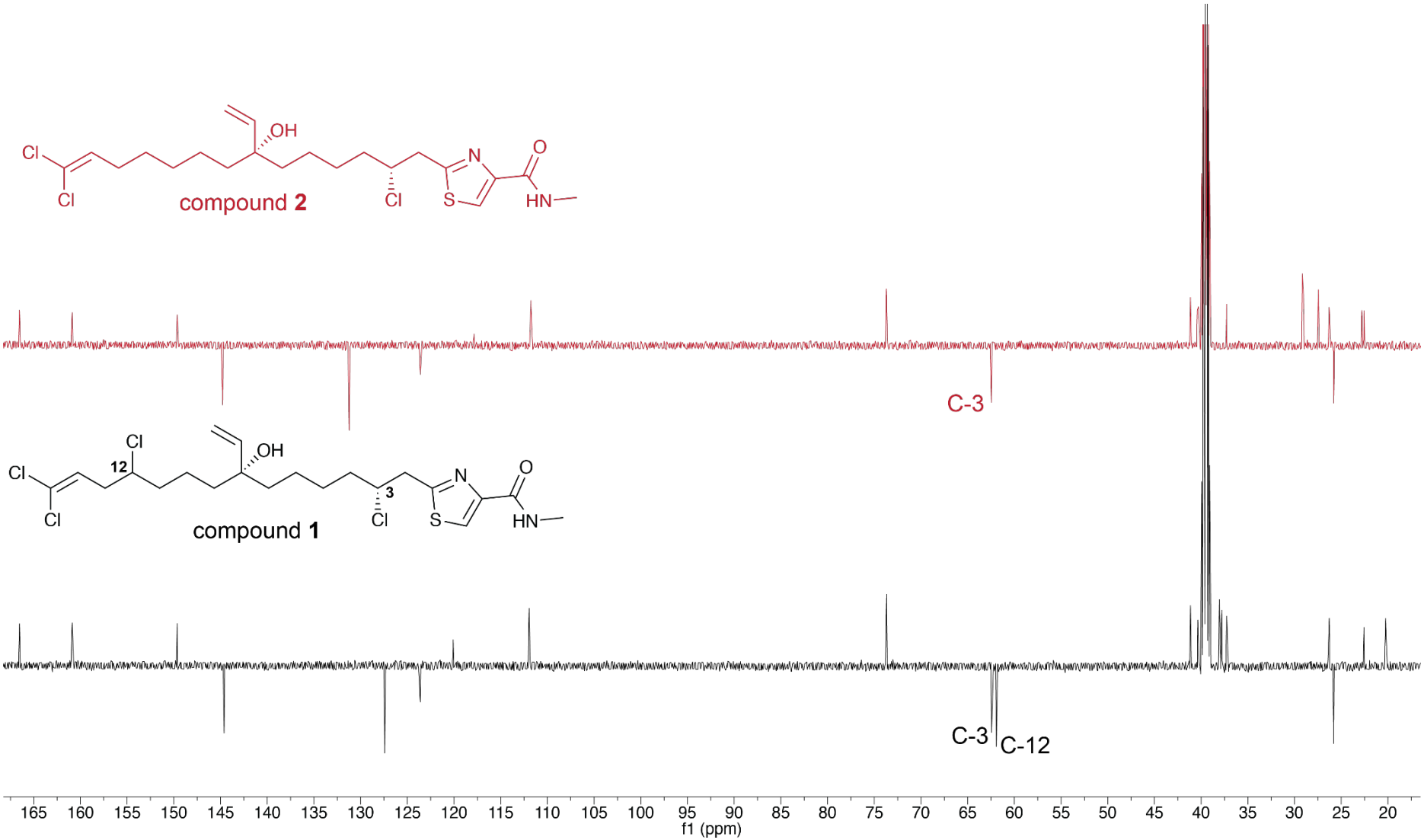

Figure S14. Comparison of the ^{13}C NMR spectra for **1** and **2**, highlighting the absent C-12 chlorinated methine carbon in **2**.

Table S2 – NMR Spectroscopic Data (^{1}H 600 MHz, ^{13}C 150 MHz, DMSO-d_6) for fischerazole C (**3**).

Position	δ_C	Type	δ_H[a]	mult., *J* (Hz)	HMB*C*[b]	COSY
1	166.5	C=N	-	-	-	-
2a	41.2	CH_2	3.53	dd, *J* = 15.4, 4.4	1, 3, 4, 19	2b, 3
2b			3.39	dd, *J* = 15.4, 8.8	1, 3, 4	2a, 3
3	62.4	CH	4.45	m	1, 2, 4, 5	2a, 2b, 4a, 4b
4a	37.3	CH_2	1.83	m	2, 5	3, 4b, 5a
4b			1.71	m	2, 5	3, 4a, 5a, 5b
5	25.7	CH_2	1.45	m	4, 6, 7, 8	4a, 4b, 5b, 6
			1.26	m	4, 6, 7, 8	4b, 5a, 6
6	25.9	CH_2	1.25	m	5, 7, 8	5a, 5b
7a	33.7	CH_2	1.34	m	6, 8	7b, 8
7b			1.22	m	6, 8	7a, 8
8	43.2	CH	1.94	ddt, *J* = 17.8, 8.9, 4.7	6, 7, 16, 17	7a, 7b, 9a, 9b, 16
9a	34.1	CH_2	1.35	m	7, 8, 10, 11	8, 9b
9b			1.19	m	7, 8, 10, 11	8, 9a
10a	23.6	CH_2	1.46	m	8, 11, 12	10b, 11a, 11b
10b			1.27	m	8, 12	10a, 11a
11a	37.8	CH_2	1.74	m	9, 10, 12, 13	10a, 10b, 12
11b			1.61	m	9, 10, 12, 13	10a, 12
12	61.9	CH	4.17	m	10, 11, 14	11a, 11b, 13a, 13b
13a	38.0	CH_2	2.64	ddd, *J* = 15.4, 6.6, 4.7	11, 12, 14, 15	12, 13b, 14
13b			2.55	ddd, *J* = 15.4, 7.8, 7.8	11, 12, 14, 15	12, 13a, 14
14	127.4	CH	6.19	dd, *J* = 7.7, 6.8 Hz	12, 15	13a, 13b
15	120.1	C	-	-	-	-
16	142.9	CH	5.53	ddd, *J* = 17.0, 10.4, 8.9	7, 8	8, 17a, 17b
17a	114.7	CH_2	4.99	dd, J = 4.6, 2.0	8, 16	16, 17b
17b			4.96	dd, *J* = 11.2, 2.0	8, 16	16, 17a
18	123.6	CH	8.14	s	1, 19	-
19	149.6	C=C	-	-	-	-
20	160.9	C=O	-	-	-	-
		NH	8.28	q, *J* = 4.8	18, 20, 21	21
21	25.8	CH_3	2.77	d, *J* = 4.8	19, 20	20-NH

[a]from HSQC; [b]from proton to indicated carbon.

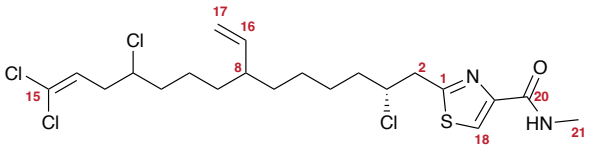

3

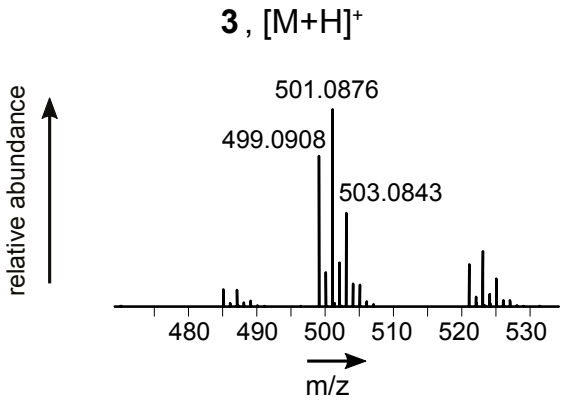

Figure S15. HRESIMS spectrum of compound **3** ($[M+H]^+$ isotope cluster).

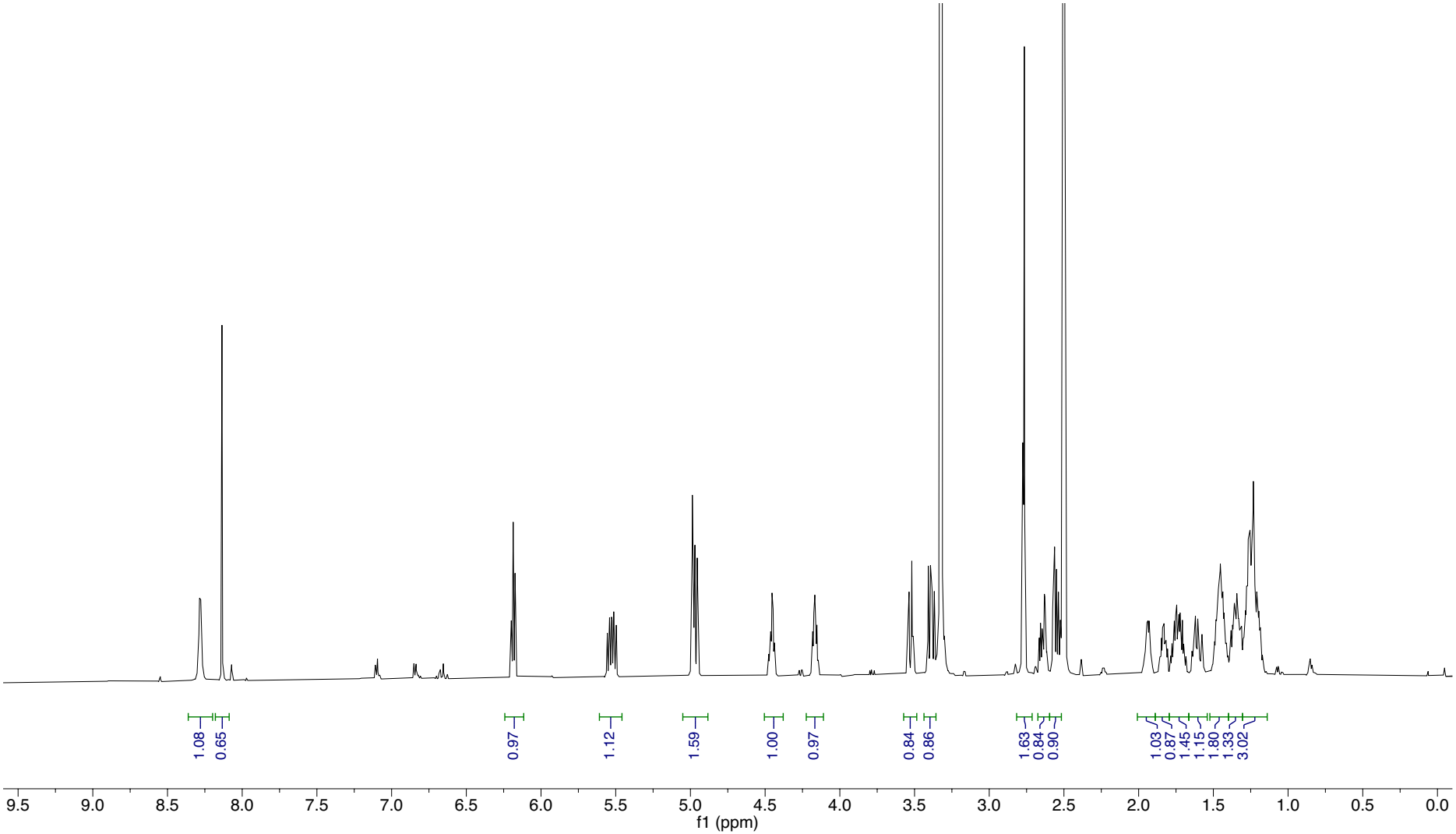

Figure S16. ^{1}H NMR (DMSO-d_6, 150 MHz) spectrum of compound **3**.

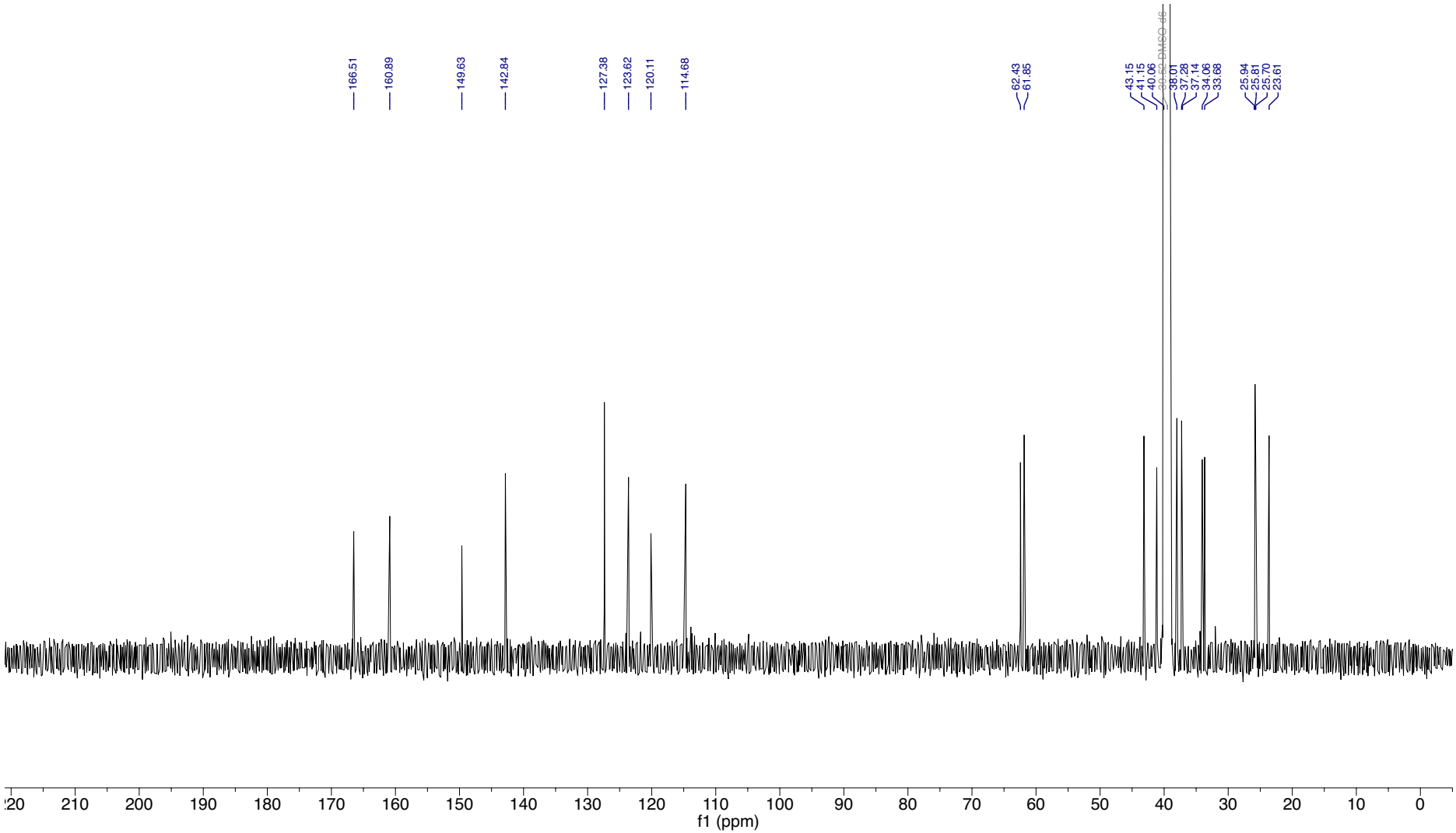

Figure S17. ^{13}C NMR (DMSO-d_6, 150 MHz) spectrum of compound **3**.

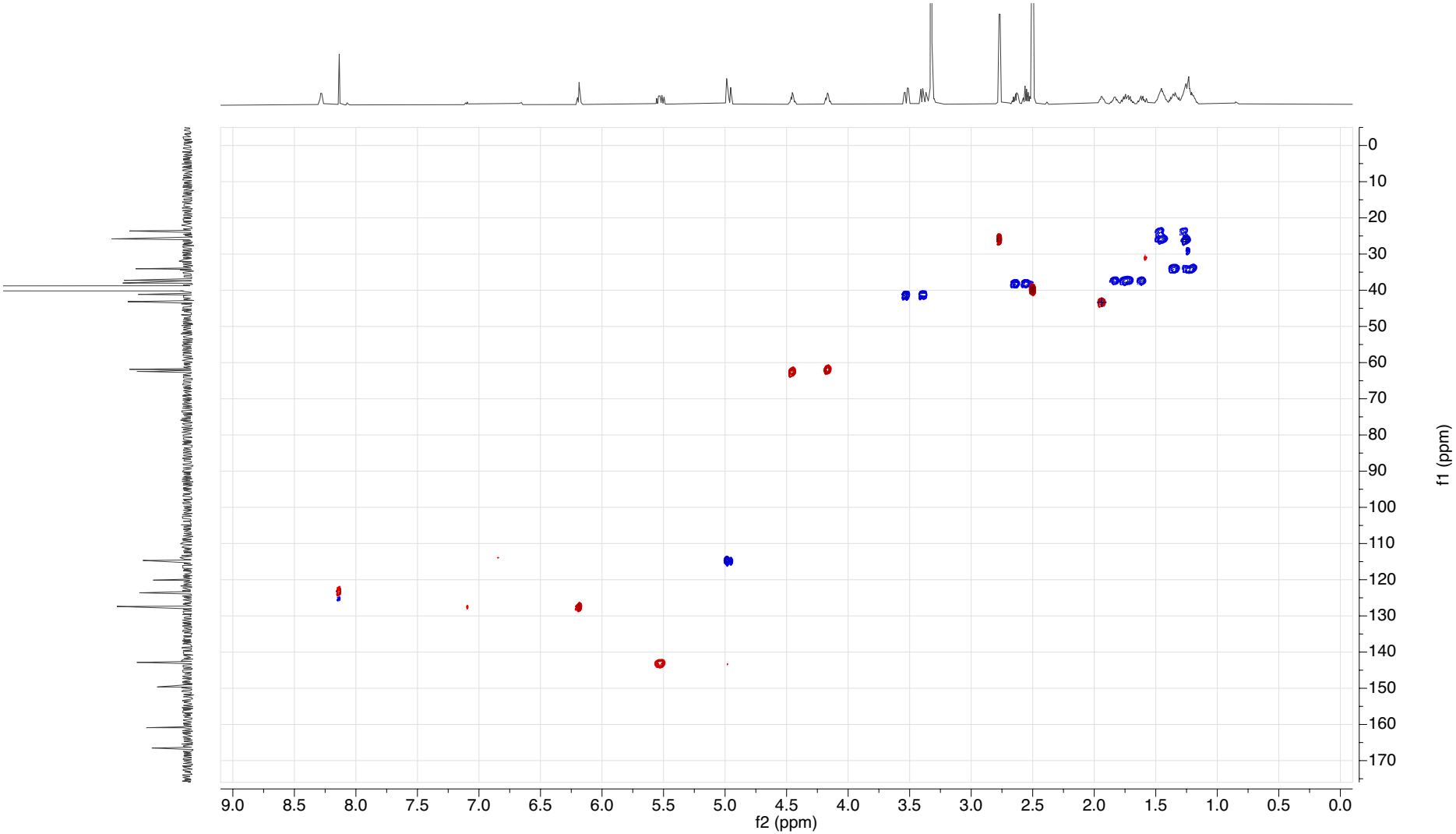

Figure S18. HSQC (DMSO-d_6, 600 MHz) spectrum of compound **3**.

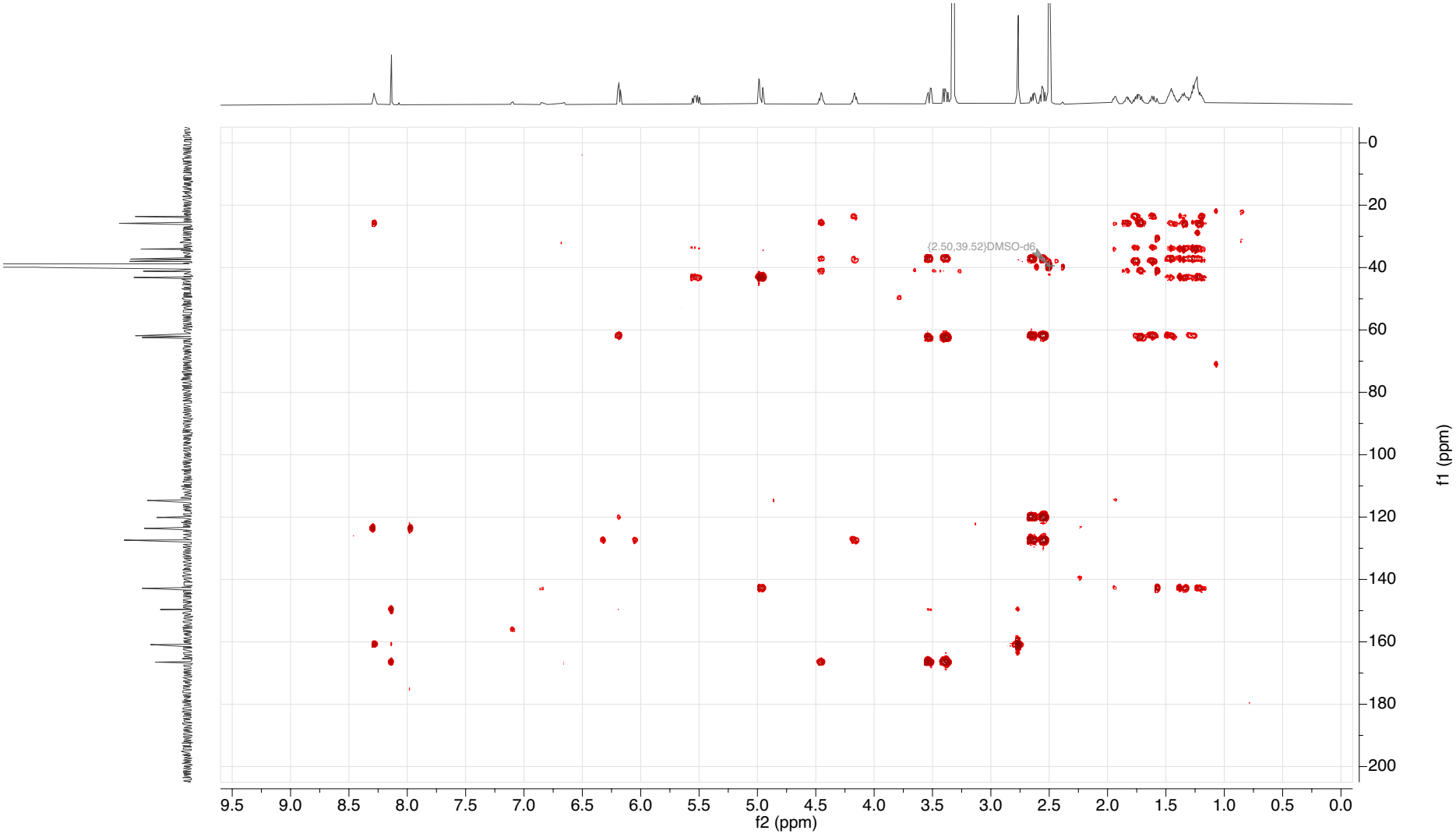

Figure S19. HMBC (DMSO-d_6, 600 MHz) spectrum of compound **3**.

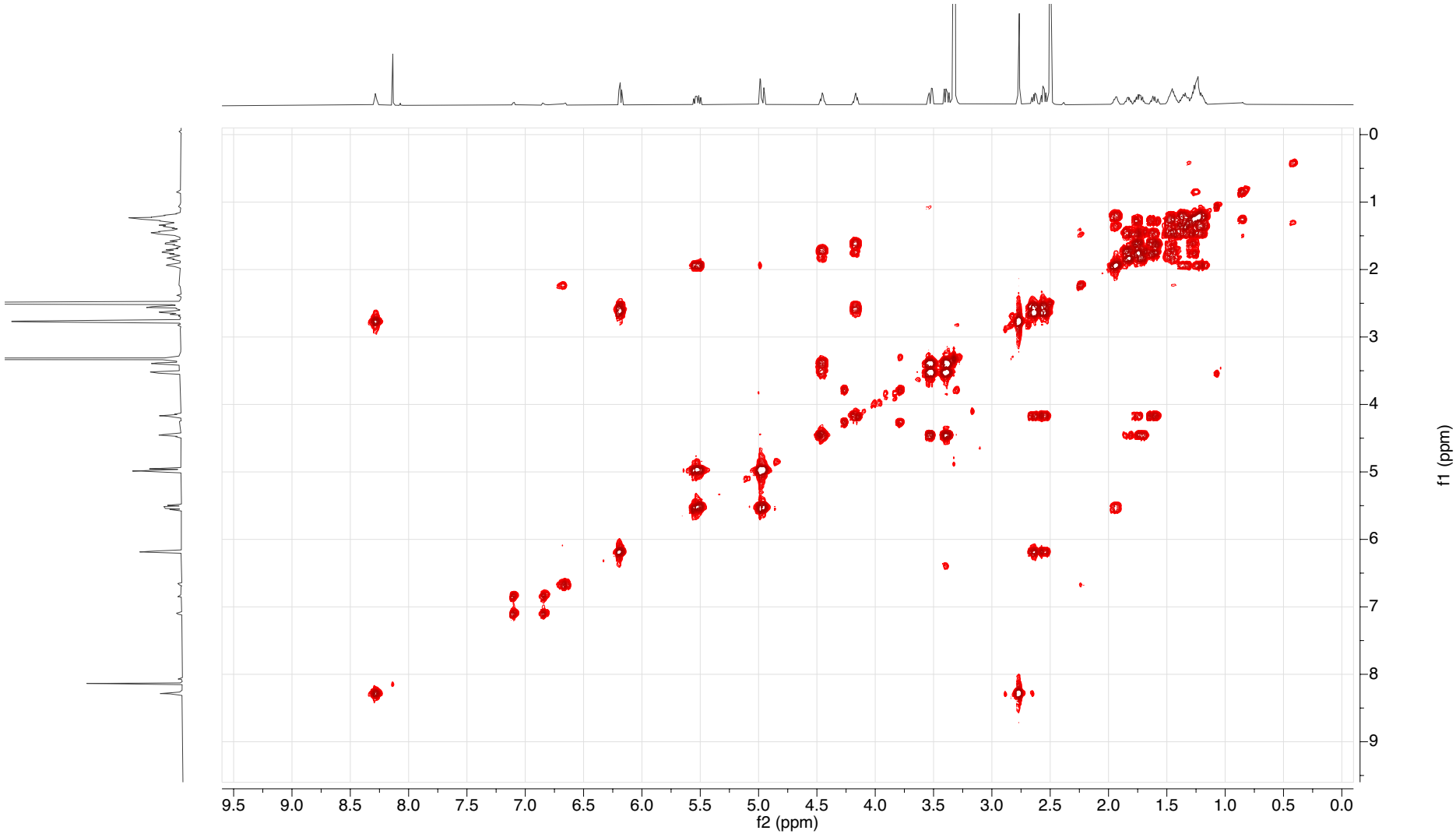

Figure S20. COSY (DMSO-d_6, 600 MHz) spectrum of compound **3**.

Table S3 – Annotation of the *fsh* biosynthetic gene cluster (BGC) locus.

Protein	Accession No.	Length [aa]	Predicted function	Closest homolog	Identity/Similarity [%]	Accession No.
-1	-	119	transposase	Insertion element protein [Fischerella thermalis JSC-11]	98/98	EHC19260.1
FshA	WP_051206792.1	610	FAAL	fatty acyl-AMP ligase [Pelatocladus maniniholoensis HA4357-MV3]	98/99	MBW4434717.1
FshB	WP_026724080.1	185	hypothetical	hypothetical protein AMR41_19650 [Hapalosiphon sp. MRB220]	97/98	KOP24608.1
FshC	WP_051206793.1	457	dimetal-carboxylate halogenase	hypothetical protein [Fischerella sp. CENA71]	98/99	MCP6757202.1
FshD	WP_231401100.1	320	FA-desaturase	acyl-CoA desaturase [Pelatocladus maniniholoensis HA4357-MV3]	97/99	MBW4434720.1
FshE	WP_026724083.1	109	ACP	acyl carrier protein [Fischerella sp. CENA71]	97/98	MCP6757200.1
FshF	WP_026724084.1	295	SAM-MT	cyclopropane-fatty-acyl-phospholipid synthase family protein [Pelatocladus maniniholoensis HA4357-MV3]	99/99	MBW4434722.1
FshG	WP_051206794.1	901	PKS (KS [4-426], AT^0 [533-826]	type I polyketide synthase [Pelatocladus maniniholoensis HA4357-MV3]	98/98	MBW4434723.1
FshH	WP_051206795.1	1084	PKS (KS^0 [4-428], AT^0 [538-832], T [982-1059]	acyltransferase domain-containing protein [Pelatocladus maniniholoensis HA4357-MV3]	98/98	MBW4434724.1
FshI	WP_035121683.1	1416	NRPS (C/Cy [75-372], A [542-941], Ox [1042-1240], T [1326-1391]	peptide synthetase [Hapalosiphon sp. MRB220]	99/99	KOP24606.1
FshJ	WP_051206796.1	2188	NRPS (C [74-374], A-Ox [561-1331], N-MT [1402-1622], T [1842-1908], TE [1930-2177]	LLM class flavin-dependent oxidoreductase [Fischerella sp. CENA71]	98/98	MCP6757194.1
FshK	WP_231401101.1	440	Fe(II)/α-ketoglutarate-dependent halogenase halogenase	hypothetical protein AMR41_19605 [Hapalosiphon sp. MRB220]	98/98	KOP24605.1
FshL	WP_051206797.1	465	Cytochrome P450	cytochrome [Hapalosiphon sp. MRB220]	99/99	KOP24604.1
FshM	WP_155959177.1	103	ACP	acyl carrier protein [Fischerella sp. CENA71]	97/99	MCP6757191.1
FshN	WP_026724087.1	468	dimetal-carboxylate halogenase	hypothetical protein AMR41_19590 [Hapalosiphon sp. MRB220]	98/98	KOP24603.1
+1	WP_026724088.1	429	transposase	hypothetical protein NIES37_44230 [Tolypothrix tenuis PCC 7101]	94/97	BAZ00432.1

FshA (FAAL)

Top Hits DDAP database C-terminal "heads"			
# identities	BGC Linker ID	Proteins	Connection
47	BGC_27_LINKER_1_HC	JamA to JamC	FAAL-ACP
18	BGC_42_LINKER_2_HC	FosB to FosC	PKS-PKS
17	BGC_17_LINKER_1_HC	GdmAI to GdmAII	PKS-PKS
17	BGC_39_LINKER_1_HC	ApoS1 to ApoS2	PKS-PKS
17	BGC_39_LINKER_2_HC	ApoS2 to ApoS3	PKS-PKS
17	BGC_88_LINKER_4_HC	RmpC to RmpD1	PKS-KS
16	BGC_91_LINKER_3_HC	SceQ to SceR	PKS-PKS
16	BGC_54_LINKER_4_HC	LobC to LobD	PKS-PKS

FshE (ACP)

Top Hits DDAP database N-terminal "tails"			
# identities	BGC Linker ID	Proteins	Connection
20	BGC_27_LINKER_1_TN	JamA to JamC	FAAL-ACP
11	BGC_63_LINKER_4_TN	BecF to BecG	PKS-PKS
11	BGC_75_LINKER_4_TN	MlaF to MlaG	PKS-PKS
11	BGC_9_LINKER_3_TN	MxaD to mxaC	PKS-PKS
10	BGC_58_LINKER_6_TN	GonP6 to GonP7	PKS-PKS
10	BGC_54_LINKER_1_TN	LobR to LobA	PKS-PKS
10	BGC_14_LINKER_1_TN	SorA to SorB	PKS-PKS
10	BGC_60_LINKER_3_TN	Ken13 to Ken14	PKS-PKS

FshM (ACP)

Top Hits DDAP database N-terminal "tails"			
# identities	BGC Linker ID	Proteins	Connection
16	BGC_27_LINKER_1_TN	JamA to JamC	FAAL-ACP
12	BGC_29_LINKER_3_TN	CurC to CurD	KS-HCS
12	BGC_39_LINKER_3_TN	ApoS3 to ApoS4	PKS-PKS
11	BGC_28_LINKER_2_TN	EryAII to EryAIII	PKS-PKS
10	BGC_20_LINKER_4_TN	MonAIV to MonAV	PKS-PKS
10	BGC_79_LINKER_1_TN	JerA to JerB	PKS-PKS
10	BGC_85_LINKER_1_TN	AmbA to AmbB	PKS-PKS
10	BGC_36_LINKER_1_TN	PikAI to PikAII	PKS-PKS

FshE (ACP)

Top Hits DDAP database C-terminal "heads"			
# identities	BGC Linker ID	Proteins	Connection
42	BGC_27_LINKER_2_HC	JamC to JamE	(FAAL-) ACP-PKS
24	BGC_26_LINKER_2_HC	BorA2 to BorA3	PKS-PKS
21	BGC_39_LINKER_1_HC	ApoS1 to ApoS2	PKS-PKS
21	BGC_88_LINKER_2_HC	RmpA2 to RmpB	PKS-PKS
20	BGC_58_LINKER_6_HC	GonP6 to GonP7	PKS-PKS
19	BGC_84_LINKER_4_HC	OlmA4 to OlmA5	PKS-PKS
19	BGC_23_LINKER_2_HC	AurB to AurC	PKS-PKS
19	BGC_46_LINKER_5_HC	PieA5 to PieA6	PKS-PKS

FshM (ACP)

Top Hits DDAP database C-terminal "heads"			
# identities	BGC Linker ID	Proteins	Connection
34	BGC_27_LINKER_2_HC	JamC to JamE	(FAAL-) ACP-PKS
18	BGC_11_LINKER_2_HC	SpnB to SpnC	PKS-PKS
17	BGC_82_LINKER_6_HC	HlsF to HlsG	PKS-PKS
16	BGC_63_LINKER_2_HC	BecD to BecE	PKS-PKS
16	BGC_9_LINKER_2_HC	MxaE to mxaD	PKS-PKS
15	BGC_13_LINKER_4_HC	StiD to StiE	PKS-PKS
15	BGC_29_LINKER_8_HC	CurH to CurI	PKS-PKS
15	BGC_29_LINKER_11_HC	CurK to CurL	PKS-PKS

FshG (PKS)

Top Hits DDAP database N-terminal "tails"			
# identities	BGC Linker ID	Proteins	Connection
32	BGC_27_LINKER_2_TN	JamC to JamE	(FAAL-) ACP-PKS
22	BGC_49_LINKER_1_TN	RevC to RevA	PKS-PKS
20	BGC_13_LINKER_2_TN	StiB to StiC	PKS-PKS
17	BGC_9_LINKER_2_TN	MxaE to mxaD	PKS-PKS
16	BGC_60_LINKER_1_TN	Ken16 to Ken12	PKS-PKS
16	BGC_46_LINKER_3_TN	PieA3 to PieA4	PKS-PKS
15	BGC_3_LINKER_2_TN	EpoB to EpoC	NRPS-PKS
15	BGC_27_LINKER_7_TN	JamL to JamM	NRPS-PKS

FshH (PKS)

Top Hits DDAP database N-terminal "tails"			
# identities	BGC Linker ID	Proteins	Connection
31	BGC_27_LINKER_2_TN	JamC to JamE	(FAAL-) ACP-PKS
23	BGC_13_LINKER_2_TN	StiB to StiC	PKS-PKS
21	BGC_49_LINKER_1_TN	RevC to RevA	PKS-PKS
19	BGC_27_LINKER_10_TN	JamO to JamP	NRPS-PKS
18	BGC_9_LINKER_2_TN	MxaE to mxaD	PKS-PKS
18	BGC_27_LINKER_7_TN	JamL to JamM	NRPS-PKS
17	BGC_46_LINKER_3_TN	PieA3 to PieA4	PKS-PKS
16	BGC_26_LINKER_3_TN	BorA3 to BorA4	PKS-PKS

FshH (PKS)

Top Hits DDAP database C-terminal "heads"			
# identities	BGC Linker ID	Proteins	Connection
35	BGC_27_LINKER_9_HC	JamN to JamO	PKS-NRPS
29	BGC_21_LINKER_1_HC	MelB to MelC	PKS-NRPS
24	BGC_32_LINKER_1_HC	CtaB to CtaC	PKS-NRPS
22	BGC_29_LINKER_2_HC	CurB to CurC	CP4-PKS
21	BGC_2_LINKER_1_HC	MtaB to MtaC	PKS-NRPS
21	BGC_27_LINKER_4_HC	JamF to JamJ	ACP-PKS
20	BGC_9_LINKER_3_HC	MxaD to mxaC	PKS-PKS
20	BGC_9_LINKER_5_HC	MxaB1 to MxaB2	PKS-PKS

FshI (NRPS)

Top Hits DDAP database N-terminal "tails"			
# identities	BGC Linker ID	Proteins	Connection
24	BGC_27_LINKER_9_TN	JamN to JamO	PKS-NRPS
21	BGC_32_LINKER_5_TN	CtaF to CtaG	PKS-NRPS
20	BGC_21_LINKER_5_TN	MelF to MelG	PKS-NRPS
18	BGC_2_LINKER_5_TN	MtaF to MtaG	PKS-NRPS
17	BGC_21_LINKER_2_TN	MelC to MelD	NRPS-NRPS
17	BGC_32_LINKER_2_TN	CtaC to CtaD	NRPS-NRPS
16	BGC_2_LINKER_2_TN	MtaC to MtaD	NRPS-NRPS
13	BGC_32_LINKER_1_TN	CtaB to CtaC	PKS-NRPS

Figure S21. Analysis of the docking domains of selected Fsh proteins encoded in the *fsh* BGC. Highest-scoring hits are highlighted with the function color code used in the main article's Figure 2.

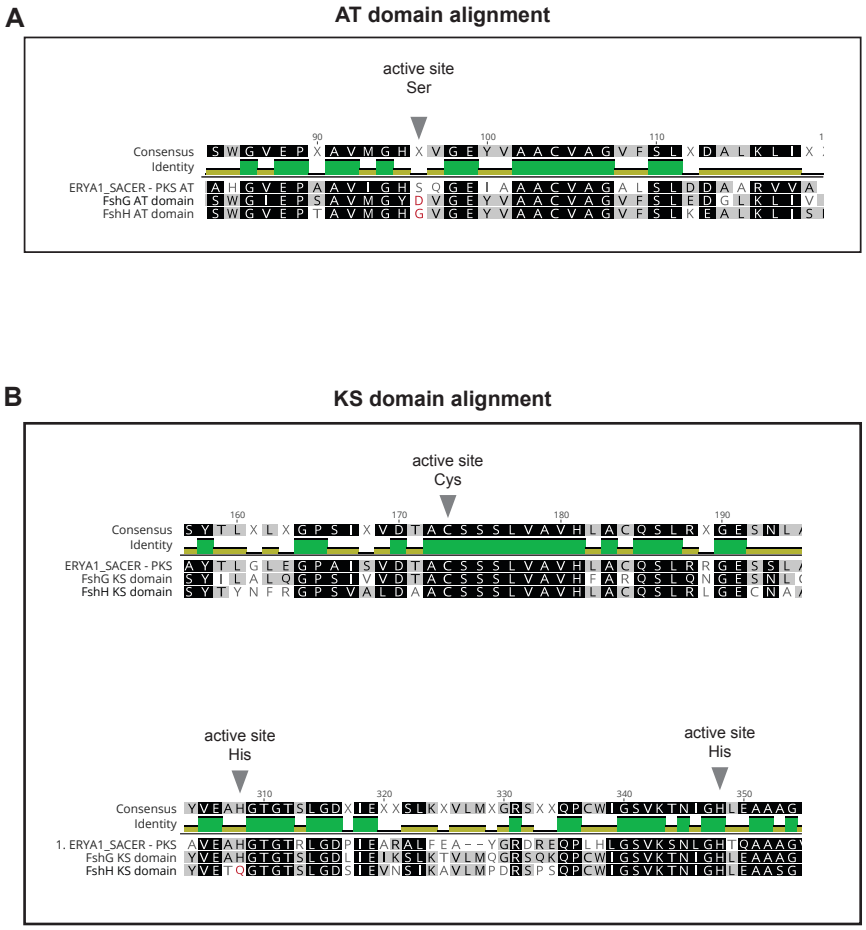

Figure S22. Alignment of the canonical DEBS 1 PKS KS and AT domains with those of FshG and FshH, highlighting the presence/absence of key catalytic residues. A – region of the AT domains containing the key Ser residue; B – regions of the KS domains containing key Cys and His residues.

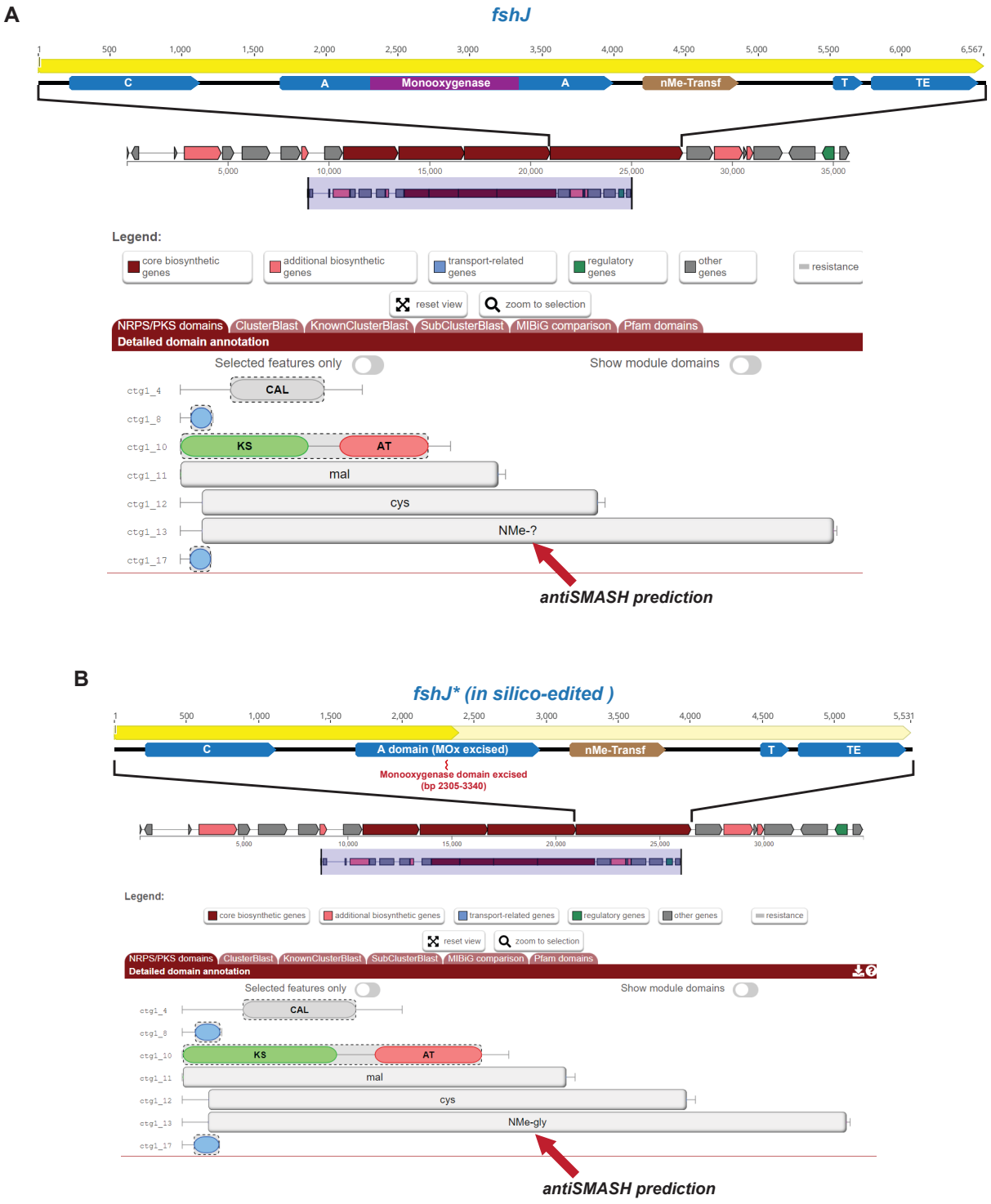

Figure S23. AntiSMASH analysis of the interrupted A-MOx domain in FshJ does not lead to a high-scoring predicted amino acid to be activated by this domain (presented graphically by the software as "NMe-**?**"). In silico excision of the MOx (monooxygenase) interrupting the A domain in FshJ leads to antiSMASH predicting Gly as the activated amino acid (presented graphically by the software as "NMe-**Gly**").

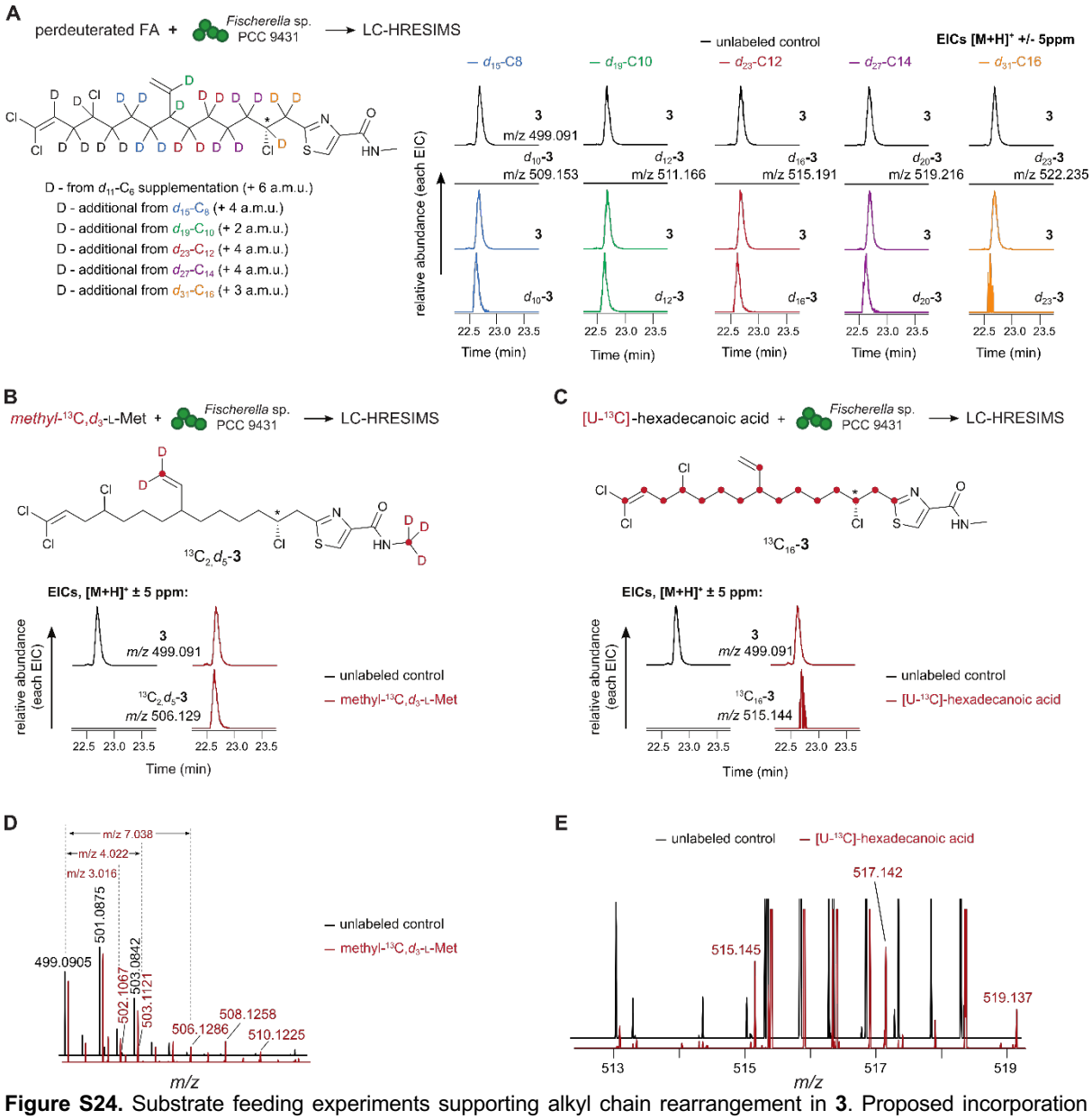

Figure S24. Substrate feeding experiments supporting alkyl chain rearrangement in **3**. Proposed incorporation pattern into **3** and LC-HRESIMS analysis of organic extracts of *Fischerella* sp. PCC 9431 cell biomass from cultures supplemented with: A – a perdeuterated fatty acid (hexanoic, octanoic, decanoic, dodecanoic, tetradecanoic and hexadecenoic acids were used in the experiments). EICs for the $[M+H]^+$ ions corresponding to non-labeled and observed deuterium-labeled **3**. (EICs for perdeuterated hexanoic acid (d_{11}-C_6) feeding experiments are as shown in Fig. 1 of the main text); B – L-Met-(*methyl*-^{13}C,d_3); C – [U-^{13}C]-hexadecanoic acid. D – LC-HRESIMS (Full MS) of the $[M+H]^+$ isotopic cluster of compound **3** (as a reference, black line) and of heavier versions resulting from $^{13}C_2$,d_5 incorporation (red lines, L -Met-(*methyl*-^{13}C,d_3) feeding), highlighting the observed +3, +4 a.m.u. and combined +7 a.m.u. from single and double incorporation of the labeled substrate. E - LC-HRESIMS (Full MS) of the M+16 isotopic cluster of compound **3** $[M+H]^+$, showing incorporation of sixteen ^{13}C atoms from labeled hexadecanoic acid into **3**. * Configuration of stereogenic centers inferred from experimental data for **2**.

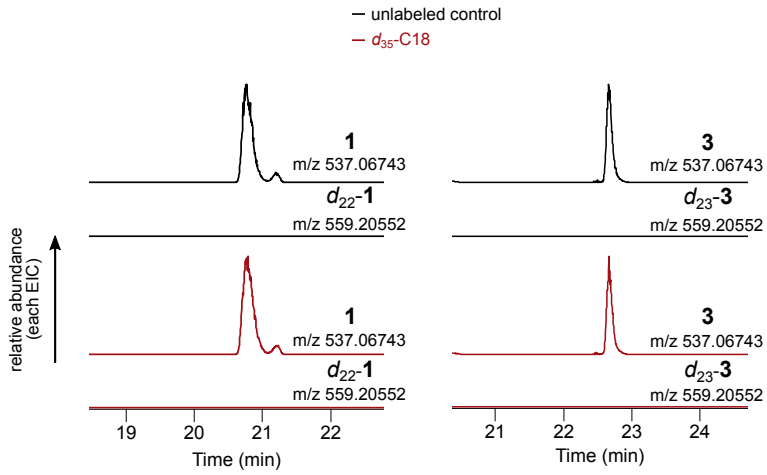

Figure S25. Supplementation of *Fischerella* sp. PCC 9431 cultures with perdeuterated octadecanoic acid does not lead to observable deuterium incorporation into the fischerazoles (**1** and **3** were analyzed), indicating that the observed incorporation of deuterium from perdeuterated hexadecanoic acid is specific to the fischerazole biosynthetic pathway. Shown are EICs for **1** and **3** and the heavier versions for which deuterium incorporation was observed in hexadecanoic supplementation.

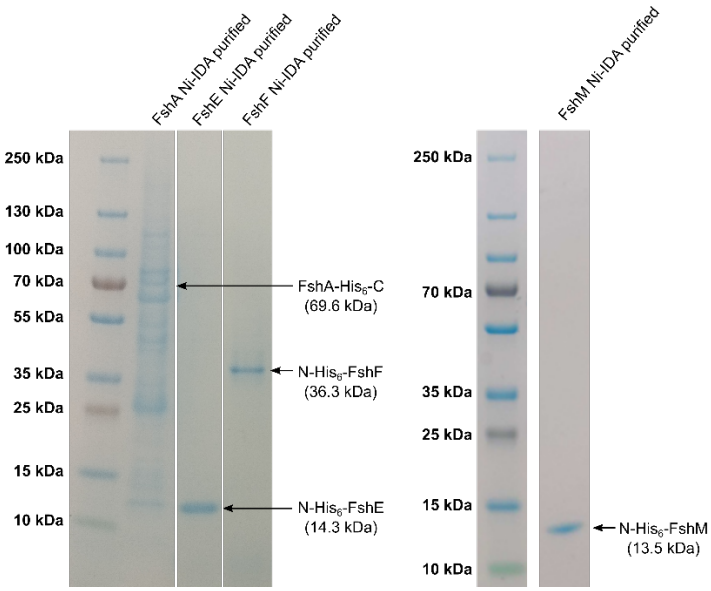

Figure S26. SDS-PAGE of purified recombinant proteins FshA, FshE, FshF and FshM.

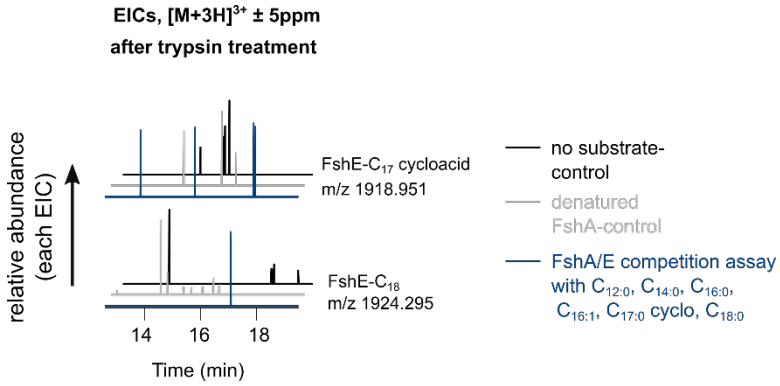

Figure S27. In a competition assay with FshA and FshE (same assay as depicted in Fig. 4B) no activation of *cis*-9,10-methylenehexadecanoic acid (C_{17} cycloacid) and octadecanoic acid (C_{18}) was observed. EICs for the $[M+3H]^{3+}$ ions corresponding to the FshE peptide containing the PPant arm (and respective loaded fatty acid) resulting from trypsinization.

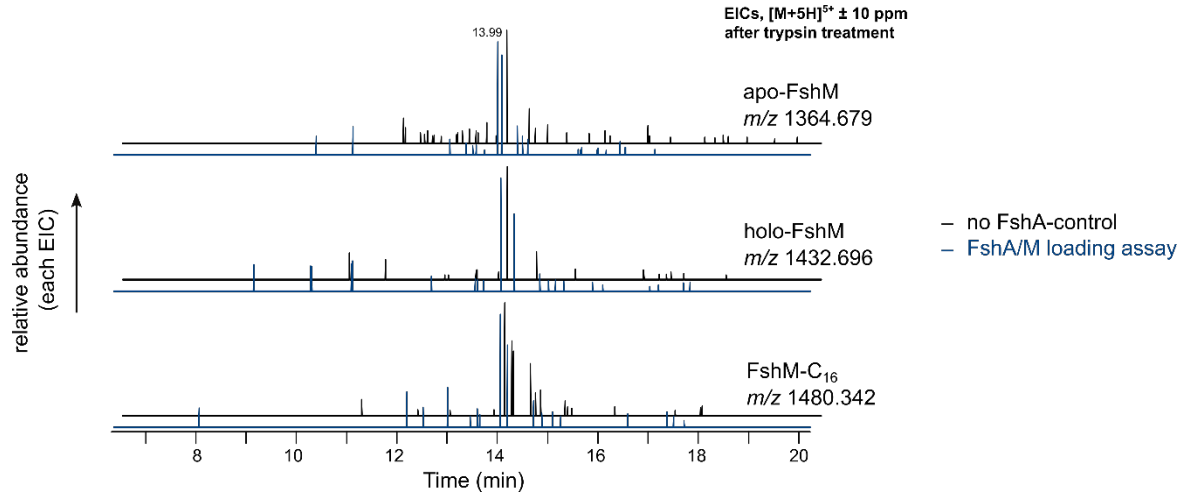

Figure S28. In a loading assay with FshA, FshM and hexadecanoic acid, no apo-, holo- or C_{16}-loaded FshM peptide was detected. EICs for the $[M+5H]^{5+}$ ions corresponding to the FshM trypsinated peptide containing the PPant arm.

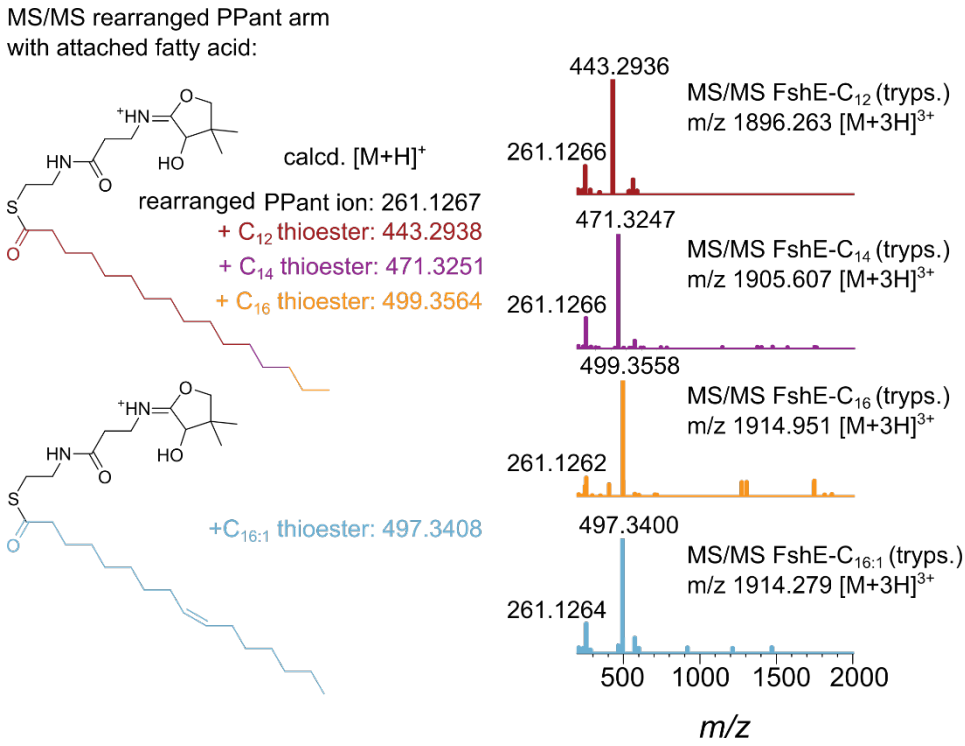

Figure S29. HRESIMS/MS spectra of PPant-containing trypsinated FshE-peptides from FshA competition assay with loaded dodecanoic, tetradecanoic, hexadecenoic and *cis*-9-hexadecenoic acid confirmed the presence of the respective diagnostic PPant-acyl-thioester ion.

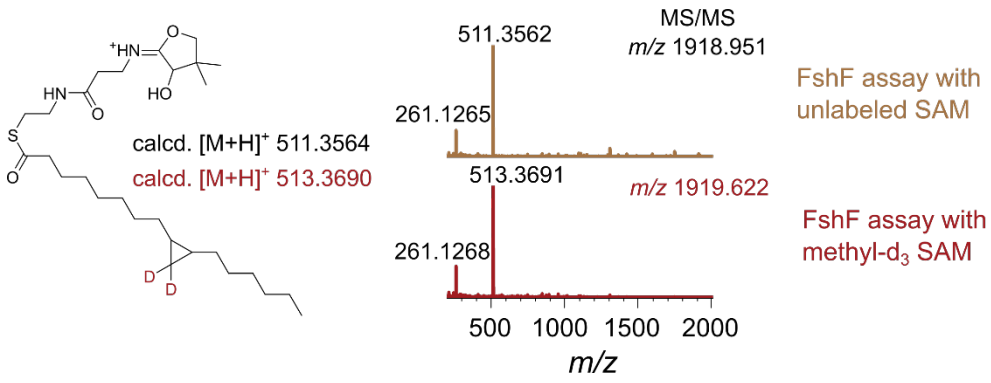

Figure S30. HRESIMS/MS spectra of PPant-containing trypsinated FshE-peptides from FshF methylation assays with labeled or unlabeled SAM confirmed the presence of the respective diagnostic PPant-acyl-thioester ion.

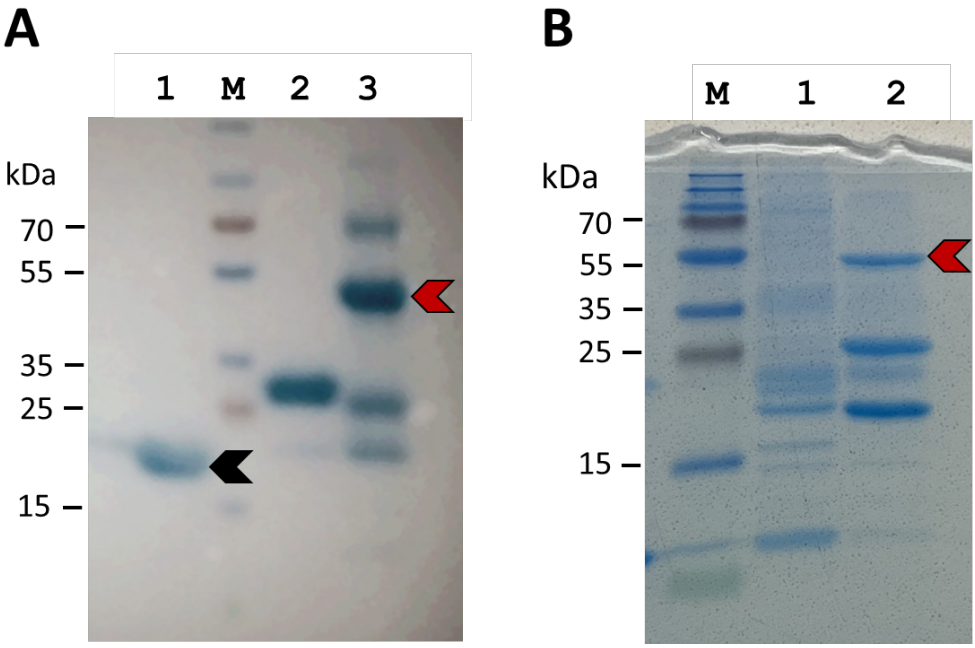

Figure S31. SDS PAGE gels of recombinant his-tagged 'tesA and 'tesA-mCherry fusion. **A:** 1 - 'tesA (black arrow) at 20 kDa; M - Thermo PAGE Ruler protein ladder; 2 - mCherry reference; 3 - 'tesA-mCh fusion (red arrow) at 50 kDa; **B:** M - Thermo PAGE Ruler protein ladder; 1 - 'tesA, apparently degraded, assays were continued with the more stable mCherry fusion; 2 - 'tesA-mCh fusion (red arrow) breaks into smaller fragments during heat treatment.

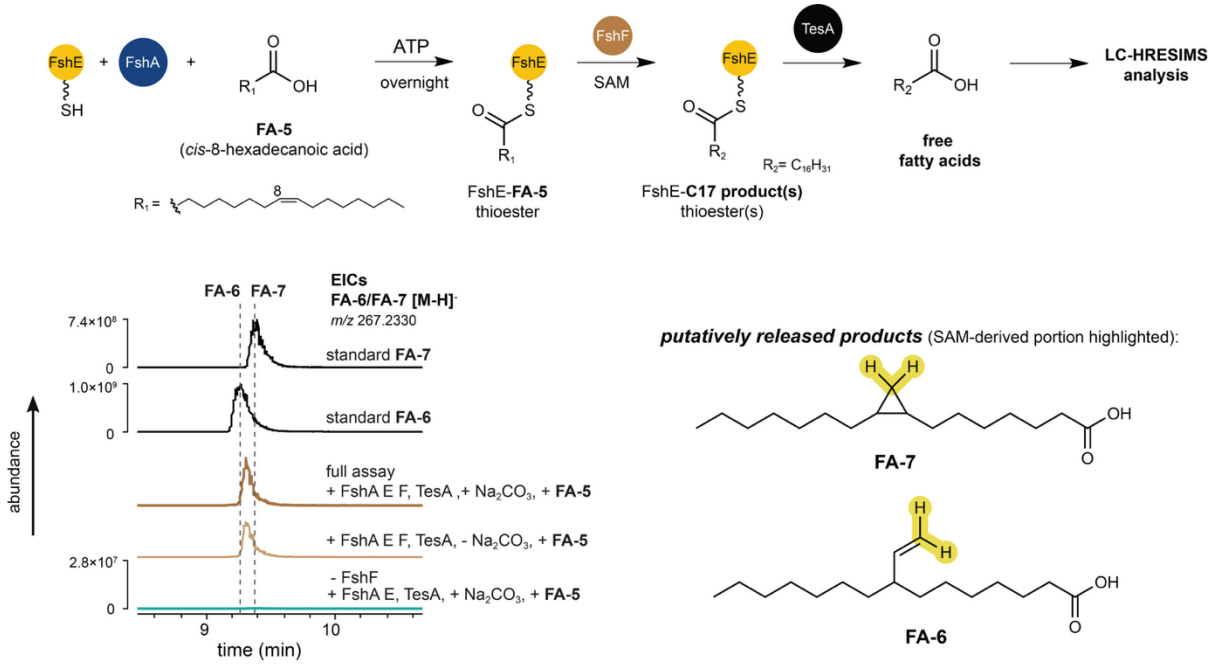

Figure S32. FshF assay followed by 'tesA-mCherry hydrolysis of the thioesters into free fatty acids for LC-HRESIMS analysis. Top – schematic representation of the assay set-up. Bottom – EICs (C17 free fatty acids) for the assay mixtures and synthetic standards **FA-6** and **FA-7.**

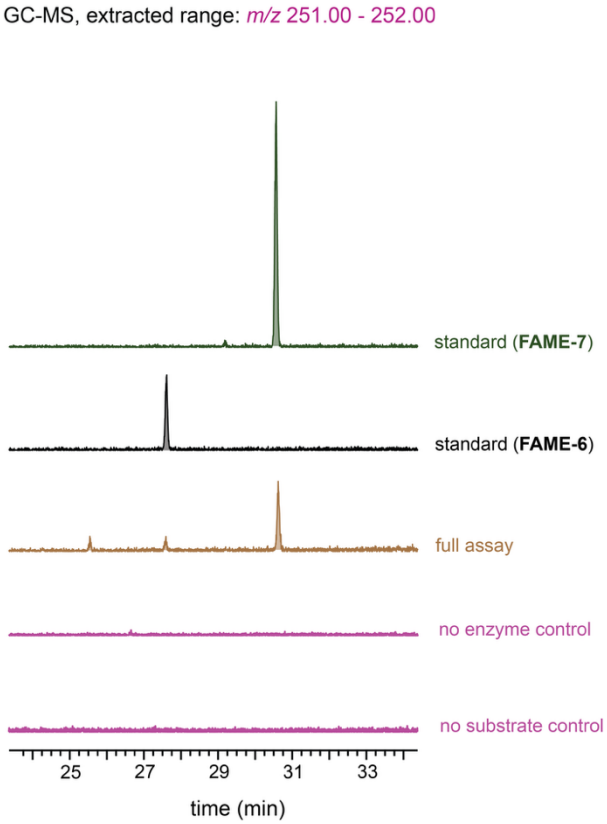

Figure S33. GC-MS extracted range chromatograms (m/z 251.0 – 252.0), corresponding to the key C17-FAME fragment formed *in-source*, showing full separation of the standard **FAME-6** and **FAME-7**, and the presence of both products in the full assay, but not in the controls.

Additional Compound Characterization Data

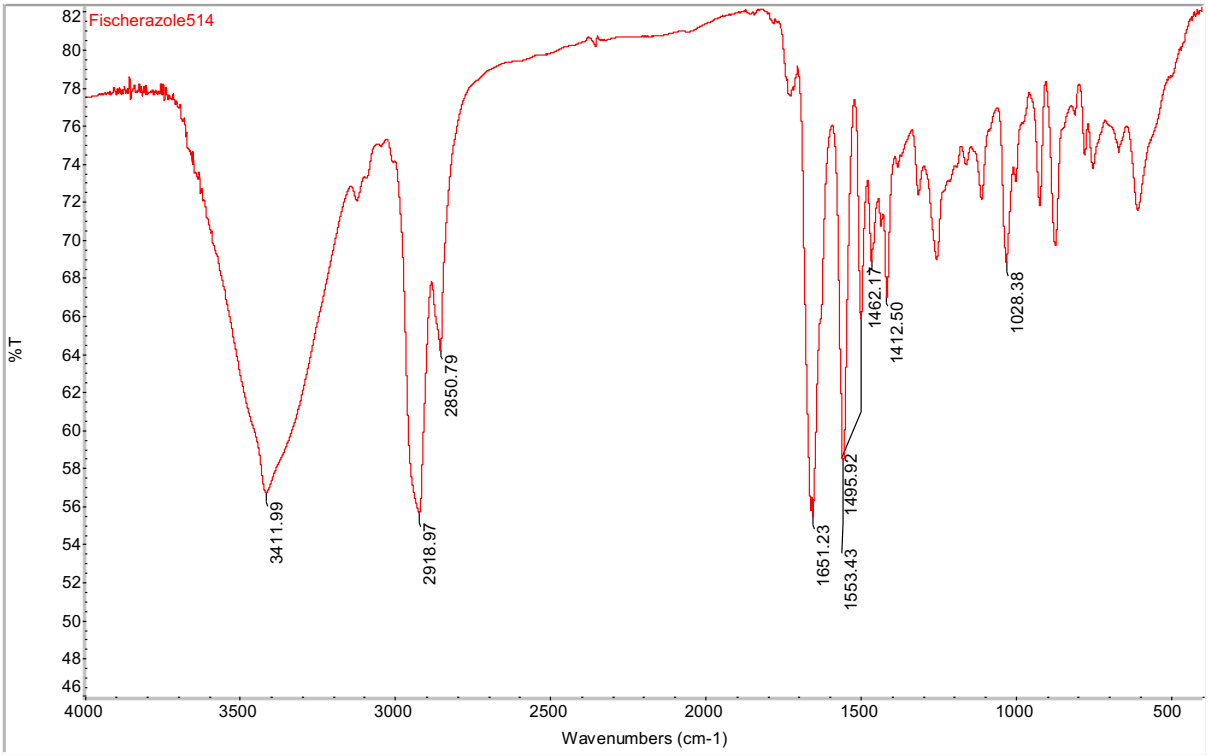

Figure S32 – FT-IR spectrum of compound **1**.

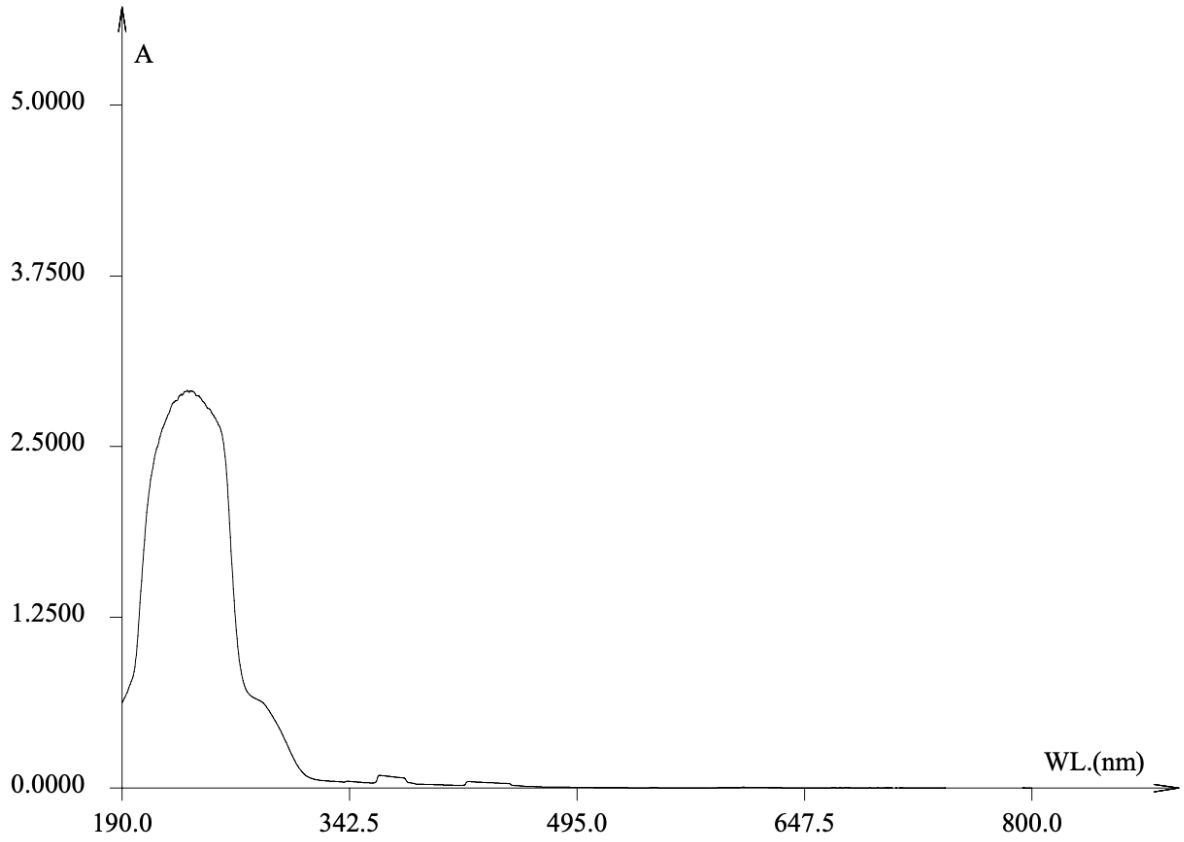

Figure S33 – UV-Vis spectrum of compound **1**.

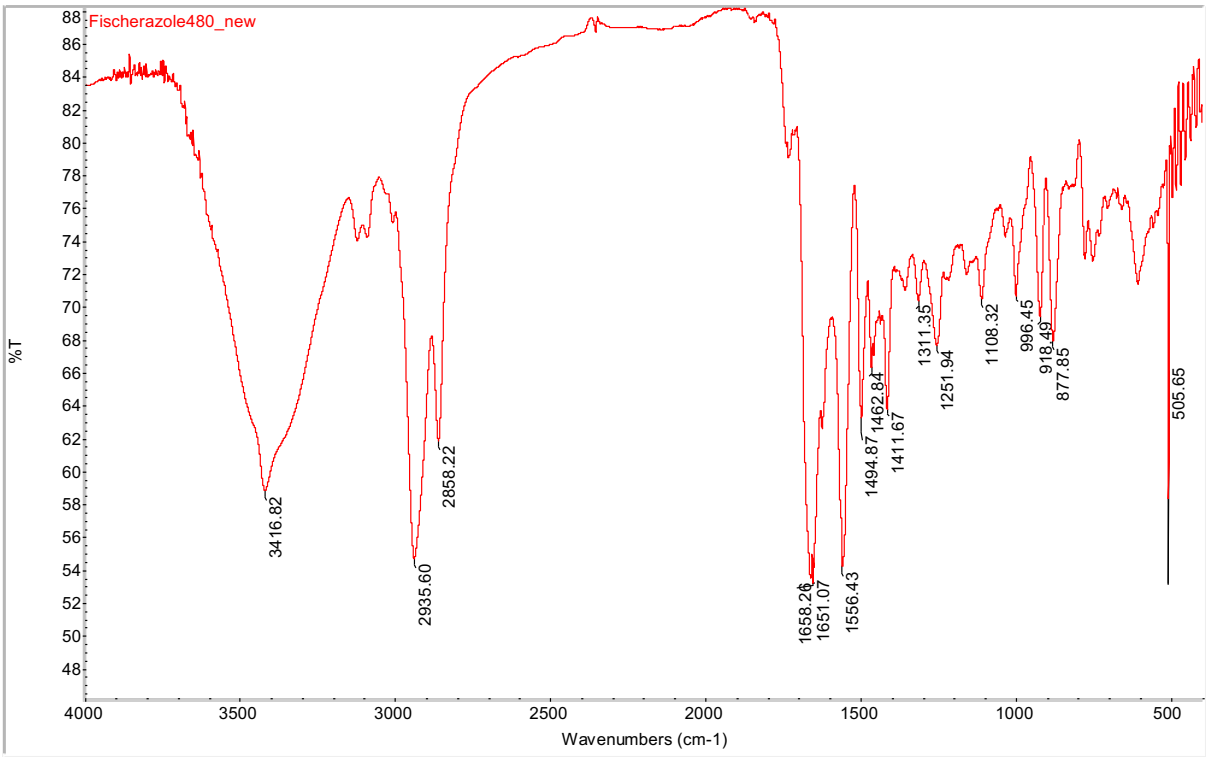

Figure S34 – FT-IR spectrum of compound **2**.

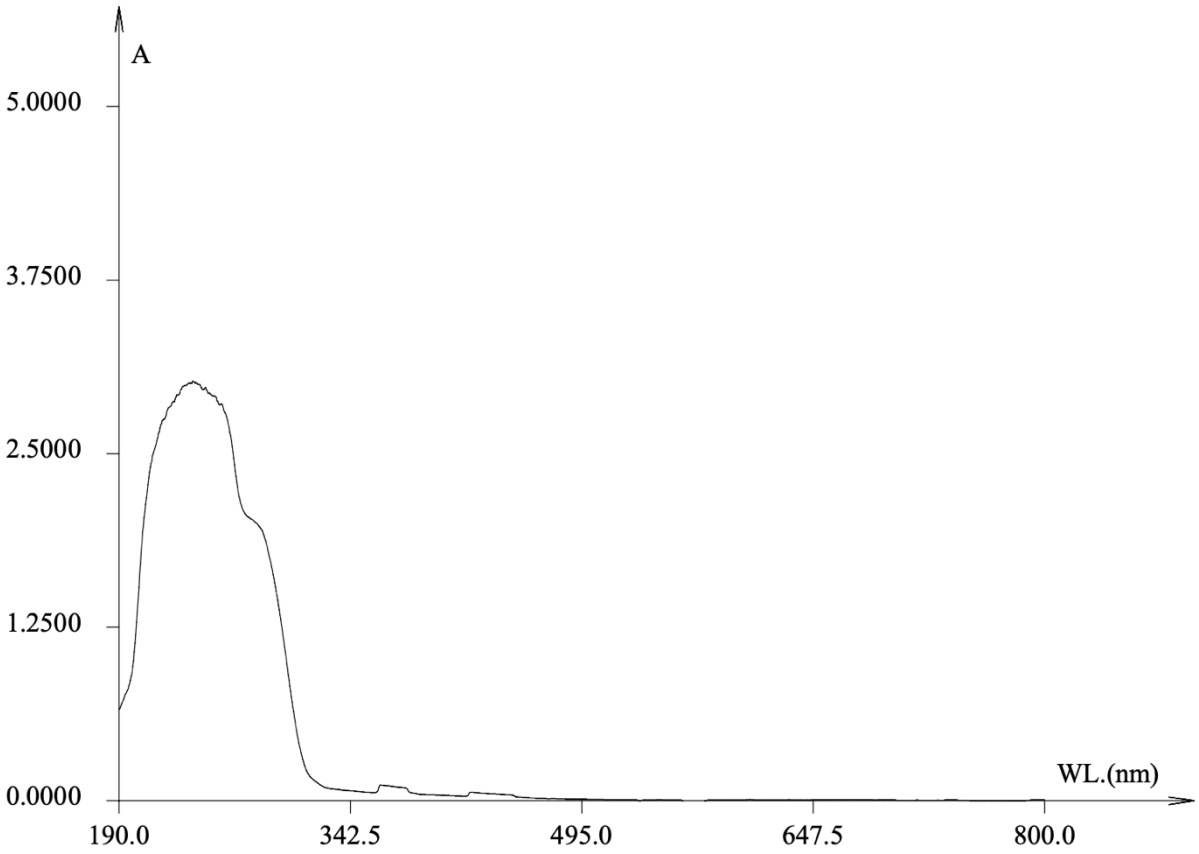

Figure S35 – UV-Vis spectrum of compound **2**.

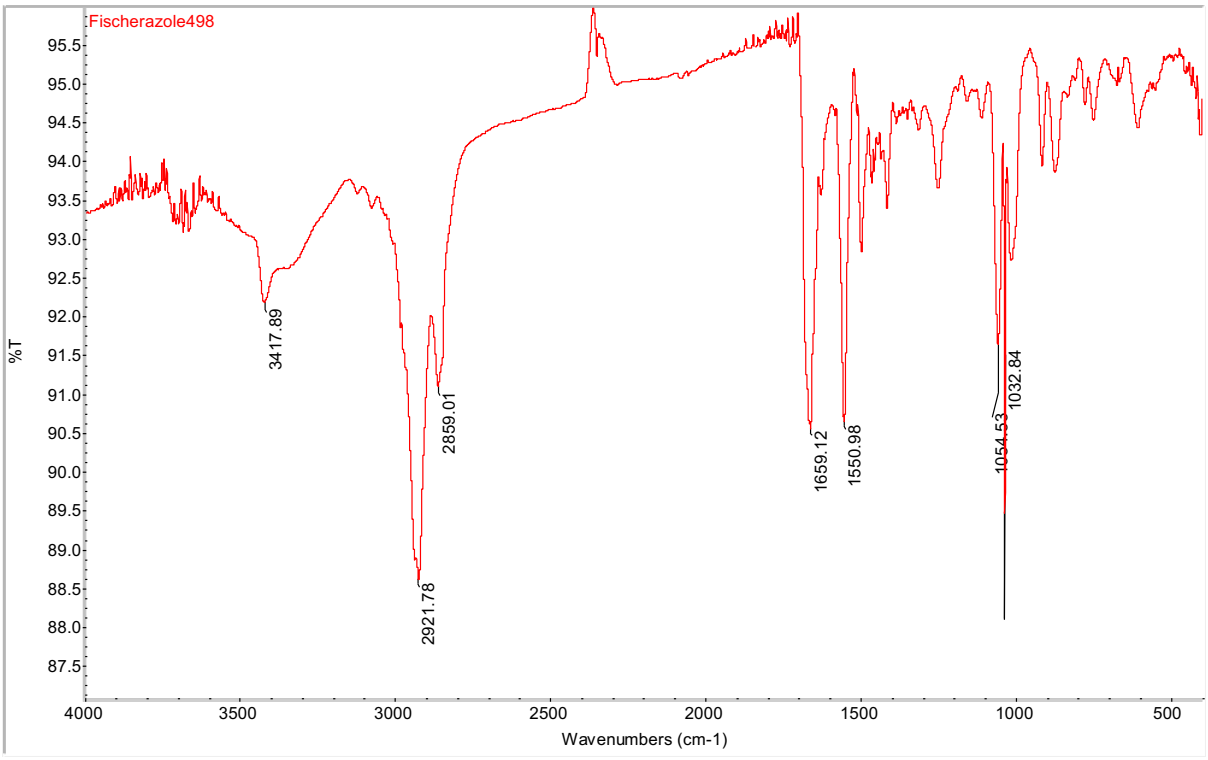

Figure S36 – FT-IR spectrum of compound **3**.

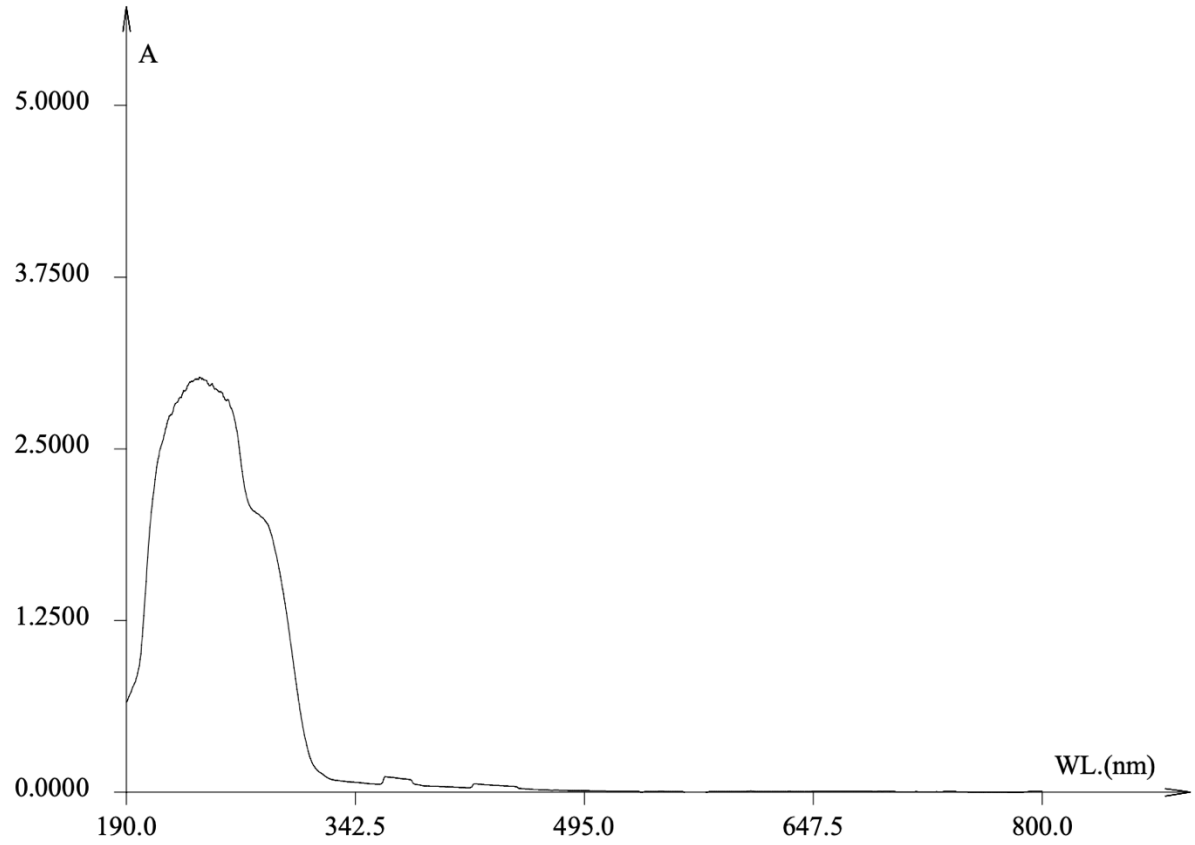

Figure S37 – UV-Vis spectrum of compound **3**.

Synthetic procedures and compound characterization

Synthetic route to 8-vinylpentadecanoic acid (FA-6)

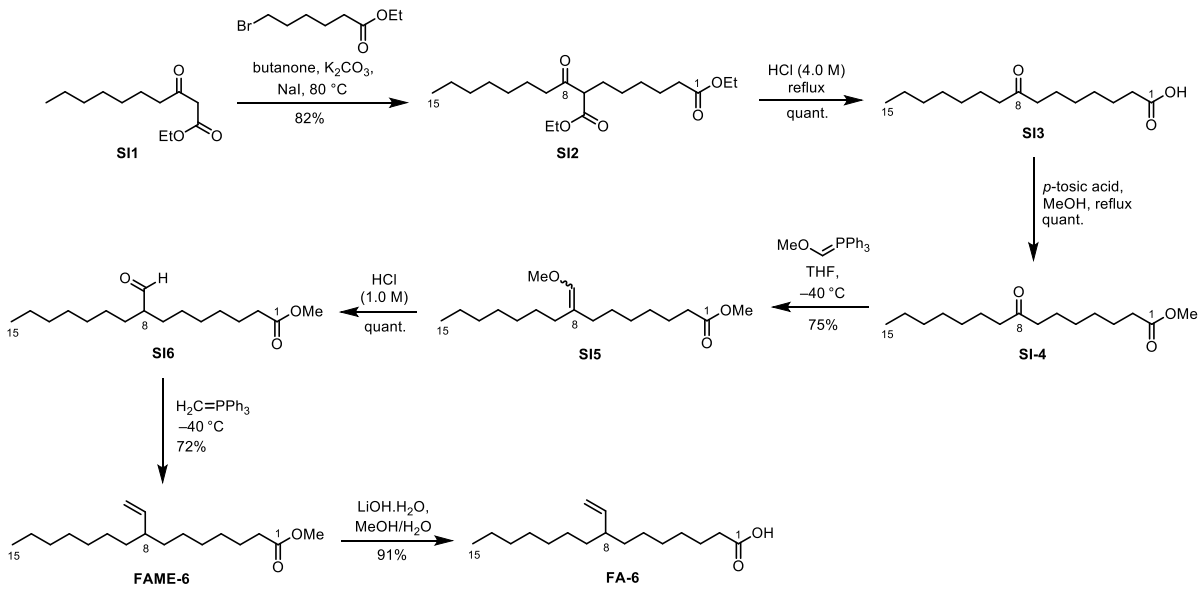

Ethyl 3-oxodecanoate (SI1)

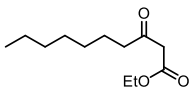

This compound was prepared as described in the literature:[SI-7] *n*-BuLi (1.50 mL of a 2.50 M solution in hexane, 3.75 mmol) was added dropwise over 2 min to a cooled (0 °C) solution of *i*-Pr_2NH (0.53 mL, 3.75 mmol) in THF (3.0 mL). This solution was stirred for 20 min at 0 °C before ethyl acetoacetate (0.19 mL, 1.50 mmol) was added dropwise over 1 min. The yellow solution was stirred at 0 °C for 1 h and then cooled to –78 °C. 1-Iodohexane (0.33 mL, 1.8 mmol) was added dropwise over 1 min and then the temperature was allowed to rise to room temperature over 14 h. HCl (5.0 mL of a 2.0 M aqueous solution) was added and the mixture was extracted with Et_2O (4 × 5.0 mL). The combined organic phase was dried (Na_2SO_4), filtered and concentrated under reduced pressure. The residue was purified by flash column chromatography (3% EtOAc in hexane) to afford ethyl 3-oxodecanoate **SI1** (keto:enol 12.5:1) as a colorless oil (340 mg, 92%); δ_H ($CDCl_3$, 400 MHz) data for keto form: 0.87 (3H, t, *J* 7.2), 1.23–1.31 (11H, m), 1.59 (2H, quintet, *J* 7.2), 2.52 (2H, t, *J* 7.2), 3.42 (2H, s), 4.19 (2H, q, *J* 7.2); selected data for enol form: 2.14–2.22 (0.16H, m), 4.96 (0.08H, s); δ_C (100 MHz) data for keto form: 14.0 (CH_3), 14.1 (CH_3), 22.5 (CH_2), 23.4 (CH_2), 28.9 (CH_2), 29.0 (CH_2), 31.6 (CH_2), 43.0 (CH_2), 49.3 (CH_2), 61.3 (CH_2), 167.2 (C), 203.0 (C); HRMS (ESI+) calcd for $C_{12}H_{22}O_3Na^+$ $[M + Na]^+$ 237.1461, found 237.1458. The data were in agreement with those described in the literature.[SI-7]

Ethyl 7-ethoxycarbonyl-8-oxopentadecanoate (SI2)

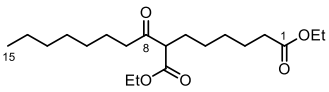

Ethyl 6-bromohexanoate (206 µL, 1.16 mmol) was added dropwise over 2 min to a stirred mixture of β-keto ester **SI1** (200 mg, 0.93 mmol) and anhydrous K_2CO_3 (386 mg, 2.79 mmol) in butanone (4.0 mL) at room temperature. The resulting suspension was then stirred at 60 °C for 48 h. The reaction mixture was filtered and then concentrated under reduced pressure. EtOAc (10 mL) and H_2O (10 mL) were added and the phases were separated. The aqueous phase was extracted with EtOAc (2 × 10 mL). The combined organic phase was washed with brine (10 mL), dried (Na_2SO_4) and concentrated under reduced pressure to afford a yellow residue, which was purified by flash column chromatography (5% EtOAc in hexane) to afford diester **SI2** as a white solid (271 mg, 82%); δ_H ($CDCl_3$, 400 MHz) 0.86 (3H, t, *J* 7.1), 1.20-1.36 (18H, m), 1.51–1.66 (4H, m), 1.75-1.90 (2H, m), 2.27 (2H, t, *J* 7.5), 2.39–2.58 (1H, m), 3.39 (2H, t, *J* 7.3), 4.11 (2H, q, *J* 7.1), 4.17 (2H, q, *J* 7.2); δ_C ($CDCl_3$, 100 MHz) 14.0 (CH_3), 14.1 (CH_3), 14.2 (CH_3), 22.6 (CH_2), 23.5 (CH_2), 24.6 (CH_2), 27.1 (CH_2), 27.9 (CH_2), 28.8 (CH_2), 28.99 (CH_2), 29.00 (CH_2), 31.6 (CH_2), 34.2 (CH_2), 41.9 (CH_2), 59.1 (CH), 60.2 (CH_2), 61.2 (CH_2), 169.9 (C), 173.6 (C), 205.4 (C); HRMS (TOF ES+) calcd for $C_{20}H_{37}O_5^+$ $[M + H]^+$ 357.2637, found 357.2631.

8-Oxopentadecanoic acid (SI3)

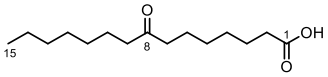

A suspension of diester **SI2** (220 mg, 0.62 mmol) in 4.0 M HCl (2.0 mL) was heated at reflux for 24 h. EtOAc (10 mL) and H_2O (10 mL) were added and the phases were separated. The aqueous phase was extracted with EtOAc (2 × 10 mL). The combined organic phase was washed with brine (10 mL), dried (Na_2SO_4) and concentrated under reduced pressure to afford **SI3** as a white solid (158 mg, quant.); δ_H ($CDCl_3$, 400 MHz) 0.88 (3H, t, *J* 7.1), 1.23–1.39 (12H, m), 1.51–1.70 (6H, m), 2.35 (2H, t, *J* 7.5), 2.38 (2H, t, *J* 7.6), 2.39 (2H, t, *J* 7.4), the exchangeable CO_2H proton was not observed; δ_C ($CDCl_3$, 100 MHz) 14.0 (CH_3), 22.6 (CH_2), 23.6 (CH_2), 23.9 (CH_2), 24.5 (CH_2), 28.79 (CH_2), 28.82 (CH_2), 29.1 (CH_2), 29.2 (CH_2), 31.7 (CH_2), 33.8 (CH_2), 42.6 (CH_2), 42.9 (CH_2), 179.2 (C), 211.6 (C); HRMS (ESI+) calcd for $C_{15}H_{28}O_3Na^+$ [M + Na]$^+$ 279.1931, found 279.1925.

Methyl 8-oxopentadecanoate (SI4)

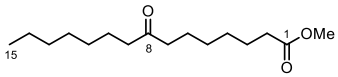

Carboxylic acid **SI3** (130 mg, 0.51 mmol) was dissolved in MeOH (3.0 mL) before $MgSO_4$ (300 mg) and *para*-toluenesulfonic acid (18 mg, 0.10 mmol) were added sequentially. The reaction mixture was then stirred at 60 °C overnight. The reaction mixture was filtered and concentrated under reduced pressure before EtOAc (10 mL) and H_2O (10 mL) were added. The phases were separated and the aqueous phase was extracted with EtOAc (2 × 10 mL). The combined organic phase was washed with brine (10 mL), dried (Na_2SO_4) and concentrated under reduced pressure to afford ester **SI4** as a white solid (138 mg, quant.): δ_H ($CDCl_3$, 400 MHz) 0.87 (3H, t, *J* 7.1), 1.21–1.37 (12H, m), 1.52–1.67 (6H, m), 2.29 (2H, t, *J* 7.5), 2.37 (2H, t, *J* 7.6), 2.38 (2H, t, *J* 7.4), 3.66 (3H, s); δ_C ($CDCl_3$, 100 MHz) 14.0 (CH_3), 22.6 (CH_2), 23.6 (CH_2), 23.9 (CH_2), 24.7 (CH_2), 28.85 (CH_2), 28.89 (CH_2), 29.1 (CH_2), 29.2 (CH_2), 31.7 (CH_2), 34.0 (CH_2), 42.6 (CH_2), 42.8 (CH_2), 51.4 (CH_3), 174.2 (C), 211.5 (C); HRMS (ESI+) calcd for $C_{16}H_{31}O_3^+$ [M + H]$^+$ 271.2268, found 271.2264.

Methyl (E/Z)-8-(methoxymethylene)pentadecanoate (SI5)

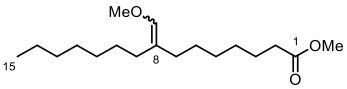

n-BuLi (332 µL of a 2.5 M in hexane, 0.83 mmol) was added dropwise to a stirred solution of (methoxymethyl)triphenylphosphonium chloride (319 mg, 0.93 mmol) in THF (3.0 mL) at –40 °C. This solution was stirred at –40 °C for 1 h before a solution of ketone **SI4** (50 mg, 0.19 mmol) in THF (3.0 mL) was added dropwise over 1 min. The reaction mixture was stirred at –40 °C for 1 h and then allowed to warm to room temperature and stirred for a further 2 h. The mixture was quenched with H_2O (10 mL) and extracted with EtOAc (2 × 10 mL). The combined organic phase was dried (Na_2SO_4), filtered and concentrated under reduced pressure. Purification of the residue by flash column chromatography (5% EtOAc in hexane) afforded enol ether **SI5** (1:1 mixture of *E*- and *Z*-isomers) as a colorless oil (42 mg, 75%); δ_H ($CDCl_3$, 400 MHz) [0.870, 0.872 (3H, t, *J* 7.0)], 1.20–1.39 (16H, m), 1.61 (2H, quintet, *J* 7.6), 1.79–1.87 (2H, m), 2.01 (2H, t, *J* 6.6), 2.29 (2H, t, *J* 7.6), [3.500, 3.502 (3H, s)], [3.65, 3.66 (3H, s)], [5.72, 5.73 (1H, s)], some peaks are doubled due to the presence of both *E*- and *Z*-isomers; δ_C ($CDCl_3$, 100 MHz) [14.07, 14.09 (CH_3)], [22.65, 22.66 (CH_2)], [24.9, 25.0 (CH_2)], [26.6, 26.7 (CH_2)], [27.5, 27.8 (CH_2)], [28.0, 28.2 (CH_2)], [28.9, 29.0 (CH_2)], [29.0, 29.1 (CH_2)], [29.18, 29.22 (CH_2)], [29.3, 29.6 (CH_2)], [31.3, 31.4 (CH_2)], [31.86, 31.89 (CH_2)], [34.07, 34.11 (CH_2)], [51.38, 51.40 (CH_3)], 59.2 (CH_3), [118.6, 118.7], [141.91, 141.93 (CH)], [174.27, 174.33 (C)], most peaks are doubled due to the presence of both *E*- and *Z*-isomers; HRMS (ESI+) calcd for $C_{18}H_{34}O_3Na^+$ [M + Na]$^+$ 321.2400, found 321.2397.

Methyl (R,S)-8-formylpentadecanoate SI6

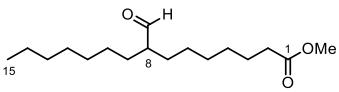

HCl (0.20 mL of a 1.0 M aqueous solution) was added to a solution of enol ether **SI5** (30 mg, 0.10 mmol) in CH_2Cl_2/MeOH (1:1, 2.0 mL) at room temperature. The resulting solution was stirred for 3 h and then diluted with CH_2Cl_2 (10 mL) and H_2O (10 mL). The phases were separated and the aqueous phase was extracted with CH_2Cl_2 (2 × 10 mL). The combined organic phase was dried (Na_2SO_4), filtered and concentrated under reduced pressure to provide aldehyde **SI6** as a colourless oil (29 mg, quant.), which was used directly in the next synthetic step without further purification; δ_H ($CDCl_3$, 400 MHz) 0.88 (3H, t, *J* 7.1), 1.20–1.36 (16H, m), 1.37–1.49 (2H, m), 1.52–1.68 (4H, m), 2.16–2.26 (1H, m), 2.30 (2H, t, *J* 7.5), 3.67 (3H, s), 9.55 (1H, d, *J* 3.2); HRMS (ESI+) calcd for $C_{17}H_{33}O_3^+$ [M + H]$^+$ 285.2424, found 285.2420.

Methyl (R,S)-8-vinylpentadecanoate (FAME-6)

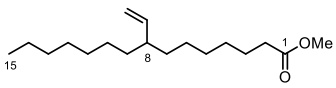

n-BuLi (62 µL of 2.5 M solution in hexane, 0.154 mmol) was added dropwise to a stirred solution of methyltriphenylphosphonium bromide (62 mg, 0.173 mmol) in THF (2.0 mL) at –40 °C. The mixture was stirred at –40 °C for 1 h before a solution of aldehyde **SI6** (10 mg, 0.035 mmol) in THF (2.0 mL) was added dropwise over 1 min. The reaction mixture was stirred at –40 °C for 1 h and then allowed to warm to room temperature and stirred for a further 2 h. The mixture was quenched with H_2O (10 mL) and extracted with EtOAc (2 × 10 mL). The combined organic phase was dried (Na_2SO_4), filtered and concentrated under reduced pressure. The residue was purified by flash column chromatography (2% EtOAc in hexane) to afford alkene **FAME-6** as a colorless oil (7.1 mg, 72%); δ_H ($CDCl_3$, 400 MHz) 0.88 (3H, t, *J* 7.0), 1.17–1.37 (20H, m), 1.57–1.67 (2H, m), 1.85–1.95 (1H, m), 2.30 (2H, t, *J* 7.6), 3.67 (3H, s), 4.87–4.97 (2H, m), 5.51 (1H, ddd, *J* 17.0, 10.4, 8.8); δ_C ($CDCl_3$, 100 MHz) 14.1 (CH_3), 22.7 (CH_2), 25.0 (CH_2), 27.0 (CH_2), 27.2 (CH_2), 29.1 (CH_2), 29.3 (CH_2), 29.4 (CH_2), 29.7 (CH_2), 31.9 (CH_2), 34.1 (CH_2), 34.9 (CH_2), 35.1 (CH_2), 44.1 (CH), 51.4 (CH_3), 113.8 (CH_2), 143.6 (CH), 174.3 (C); HRMS (ESI+) calcd for $C_{18}H_{35}O_2^+$ $[M + H]^+$ 283.2632, found 283.2638.

(R,S)-8-Vinylpentadecanoic acid (FA-6)

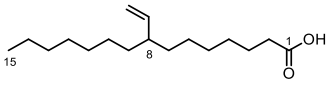

$LiOH·H_2O$ (7.6 mg, 0.18 mmol) was added to a vigorously stirred solution of ester **SI6** (5.0 mg, 0.018 mmol) in $MeOH/H_2O$ (1:1, 2.0 mL) at rt. After stirring for 1 h, the mixture was quenched by the addition of HCl (10 mL, 0.5 M solution). EtOAc (10 mL) was added and the phases were separated. The aqueous phase was extracted with EtOAc (3 × 10 mL) and the combined organic extracts were washed with brine (10 mL), dried (Na_2SO_4), filtered and concentrated under reduced pressure. Purification of the residue by flash column chromatography (30% EtOAc in hexane) afforded fatty acid **FA-6** as a colorless oil (4.4 mg, 91%); δ_H (300 MHz, $CDCl_3$) 0.88 (3H, t, *J* 6.9), 1.16–1.37 (20H, m), 1.58–1.68 (2H, m), 1.63 (1H, app. quintet, *J* 7.4), 2.34 (2H, t, *J* 7.4), 4.88–4.96 (2H, m), 5.51 (1H, ddd, *J* 16.9, 10.4, 8.8), the exchangeable CO_2H proton was not observed; δ_C (100 MHz, $CDCl_3$) 14.1 (CH_3), 22.7 (CH_2), 24.7 (CH_2), 27.0 (CH_2), 27.2 (CH_2), 29.0 (CH_2), 29.31 (CH_2), 29.33 (CH_2), 29.7 (CH_2), 31.9 (CH_2), 33.6 (CH_2), 34.9 (CH_2), 35.1 (CH_2), 44.1 (CH), 113.8 (CH_2), 143.6 (CH), 177.7 (C); HRMS (ESI–) calcd for $C_{17}H_{31}O_2^-$ $[M – H]^+$ 267.2331, found 267.2341.

Synthetic route to *cis*-8,9-methylenehexadecanoic acid (FA-7)

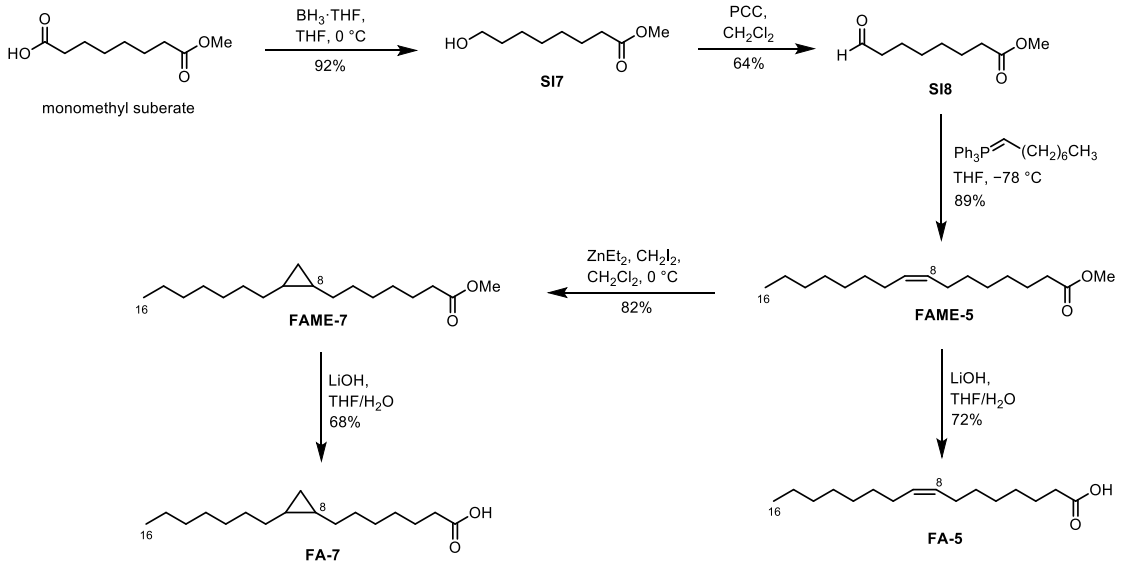

Methyl 8-hydroxyoctanoate (SI7)

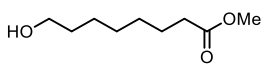

$BH_3·THF$ (31.5 mL of a 1.0 M solution in THF, 31.5 mmol) was added dropwise to a mixture of monomethyl suberate (5.65 g, 30.0 mmol) in THF (1.0 M) at 0 °C under N_2. After stirring for 10 min at 0 °C, the reaction mixture was allowed to warm to room temperature and stirred overnight. The reaction was then quenched with saturated aqueous Na_2CO_3 solution (20 mL). The mixture was extracted with Et_2O (3 × 30

mL) and the combined organic layers were washed with brine, dried ($MgSO_4$), and concentrated under reduced pressure. The residue was purified by flash column chromatography (20% EtOAc in petroleum ether) to afford **SI7** as a colorless oil (4.82 g, 92%); δ_H ($CDCl_3$, 400 MHz) 1.25–1.39 (6H, m), 1.48–1.68 (4H, m), 2.29 (2H, t, *J* 7.5), 3.62 (2H, t, *J* 6.7), 3.65 (3H, s), the exchangeable O*H* proton was not observed; δ_C (100 MHz, $CDCl_3$) 25.0, 25.7, 29.1, 29.2, 32.8, 34.2, 51.6, 63.1, 174.4. The data were in agreement with those described in the literature.[SI-8]

Methyl 8-oxooctanoate (SI8)

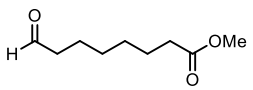

Alcohol **SI7** (871.0 mg, 5.00 mmol) was added to a mixture of PCC (1.62 g, 7.50 mmol) and Celite (1.62 g) in CH_2Cl_2 (15 mL) under N_2. The reaction mixture was stirred at room temperature for 2 h and then filtered through a pad of Celite and silica gel. This pad was washed with portions of Et_2O (3 × 20 mL) and the combined filtrate was concentrated under reduced pressure. The crude product was purified by flash column chromatography (5% EtOAc in petroleum ether) to afford aldehyde **SI8** as a colorless oil (556 mg, 64%); δ_H ($CDCl_3$, 400 MHz) 1.28–1.42 (4H, m), 1.56–1.72 (4H, m), 2.31 (2H, t, *J* 7.5), 2.43 (2H, dd, *J* 7.4, 1.8), 3.67 (3H, s), 9.76 (1H, t, *J* 1.9); δ_C (100 MHz, $CDCl_3$) 21.9, 24.7, 28.8, 28.9, 34.0, 43.8, 51.5, 174.1, 202.9. The data were in agreement with those described in the literature.[SI-8]

Methyl (Z)-hexadec-8-enoate (FAME-5)

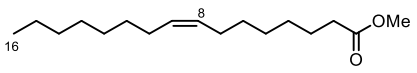

NaHMDS (4.0 mL of a 1.0 M solution in THF, 4.00 mmol) was added dropwise to a suspension of octyltriphenylphosphonium bromide (2.0 g, 4.40 mmol) in dry THF (10 mL) at 0 °C under N_2. The resulting orange mixture was stirred for 40 min at room temperature. The mixture was then cooled to −78 °C before aldehyde **SI8** (344 mg, 2.00 mmol) was added dropwise. After 30 min, the mixture was allowed to slowly warm to room temperature and stirred overnight. The reaction was quenched with saturated aqueous NH_4Cl solution (20 mL) and then extracted with Et_2O (3 × 20 mL). The combined organic layers were washed with brine, dried ($MgSO_4$), and concentrated under reduced pressure. The residue was purified by flash column chromatography (gradient 20–50% CH_2Cl_2 in petroleum ether) to afford alkene **FAME-5** as a colorless oil (480 mg, 89%); δ_H ($CDCl_3$, 400 MHz) 0.83–0.90 (3H, m), 1.19–1.36 (16H, m), 1.56–1.68 (2H, m), 1.89–2.07 (4H, m), 2.29 (2H, t, *J* 7.5), 3.65 (3H, s), 5.25–5.40 (2H, m); δ_C (100 MHz, $CDCl_3$) 14.1, 22.6, 24.9, 27.15, 27.21, 28.9, 29.07, 29.12, 29.14, 29.67, 29.72, 31.8, 34.1, 51.4, 129.8, 130.0, 174.3. HRMS (ESI+) calcd for $C_{17}H_{33}O_2^+$ $[M + H]^+$ 269.2475, found 269.2472.

(Z)-Hexadec-8-enoic acid (FA-5)

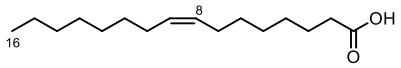

LiOH (45.6 mg, 1.90 mmol) was added to a mixture of ester **FAME-5** (170 mg, 0.63 mmol) in THF/H_2O (2.0 mL, 7:3, v/v) at room temperature. After stirring overnight, the reaction mixture was quenched with 1.0 M HCl (20 mL) and then extracted with EtOAc (3 × 20 mL). The combined organic layers were washed with brine, dried ($MgSO_4$), and concentrated under reduced pressure. The residue was purified by flash column chromatography (9% EtOAc in petroleum ether with 0.1% AcOH) to afford fatty acid **FA-5** as a colorless oil (115.4 mg, 72%); δ_H ($CDCl_3$, 400 MHz) 0.88 (3H, t, *J* 6.7), 1.22–1.39 (16H, m), 1.57–1.69 (2H, m), 1.93–2.08 (4H, m), 2.35 (2H, t, *J* 7.5), 5.30–5.40 (2H, m), the exchangeable CO_2H proton was not observed; δ_C (100 MHz, $CDCl_3$) 14.3, 22.8, 24.8, 27.3, 27.4, 29.0, 29.1, 29.38, 29.43, 29.7, 29.9, 32.0, 129.8, 130.3, 177.6 (one resonance not observed due to overlap). HRMS (ESI+) calcd for $C_{16}H_{29}O_2^+$ $[M + H]^+$ 253.2173, found 253.2178.

Methyl cis-8,9-methylenehexadecanoate (FAME-7)

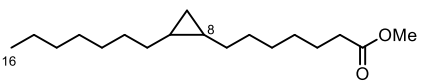

Diethyl zinc (6.0 mL of a 1.0 M solution in hexane, 6.0 mmol) was added dropwise to a mixture of alkene **FAME-5** (268.4 mg, 1.00 mmol) in dry CH_2Cl_2 (10 mL) at 0 °C under N_2. After stirring for 1 h at 0 °C, diiodomethane (3.21 g, 12.0 mmol) was added to the reaction mixture. A milky dispersion was formed and the reaction mixture was allowed to slowly warm to room temperature and stirred overnight. The reaction was quenched with saturated aqueous NH_4Cl solution (10 mL) and extracted with CH_2Cl_2 (3 × 10 mL). The combined organic layers were washed with brine, dried ($MgSO_4$), and concentrated under reduced pressure. The residue was purified by flash column chromatography (gradient 20–50% CH_2Cl_2 in petroleum ether) to afford cyclopropane **FAME-7** as a colorless oil (234 mg, 82%); δ_H ($CDCl_3$, 400 MHz) –0.38 – –0.30 (1H, m), 0.51–0.59 (1H, m), 0.59–0.70 (2H, m), 0.85–0.90 (3H, m), 1.06–1.19 (2H, m), 1.22–1.41 (18H, m), 1.58–1.67 (2H, m), 2.30 (2H, t, *J* 7.5), 3.66 (3H, s); δ_C (100 MHz, $CDCl_3$) 11.1, 14.3, 15.8, 15.9, 22.8, 25.1, 28.8, 28.9, 29.35, 29.39, 29.5, 29.8, 30.1, 30.4, 32.1, 34.3, 51.6, 174.5. HRMS (ESI+) calcd for $C_{18}H_{35}O_2^+$ $[M + H]^+$ 283.2632, found 283.2630.

***cis*-8,9-Methylenehexadecanoic acid (FA-7)**

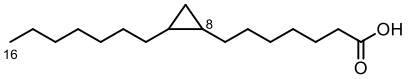

LiOH (51.1 mg, 2.10 mmol) was added to a mixture of ester **FAME-7** (200 mg, 0.71 mmol) in THF/H_2O (2.0 mL, 7:3, v/v) at room temperature. After stirring overnight, the reaction mixture was quenched with 1.0 M HCl (20 mL) and then extracted with EtOAc (3 × 20 mL). The combined organic layers were washed with brine, dried ($MgSO_4$), and concentrated under reduced pressure. The residue was purified by flash column chromatography (9% EtOAc in petroleum ether with 0.1% AcOH) to afford **FA-7** as a colorless oil (92.5 mg, 68%); δ_H ($CDCl_3$, 400 MHz) –0.33 (1H, app. td, *J* 5.2, 5.0), 0.51–0.61 (1H, m), 0.61–0.70 (2H, m), 0.89 (3H, t, *J* 6.6), 1.08–1.19 (2H, m), 1.24–1.44 (18H, m), 1.57–1.70 (2H, m), 2.35 (2H, t, *J* 7.5), the exchangeable CO_2H proton was not observed; δ_C (100 MHz, $CDCl_3$) 11.1, 14.3, 15.8, 15.9, 22.9, 24.8, 28.8, 28.9, 29.3, 29.4, 29.6, 29.8, 30.1, 30.4, 32.1, 34.2, 180.4. HRMS (ESI–) calcd for $C_{17}H_{31}O_2^-$ $[M - H]^+$ 267.2331, found 267.2325.

*Ethyl 7-ethoxycarbonyl-8-oxopentadecanoate (**SI2**)*

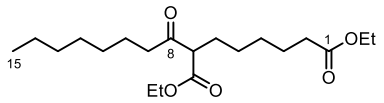

$CDCl_3$, 400 MHz

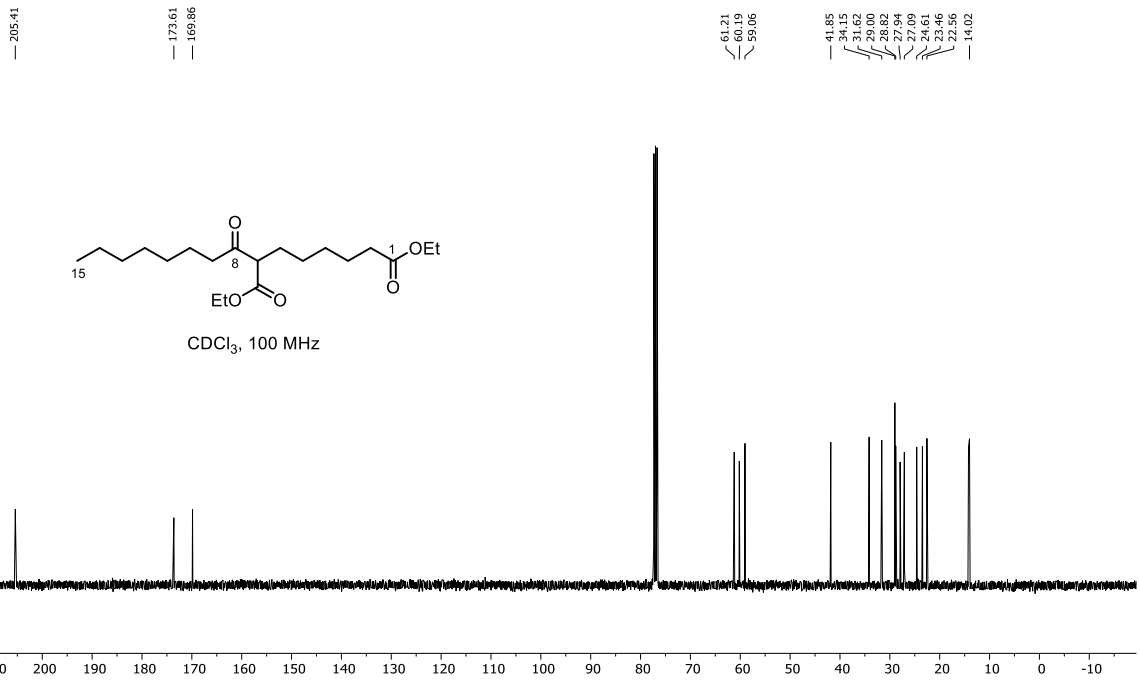

$CDCl_3$, 100 MHz

*8-Oxopentadecanoic acid (**SI3**)*

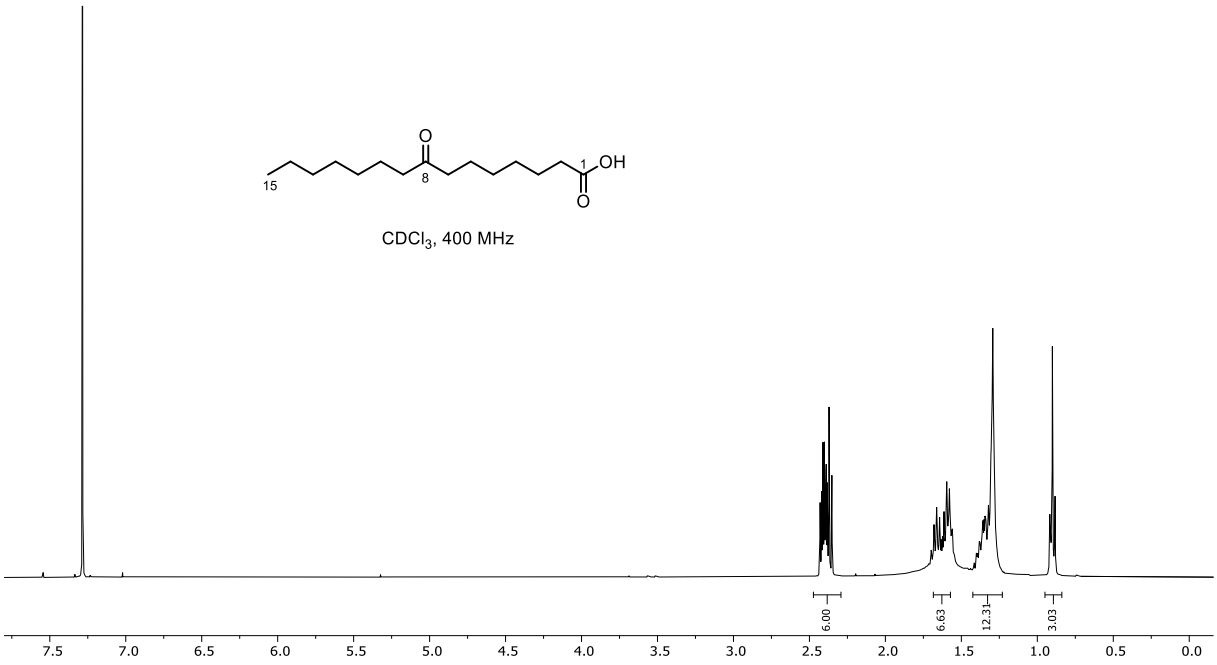

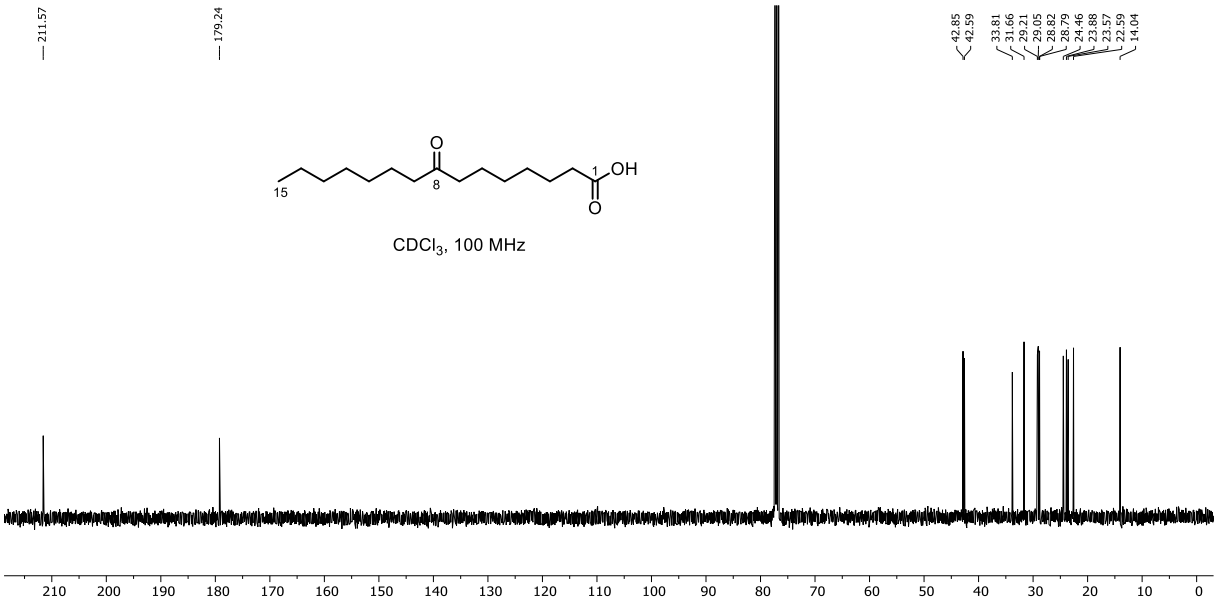

*Methyl 8-oxopentadecanoate (**SI4**)*

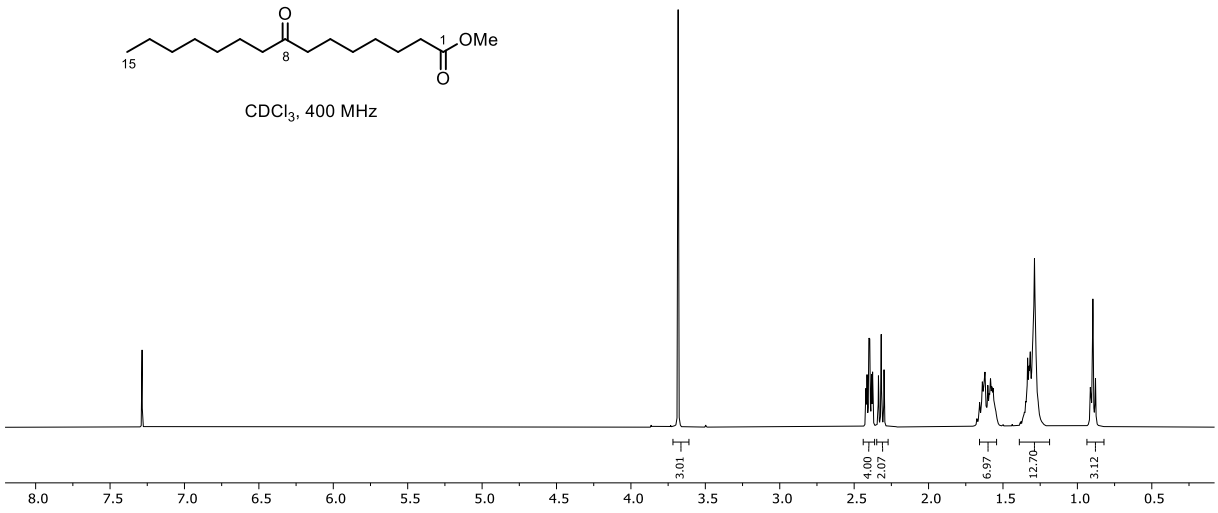

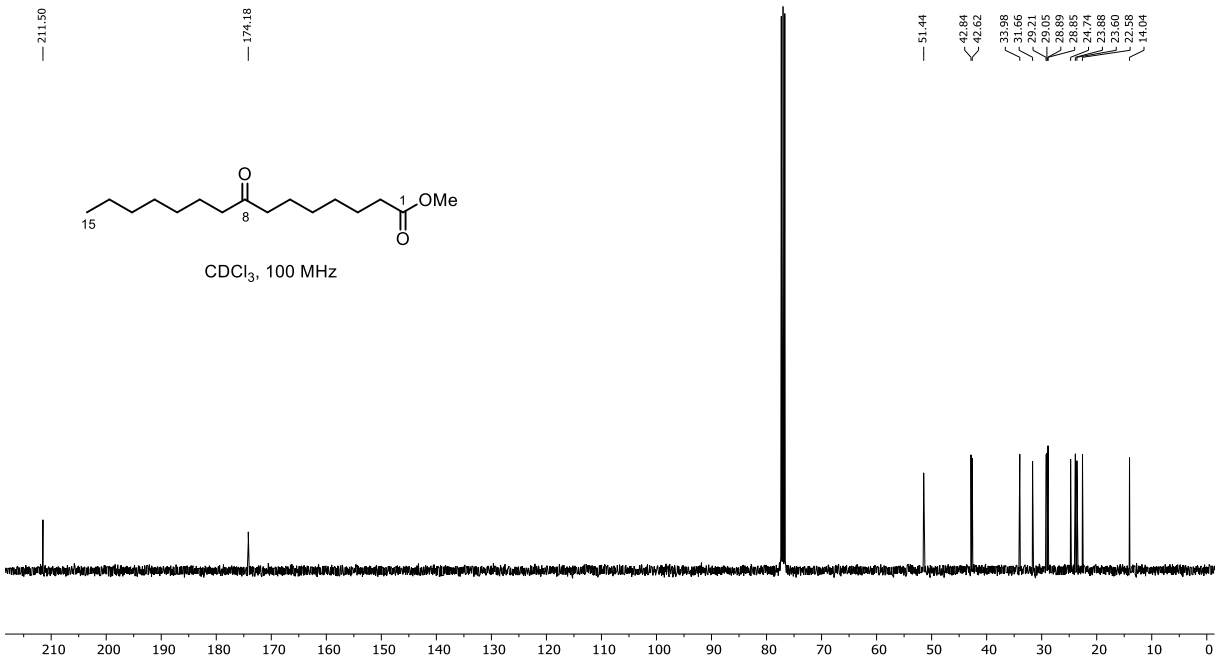

*Methyl (E/Z)-8-(methoxymethylene)pentadecanoate (**SI5**)*

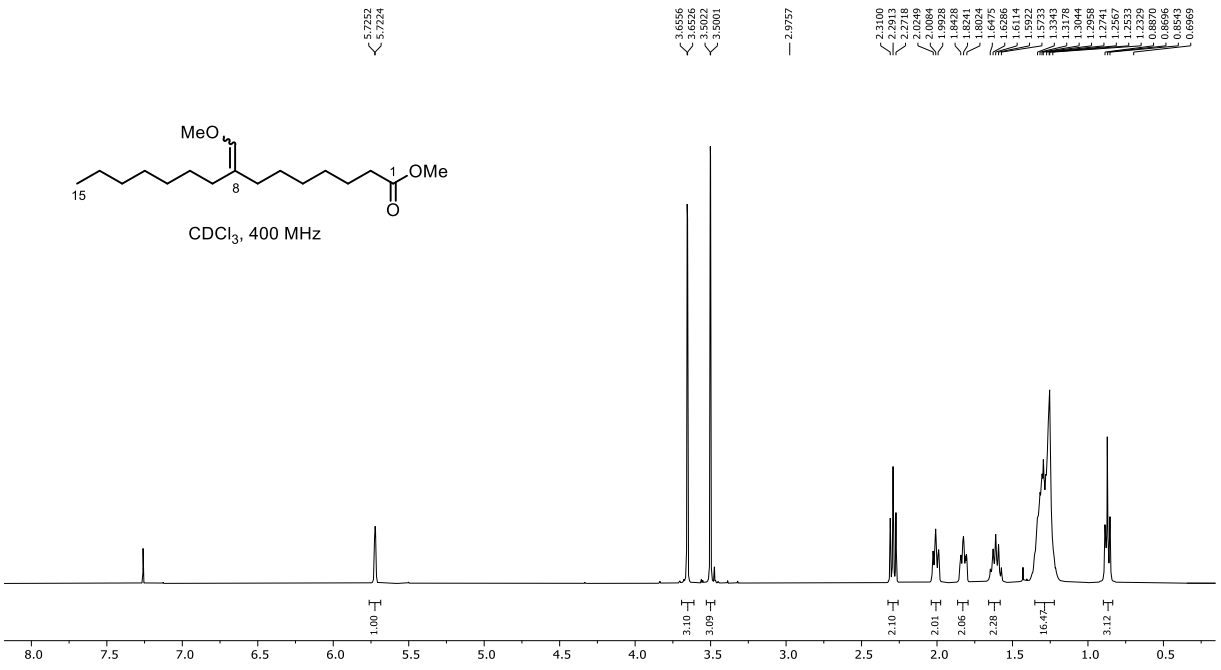

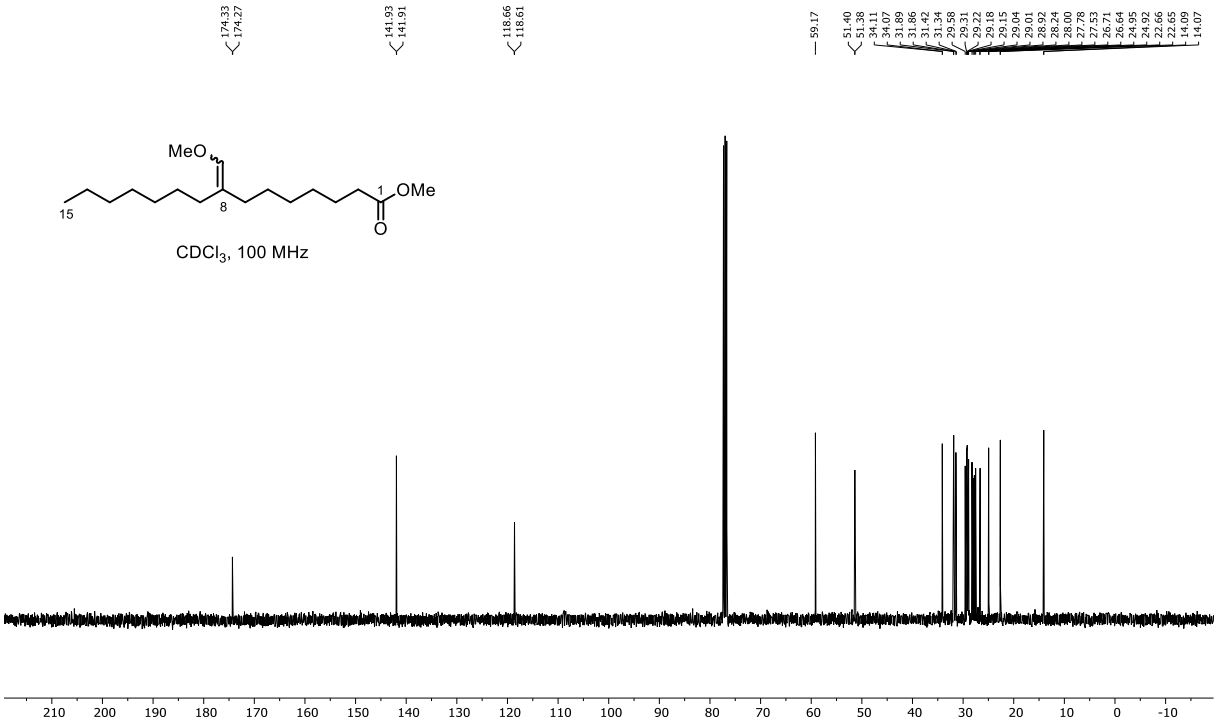

*Methyl 8-vinylpentadecanoate (**FAME-6**)*

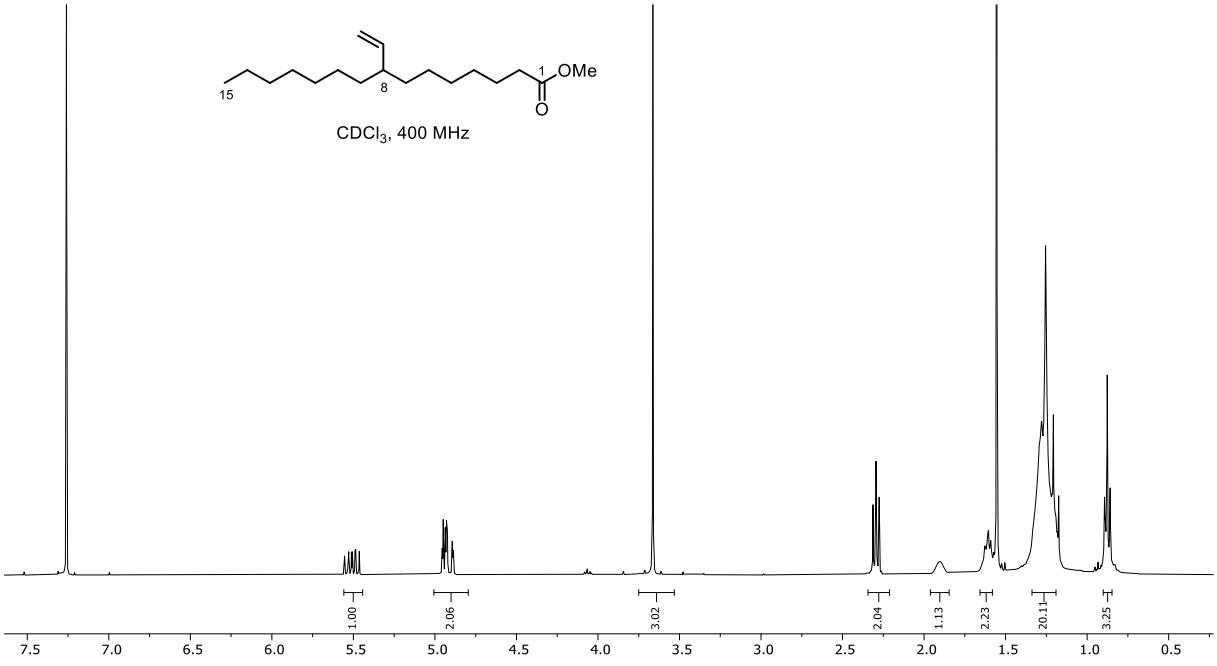

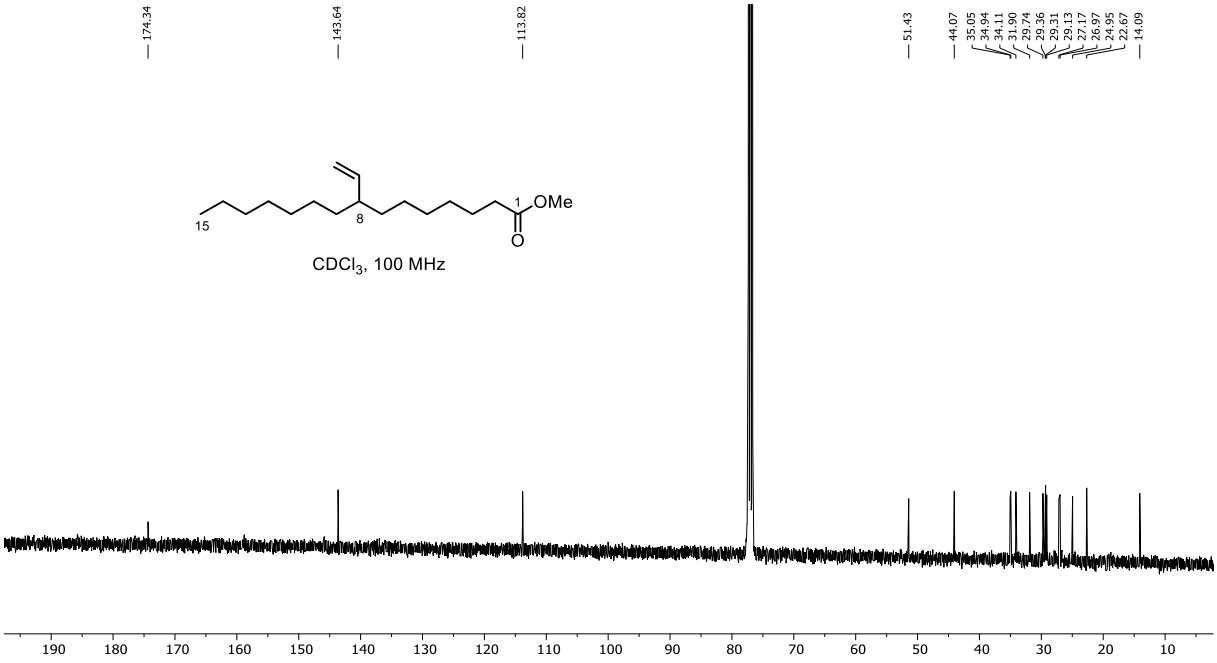

8-vinylpentadecanoic acid (***FA-6***)

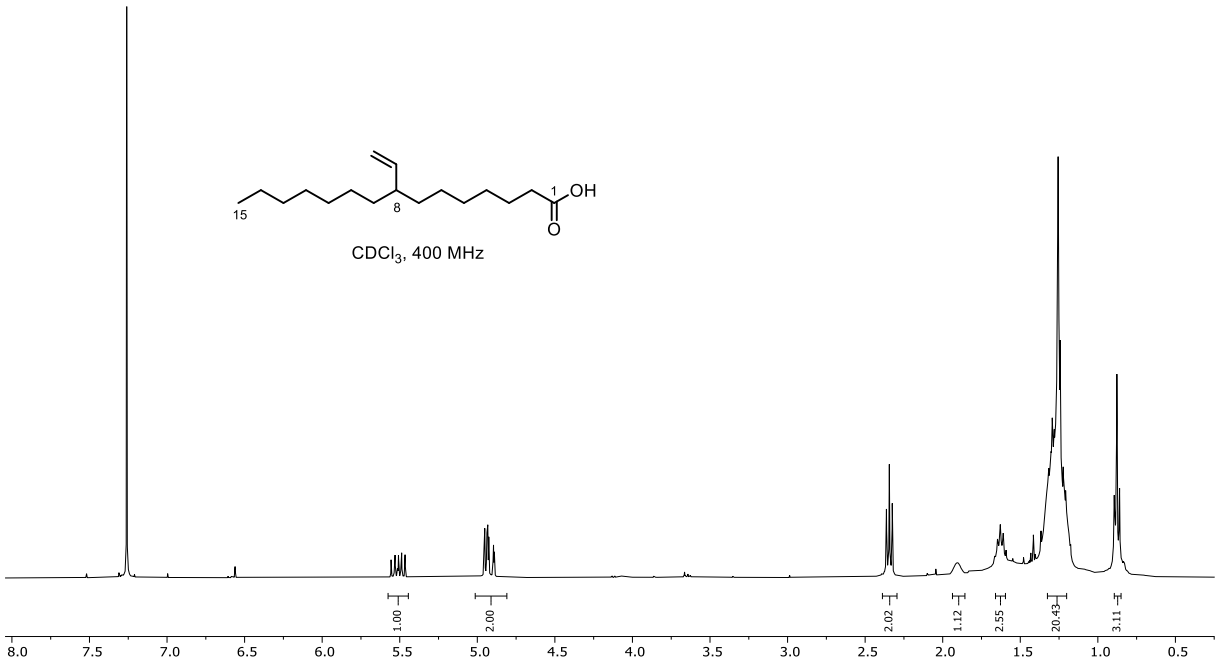

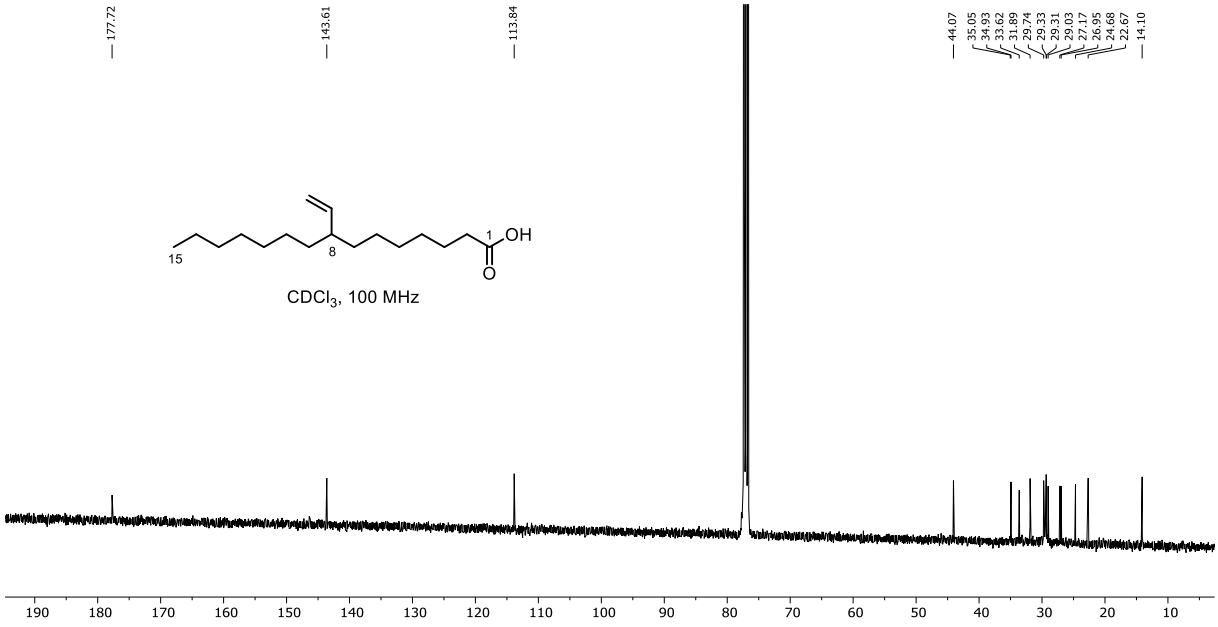

*Methyl 8-hydroxyoctanoate (**SI7**)*

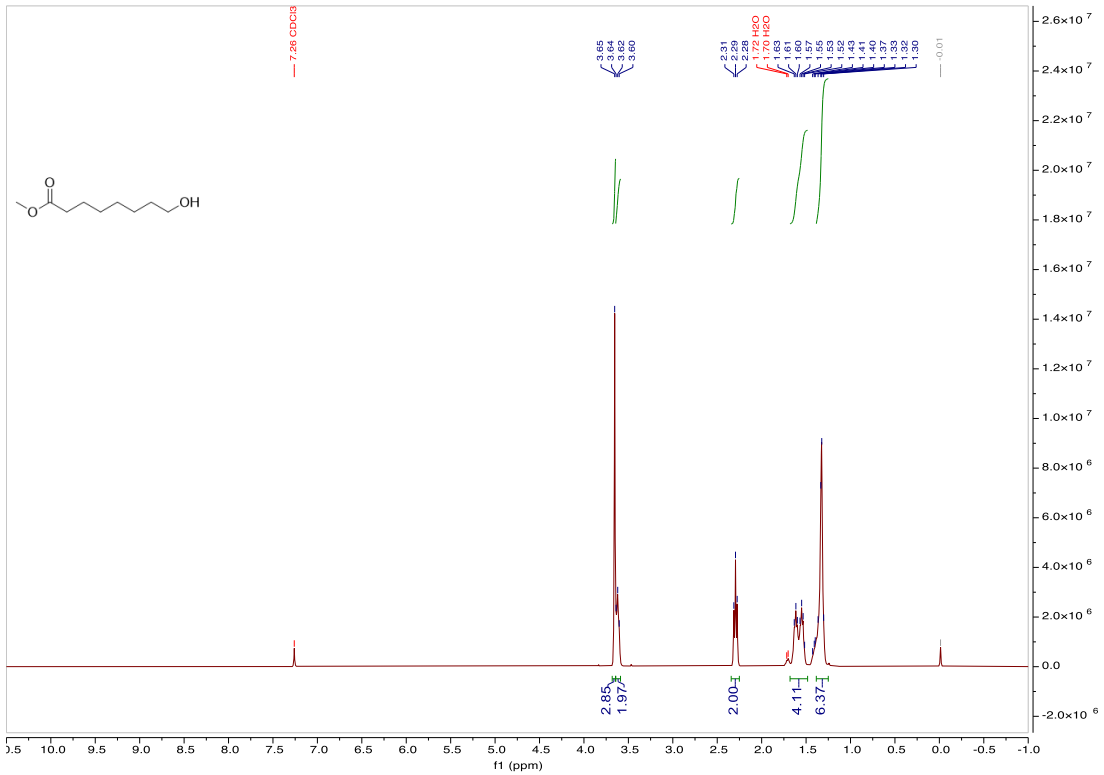

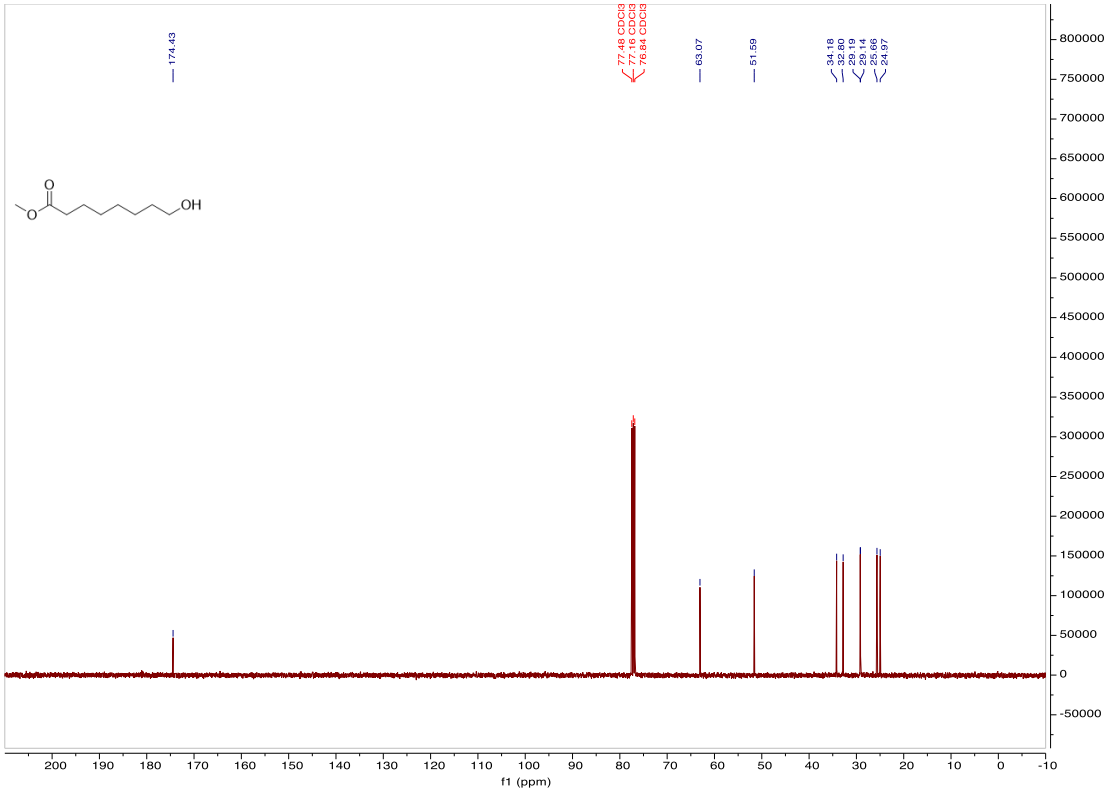

*Methyl 8-oxooctanoate (**SI8**)*

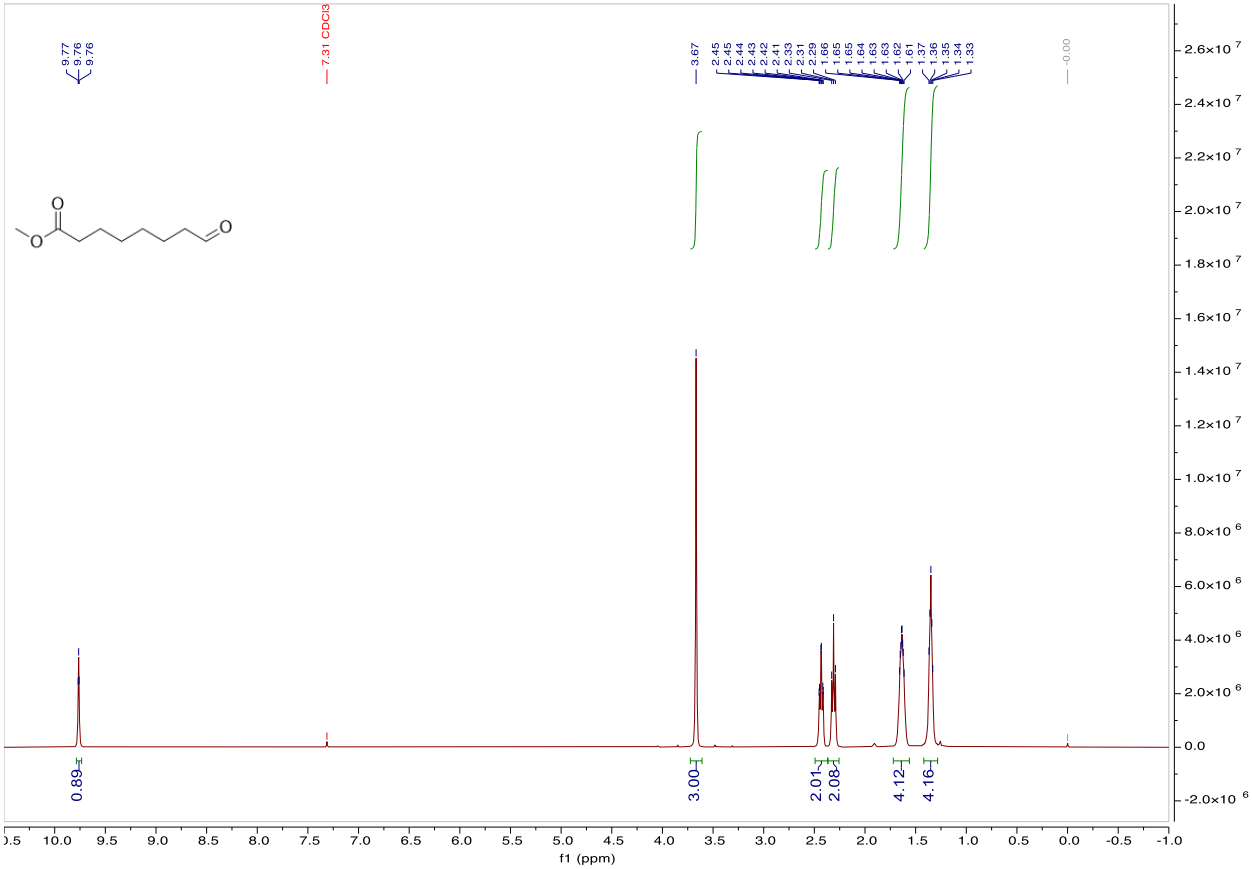

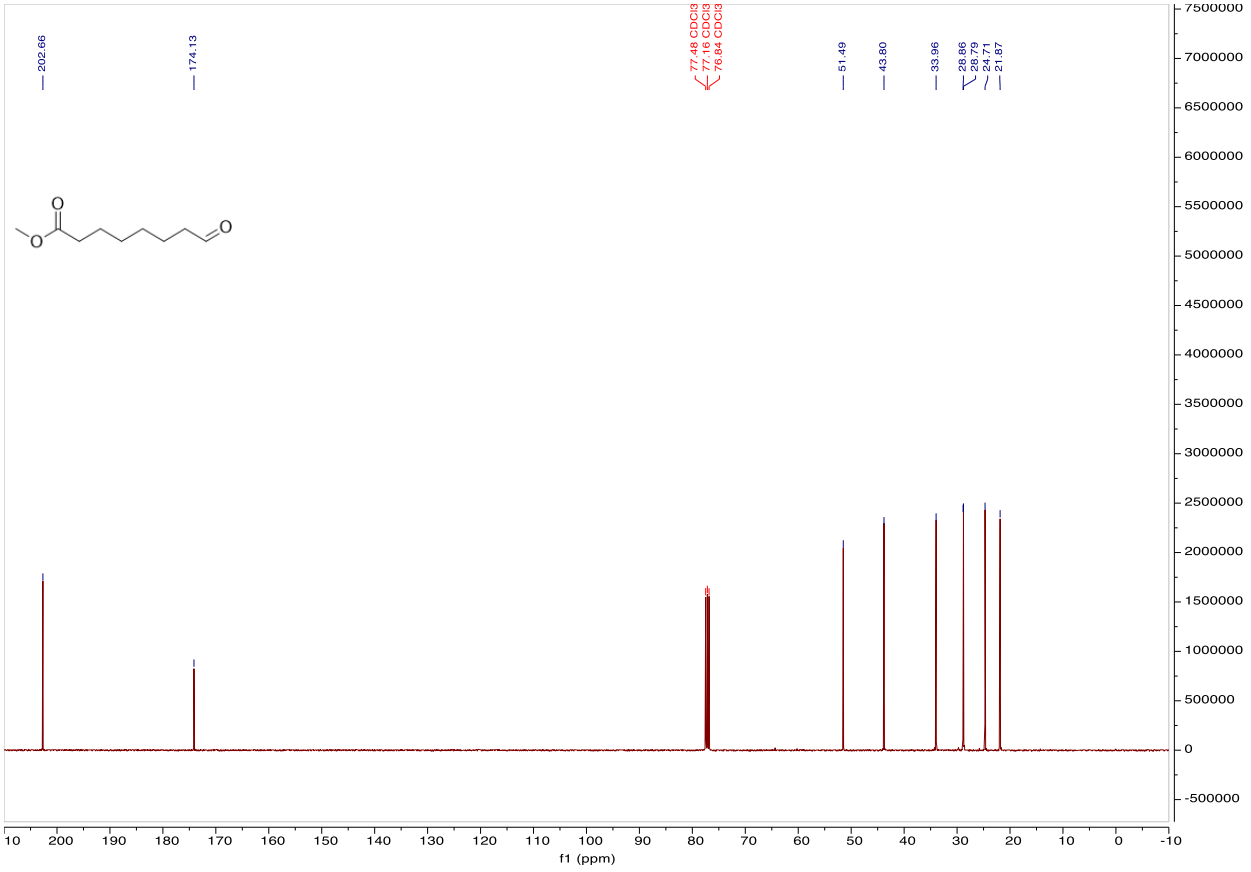

*Methyl (Z)-hexadec-8-enoate (**FAME-5**)*

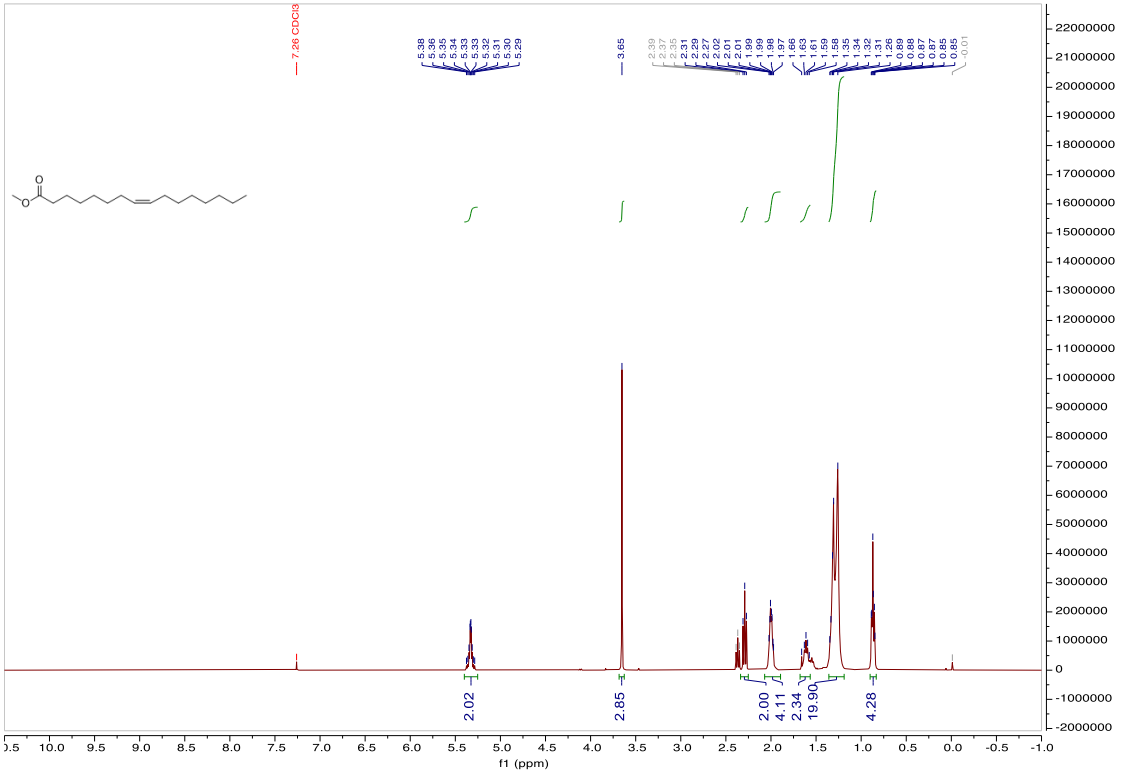

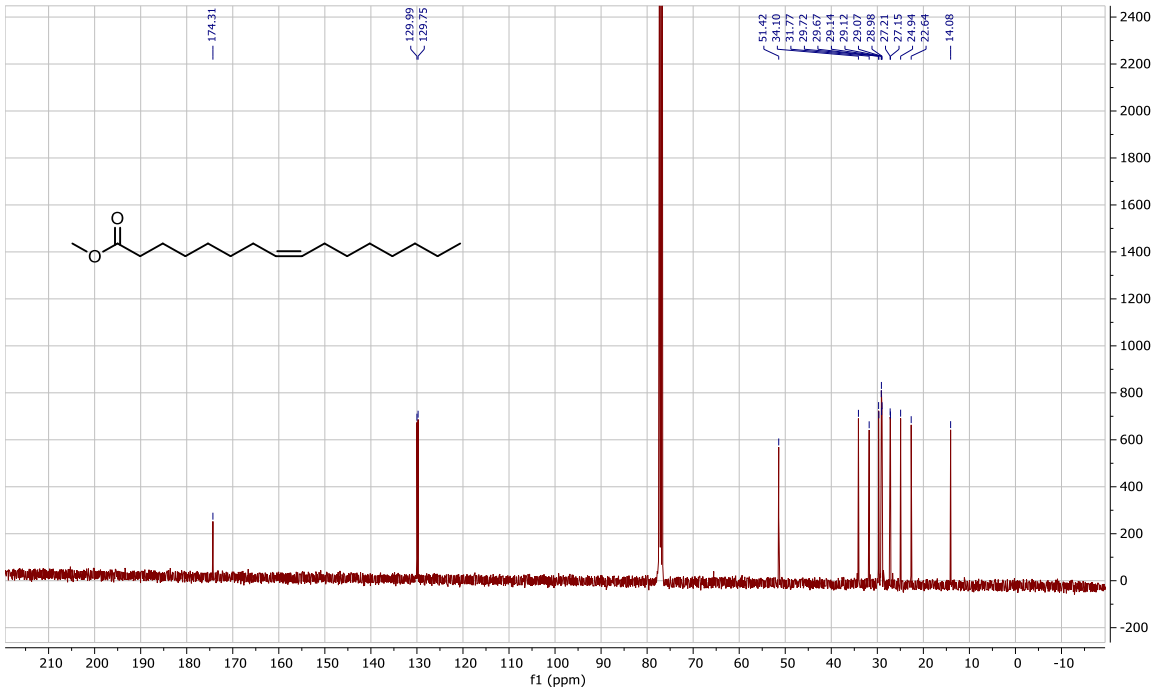

*(Z)-hexadec-8-enoic acid (**FA-5**)*

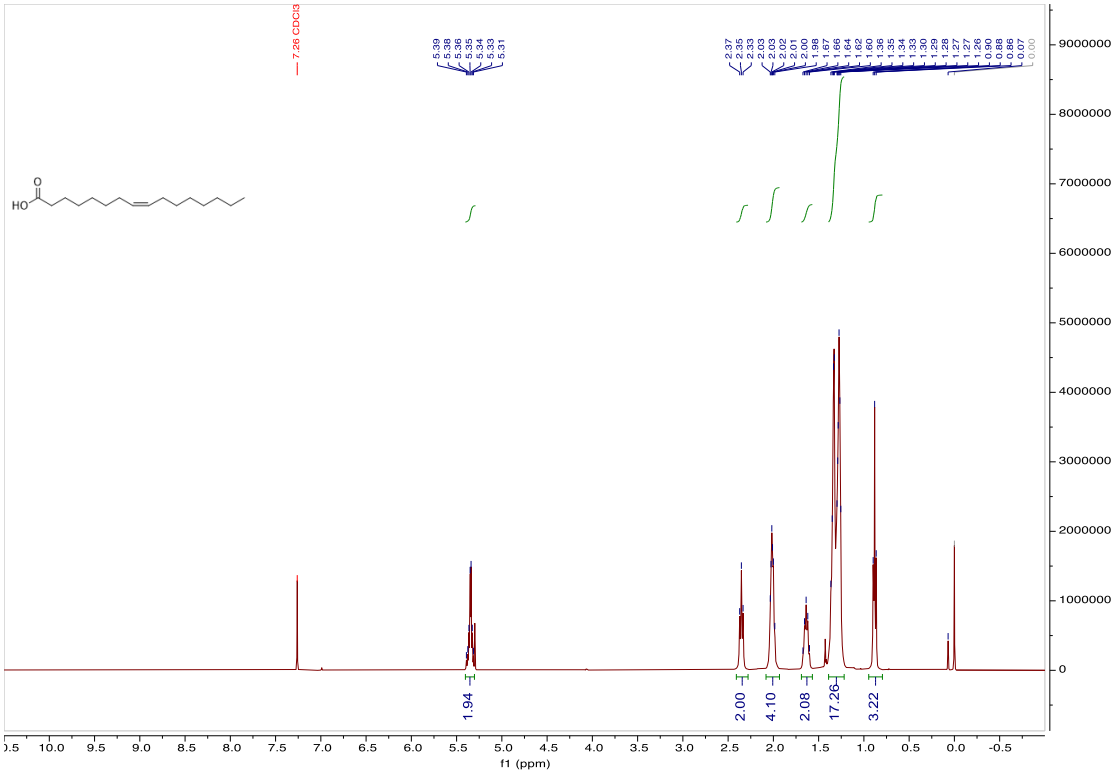

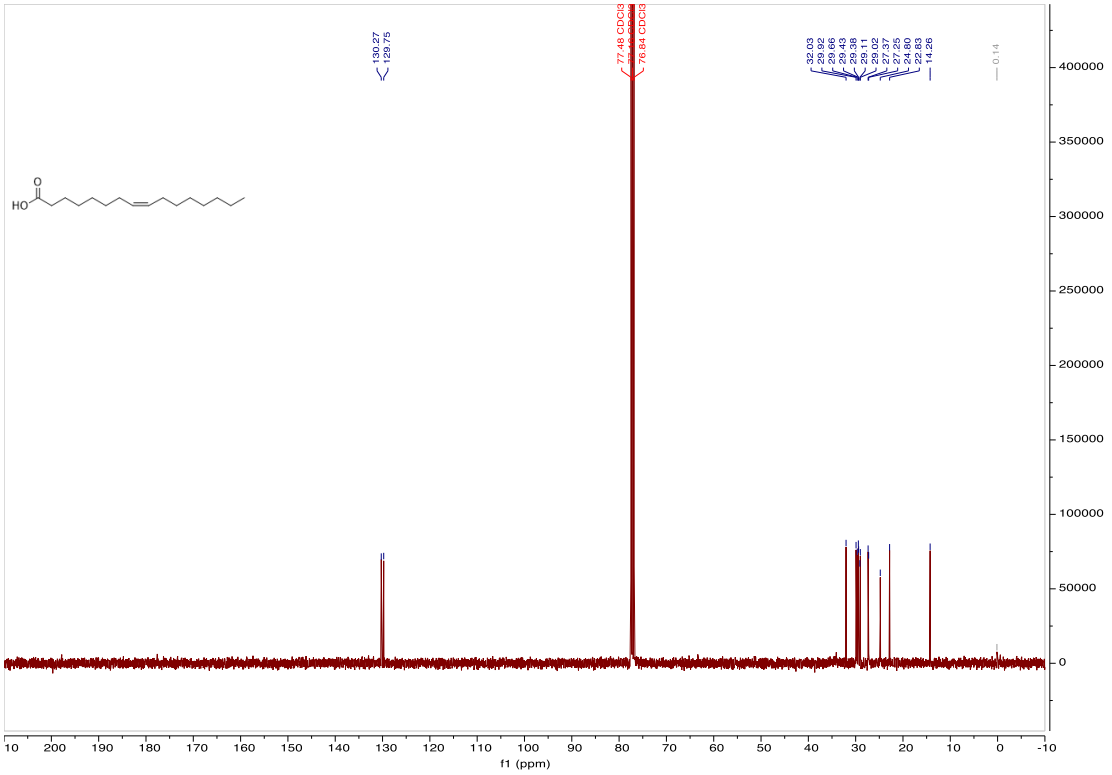

*Methyl cis-8,9-methylenehexadecanoate (**FAME-7**)*

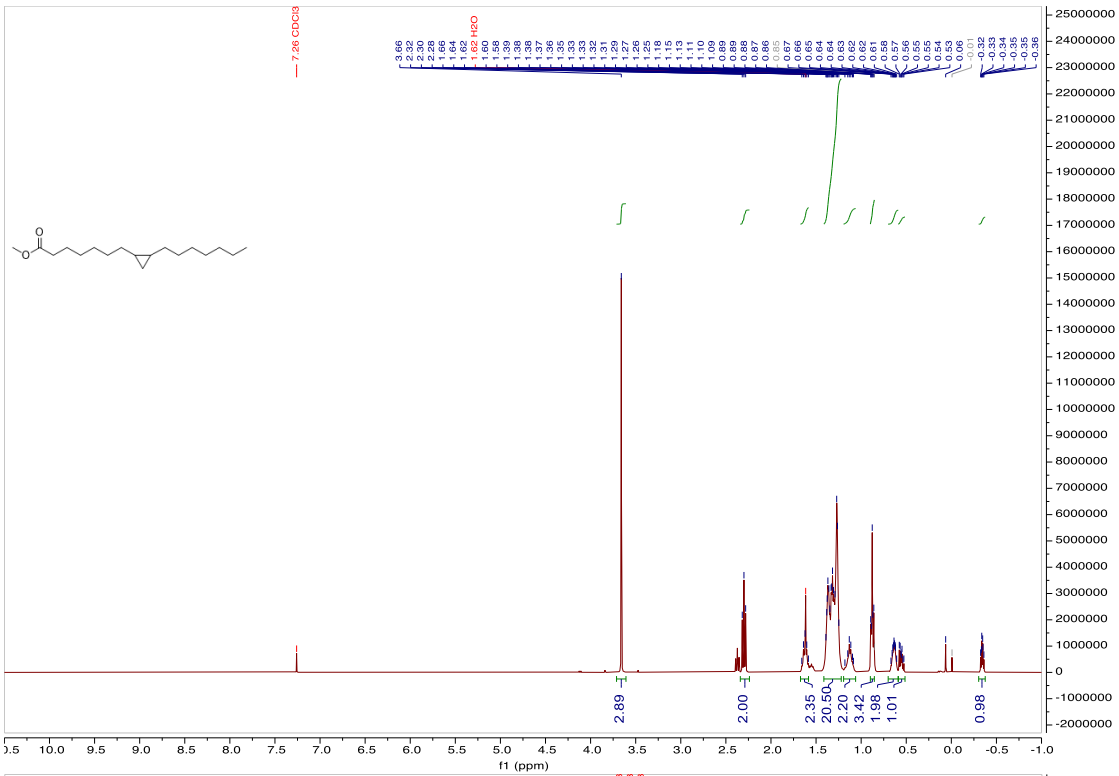

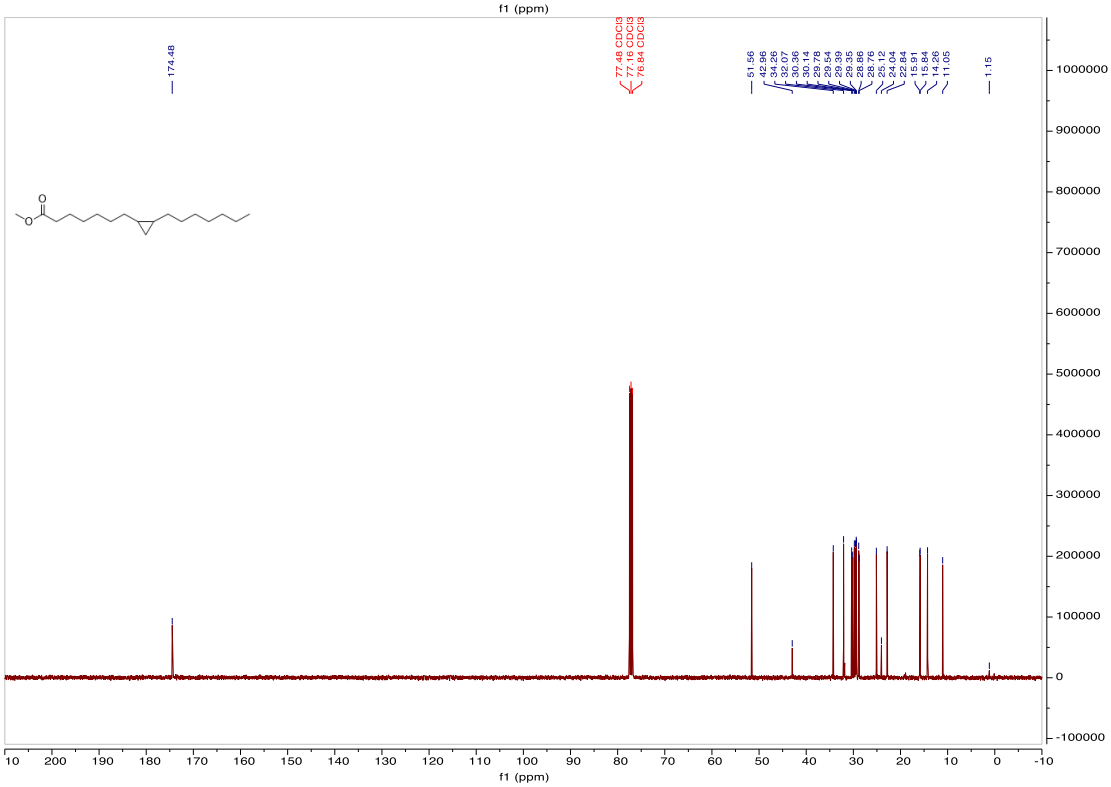

*cis-8,9-methylenehexadecanoic acid (**FA-7**)*

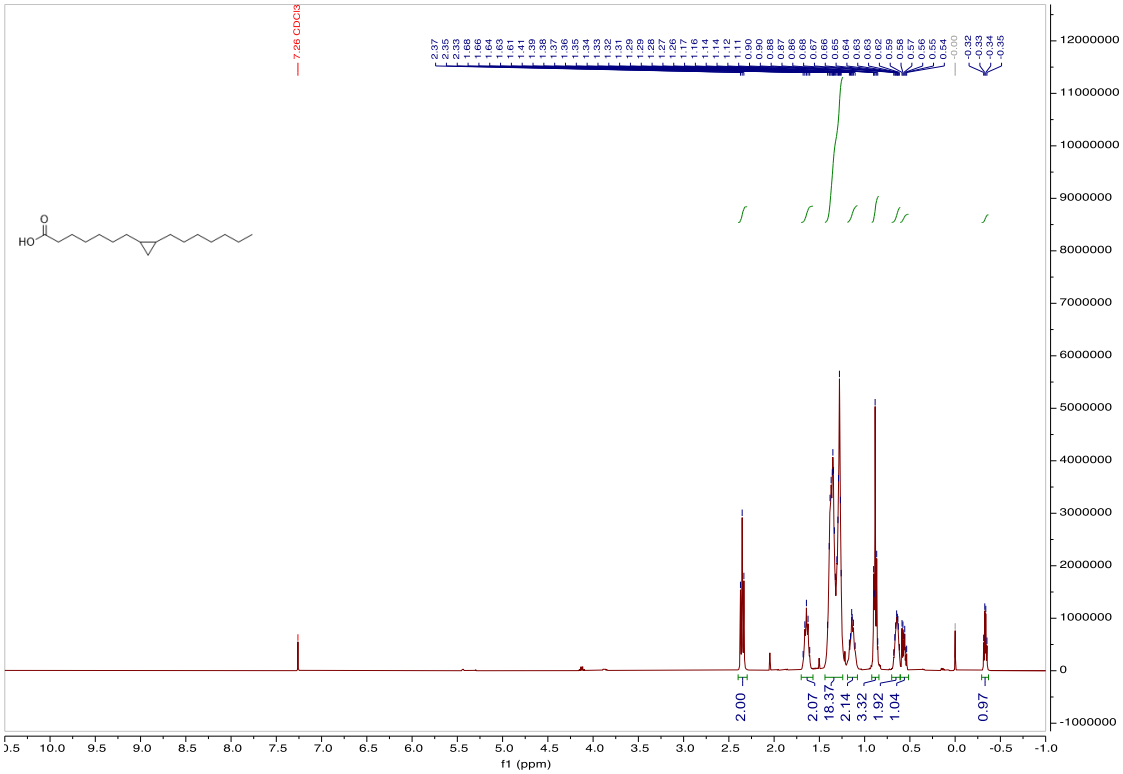

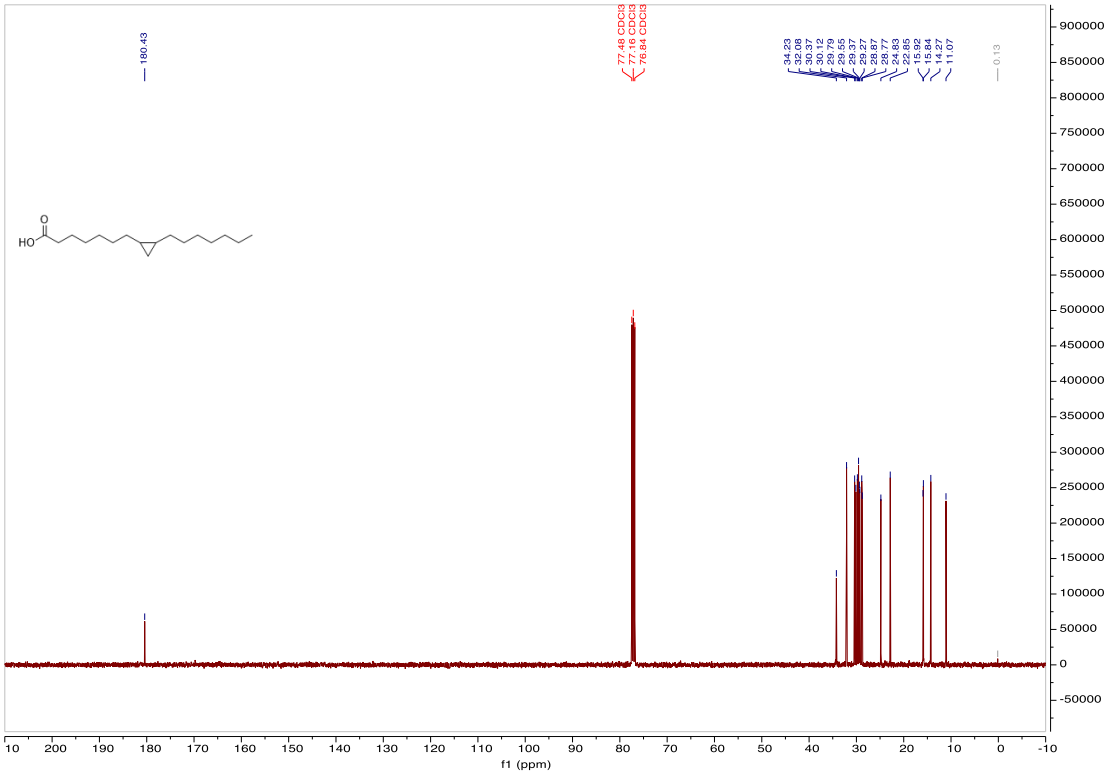

References

SI-1. Figueiredo, S. A. C. *et al.* Discovery of Cyanobacterial Natural Products Containing Fatty Acid Residues. *Angew. Chem. Int. Ed.* **60**, 10064–10072 (2021).

SI-2. van Santen, J. A. *et al.* The Natural Products Atlas: An Open Access Knowledge Base for Microbial Natural Products Discovery. *ACS Cent. Sci.* **5**, 1824–1833 (2019).

SI-3. Li, T., Tripathi, A., Yu, F., Sherman, D. H. & Rao, A. DDAP: docking domain affinity and biosynthetic pathway prediction tool for type I polyketide synthases. *Bioinforma. Oxf. Engl.* **36**, 942–944 (2020).

SI-4. Martins, T. P. *et al.* Biosynthesis of the Unusual Carbon Skeleton of Nocuolin A. *ACS Chem. Biol.* **17**, 2528–2537 (2022).

SI-5. Dayal, B., Speck, J., Bagan, E., Tint, G. S. & Salen, G. p-Toluenesulfonic acid/methanol: Mild reagent for the preparation of bile acid methyl esters. *Steroids* **37**, 239–242 (1981).

SI-6. Moosmann, P., Ueoka, R., Gugger, M. & Piel, J. Aranazoles: Extensively Chlorinated Nonribosomal Peptide–Polyketide Hybrids from the Cyanobacterium *Fischerella* sp. PCC 9339. *Org. Lett.* **20**, 5238–5241 (2018).

SI-7. Nguyen, V., Bellur, E., Appel, B. & Langer, P. Synthesis of 4-Alkyl- and 4-(ω-Chloroalkyl)-3-hydroxy-5-alkylidenebuten-olides Based On Cyclizations of 4-Alkyl- and 4-(ω-Chloroalkyl)-1,3-bis(tri-methylsilyloxy)buta-1,3-dienes with Oxalyl Chloride. *Synthesis* **2006**, 2865–2872 (2006).

SI-8. Okuma, K. *et al.* An efficient synthesis of (R)-(+)-recifeiolide and related macrolides by using enantiomerically pure (R)-(−)-5-methyl-2,2,2-triphenyl-1,2λ5-oxaphospholane. *Tetrahedron* **54**, 4243–4250 (1998).